MODELLING THE LONG-RANGE TRANSPORT AND TRANSFORMATION OF AIR POLLUTANTS OVER THE SOUTHERN AFRICAN REGION

by

Gerhardus Dirk Fourie
M.Sc. (P.U. vir C.H.O.)

Thesis submitted in fulfilment of the requirements for the degree

PHILOSOPHIAE DOCTOR

in the

School of Chemistry, Faculty of Natural Science
North-West University
Potchefstroom, South Africa

Supervisor: Prof. J.J. Pienaar (North-West University, South Africa)
Co-supervisor: Prof. G.D. Djolov (University of Limpopo, South Africa)

Potchefstroom
May 2006

Vir Zelda

Contents

List of Tables

List of Figures

ACKNOWLEDGEMENTS

I wish to express my sincere appreciation and gratitude to the following persons and institutions for their contributions to the successful completion of this study:

Prof. Kobus Pienaar, School of Chemistry and Biochemistry, North-West University (Potchefstroom Campus), for the scientific freedom provided, his able guidance and constructive critique throughout the study, and for his friendship;

Prof. George Djolov, School of Physical and Mineral Sciences, University of Limpopo, for his extraordinary insight, untiring and uncompromising dedication, commitment and support, both to me and to the accomplishment of the task ahead;

Mr. Herman van der Walt, Sasol SHE Center, for his leadership, guidance, patience and willingness to help me during my formative years at Sasol Technology Research and Development;

Dr. Trevor Phillips, Group Manager, Environmental Sciences and Technology, Sasol Technology Research and Development, for his interest, motivation and support, especially during the most stressfilled periods of my work;

The staff of the Environmental Sciences and Technology department, Sasol Technology Research and Development, Sasolburg, for their friendship and support, and numerous other people not mentioned by name, who in some way contributed to this study;

My wife, Zelda, for her love, patience, indulgence and support throughout the entire study;

My daughter, Megan, who without understanding, had to endure many hours of absence;

My parents, for their love, continuous encouragement and moral support throughout the entire study;

My brother Dries, for this enthusiasm, inspiration and continuous support throughout the entire study, as well as my life; and

Above all, God Almighty, for the opportunity, health, motivation, guidance and love He bestowed on me during this period.

SUMMARY

Dispersion modelling of transport, diffusion and chemical transformation of pollutants and trace gases over the Southern African region which spans between 52 ° South to 1 ° North, 28 ° West to 68 ° East, presents a special challenge due to three major factors. The first factor is associated with the frequent occurrence of a stable anticyclonic environment. This environment inhibits the vertical exchange of air masses and stratifies the troposphere into persistent layers, in which residence times of pollutants are prolonged from several days to weeks over the region. The second factor stems from the different distribution of emission sources in Africa. Biogenic emissions from biomass burning, vegetation and soils are equal to, or substantially bigger than anthropogenic emissions over larger parts of the region. Thirdly, long-range transport is vital for the existence or destruction of many fragile ecosystems that receive nutrients or pollutants mainly from the atmosphere. In addition to these major factors, experimental studies on the tropical meteorological factors affecting the long-range transport and chemical transformation of pollutants are limited, and theoretical understanding of the atmospheric processes in the regions with negligible Coriolis force, is still lacking. Special emphasis should be placed on the identification of key linkages between the physical, chemical and anthropogenic processes governing the functioning of the biogeophysical and biogeochemical systems of Southern Africa that lead to significantly elevated ozone concentrations over considerable sections of the tropics.

This thesis describes the development and application of an appropriate dispersion package for studying the peculiarities of the long-range transport, diffusion and chemical transformation of pollutants and trace gases in the Southern Africa region. Special attention is given to the transport of harmful substances from the highly industrialized regions to the predominantly rural areas of the region as well as wet- and dry deposition over sensitive land and water ecosystems.

The Lagrangian-Eulerian Diffusion (LED) model developed in this thesis, utilizes in a complimentary way the positive features of the Lagrangian and Eulerian description of hydrodynamic flows. It is well-known that the essence of the Lagrangian method consists of studying the properties and variation of a fixed fluid volume during its motion. Using this idea in the model, any volume of polluted air is identified by the trajectory of its center of mass. The diffusion and transformation processes of pollutants are investigated on the basis of analytical solutions of the appropriate differential equations in Eulerian coordinates with origin at the center of mass of puffs. As part of the basic structural element of the model, the puff allows for approximation of any type of emission source by using proper puff volume and emission time intervals. A unique feature of LED is the use of an appropriate ABL model calculating its dynamics and turbulent characteristics. In the LED model the two-layer parametric ABL model proposed by Yordanov et al. (1983) is included. LED incorporates a linear chemical mechanism for the transformation of sulphur and nitrogen species, as well as modules to calculate dry and wet deposition parameters.

LED model results for ambient concentrations, as well as deposition fields, were produced for all months during the year 2000, and compared with the available experimental data at the Deposition of Biogeochemically Important Trace Species (DEBITS) international sites. Data obtained for the evaluation, were in the framework of SAFARI 2000 research campaign. However, the ground measurements needed for the evaluation of LED were not sufficient due to the small number of observation points (5), and the geographical location which does not

comply with the WMO criteria for baseline regional air quality stations. Another shortcoming stems from the fact that some of the DEBITS stations were not fully operational during the year 2000. The predetermined SAFARI 2000 research plan for the period of integration (2000), did not allow the use of previous years measured data (where the availability of experimental data is somewhat more complete) for the evaluation exercise. Therefore data from before the year 2000, has been used to only evaluate LED capability of producing results which are in the range of the observed inter-annual observations. Despite these inherent difficulties of not having a complete set of experimental data for the evaluation process, the study presents enough evidence that LED is producing reliable results. The annual quantities compare quite accurately. The bigger variation in differences of the monthly quantities is also within the acceptable range. A numerical experiment, carried out with an alternative emission data set, clearly shows the importance of revisiting the existing emission data set accepted by the SAFARI 2000 research group. It gives a reasonable explanation for some of the monthly deviations observed at the most northern DEBITS station.

LED was also implemented to study the long-range transport from the highly industrialised Highveld region of South Africa, where the versatility of the LED model was clearly demonstrated. Ambient concentration fields, accumulated dry- and wet deposition fields, as well as pH values of precipitation over the modelling region were calculated. These outputs allow the environmental footprint characteristics to be determined. For the specific case study, the environmental impact region is located approximately 500 to 600 kilometers around the industrial region. The comparison of the calculated model results with limited experimental data for the region, and lack of outputs from other models and observations, substantiate the use of LED for environmental impact studies, regulatory purposes and decision making.

The results in Chapter 7 clearly demonstrate that the phenomena of long-range transport of air pollutants is a serious, complex and significant problem for the countries in the southern African region. The results also indicate that impacts from highly industrial countries in the region may pose significant risks to developing countries, who relies for example on agriculture as a major contributor to the specific country's gross domestic product (GDP). The LED model supplies objective data, which lays the foundation for the development of holistic regional air quality management plans. The implementation of such a management plan will be obviously beneficial to all countries in the region. The results obtained from this modelling scenario highlights the complexity of transboundary air pollutant transport, as well as its serious developmental consequences.

After development, modification and evaluation of the LED, it can be used to assist in identifying potentially high impact areas. Concentration and deposition fields for specific regions allow the study of anthropogenic impacts caused by the transport of major air pollutants such as sulphates and nitrogen oxides. The ability to define the relative importance of each source in the total pollution and deposition fields can be used to determine the most effective strategy for decreasing the emissions of a given region. LED can be applied with confidence as a diagnostic and prognostic tool for air pollution studies at different time and space scales in the southern African region.

LIST OF ABBREVIATIONS

ABL: Atmospheric Boundary Layer.

APPA: Air Pollution and Prevention Act, South Africa.

CAA: Clean Air Act, United States.

DEAT: Department of Environmental Affairs and Tourism, South Africa.

DEBITS: Deposition of Biogeochemical Important Trace Species.

EPA: Environmental Protection Agency, United States.

EU: European Union.

GEMS: Global Environmental Monitoring Network.

Gg: Gigagrams.

IDAF: IGAC (International Global Atmospheric Chemistry) / DEBITS / Africa.

IGAC: International Global Atmospheric Chemistry.

IPCC: International Panel on Climate Change.

LAI: Leaf Area Index.

LED: Lagrangian-Eulerian Diffusion model.

$mg.m^{-3}$: milligrams per cubic meter.

$mol.m^{-3}$: molecules per cubic meter.

NAAQS: National Ambient Air Quality Standards, United States.

NCEP: National Center for Environmental Prediction, United States.

NDVI: Normalised Difference Vegetation Index.

NGM: Nested Grid Model.

PBL: Planetary Boundary Layer.

PSD: Prevention of Significant Deterioration.

SADC: Southern African Development Community.

SAFARI: South African Fire-Atmosphere Research Initiative.

SAWS: South African Weather Service.

STP: Standard Temperature and Pressure.

Tg: Terragrams.

UNFCCC: United Nations Framework Convention on Climate Change.

US: United States of America.

WHO: World Health Organisation.

WMO: World Meteorological Organisation.

$\mu g.m^{-3}$: micrograms per cubic meter.

Chapter 1

MOTIVATION AND GOALS

In this Chapter...

The project is motivated by giving a short overview and atmospheric relevance of the long-range air pollution transport phenomena in Section 1.1. This short chapter is concluded by Section 1.2, which sets the objectives and envisaged outputs of the study.

1.1 PROJECT MOTIVATION

"Fair is foul, and foul is fair:
Hover through the fog and filthy air"
Macbeth, William Shakespeare

Although penned 400 years ago, the prophecies of the three witches of *Macbeth* bear some resemblance to the events and perceptions surrounding our understanding of air pollution as they developed over the later half of the 20th century. For example December 2002 marked the 50th anniversary of the infamous 1952 air pollution disaster in London, in which thousands died during a week of intense pollution and more succumbed prematurely years after the exposure. Less well known is that this palpable "filthy air" helped create and perpetuate the famous London fogs, which diminished in frequency and degree as the eventual cleanup progressed. Also in 1952, the International Council of Scientific Unions proposed the International Geophysical Year (1957-1958), which would see an unprecedented scientific effort to explore all areas of the globe, including the more pristine, or "fair", reaches of the atmosphere. For the larger remaining part of the century, the growing field of global atmospheric science would generally distance itself from the more specialized concerns of urban air pollution (Bachmann, 2003).

From the 1950s through the early 1970s, air pollution was commonly understood to be largely a localized urban phenomenon, and early measures to address it in Europe and the United States focused on relatively small urban "airsheds". This common understanding, along with societal demands for cleaner air and more convenient heating sources, produced remarkable success that was accelerated in many countries with the passage of air quality legislation in the 1960s and 70s. Progress from local control programs has continued and today the air in formerly polluted world cities is markedly cleaner. It may be a stretch to say that "foul is fair", but if you look at old photos of these cities, the difference is clear (Bachmann, 2003).

Meanwhile, air pollution scientists began to notice more disturbing trends in rural locations. Surprisingly, the air in many of these areas was becoming polluted. In the 1970s, both Europe and the United States recognized the emergence of regional-scale air pollution issues, including acid rain, regional haze, fine particles, and ozone smog. These were the result of increased regional emissions and long-range transport of air pollution. The next two decades brought more evidence that such regional-scale air pollution was contributing to significant effects on public health and welfare. "Fair" was becoming "foul" (Bachmann, 2003).

It was not until the 1990 Clean Air Act (CAA) Amendments in the United States, that U.S. policymakers took serious steps to address the growing scientific evidence on the regional component of air pollution. This evidence prompted a "rethinking" of conventional wisdom, particularly those concerning ozone and acid rain. The realization that natural sources contributed significant amounts of volatile organic compounds on a regional scale meant that the focus of regional ozone control needed to be weighed up heavily against man-made sources of nitrogen oxides, and not against non-methane hydrocarbons. Obviously, the scale addressed by air pollution science and policy has continued to grow during the 50 years since the London disaster. More recently, continuing scientific developments and insights have progressed to a point where the scientific and policy communities that have focused on conventional air pollution, and those studying global phenomena, can no longer afford to ignore one another.

Atmospheric pollution consists of a variety of contaminants emitted into the atmosphere by biogenic and anthropogenic processes, which adversely affect human health and ecosystems. This phenomenon is further complicated because the contaminants can be transformed by chemical reactions into more toxic and harmful chemical compounds, during their transport and diffusion in the atmosphere (Fourie, 2000).

In all cases of pollution there is a particular source of pollutants, in addition to the pollutants themselves, as well as the transport medium (air, water or direct dumping onto land), the target (or receptor) which includes ecosystems, individual organisms (e.g. humans), and structures. Pollution can be classified in several ways according to the source (e.g. agricultural pollution), the media affected (e.g. air pollution or water pollution) or by the nature of the pollutant (e.g. heavy metal pollution) (Alloway and Ayres, 1997).

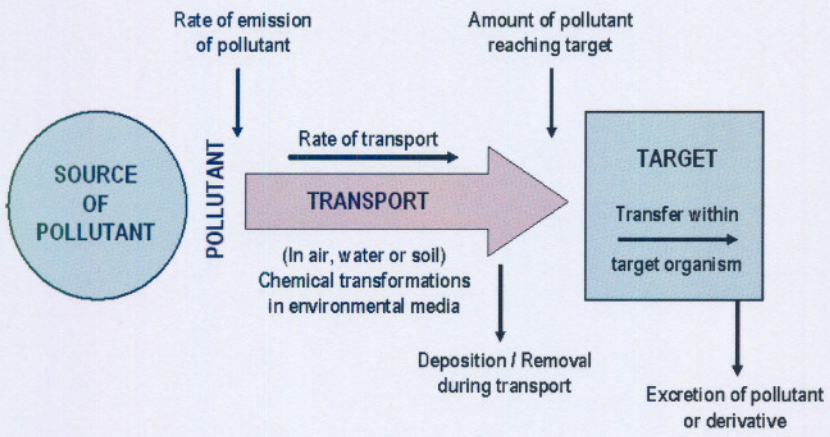

Figure 1.1: A simplified model of environmental pollution (Alloway and Ayres, 1997)

Understanding the relationship between primary pollutant emissions and air quality, represented by ambient concentrations of the atmospheric pollutants, is essential to developing emission control strategies. The better this understanding, the more effective the strategies, and the greater the opportunity for minimizing control costs while maintaining an acceptably low risk of exceeding ambient air quality standards.

The growing interest in the long-range air pollution transport phenomena, and global effects of air pollution, highlights the fact that air pollution under the relevant meteorological conditions is not a localized problem. It has been shown that large emissions of "primary" pollutants, such as sulphur dioxide (SO_2), undergo chemical transformations in the atmosphere. These transformations generate new chemical species known as "secondary" pollutants, such as sulphates (SO_4^{2-}), hundreds or thousands kilometres downwind. These secondary species are responsible for new adverse effects, such as acidic deposition (or, as commonly and improperly called in the media, acid rain). The long-range transport of air pollutants is becoming a highly debated topic, with increased public awareness and political consequences.

Understanding long-range air pollution is a challenge. Experimental data shows that background air quality in various regions is affected by the long-range transport of pollutants. This is considered to be a major reason for the observed increase of acidic deposition over Scandinavia during the last decades.

Nature has given a comprehensive example of this phenomenon. The smoke cloud from a large forest fire in Alberta, Canada, that had burned from the 17th to the 24th of September 1950 was observed on the 25th of September over the East coast of the USA (Munn and Bolin, 1971). On the 26th of September it was seen over the British islands, and on the 28th of September over Europe: from Scandinavia to Gibraltar. The progressive change of the cloud's thickness was 2.5 - 4.5 km over USA, 5 - 6 km over the Atlantic Ocean, 9 - 10 km over England and more than 11 km over Europe. Similar pictures have been observed during volcanic eruptions, nuclear explosions, dust storms, and other phenomena.

These examples indicate that long-range transport of air pollutants caused by general atmospheric circulation is essentially a three-dimensional process. Its modelling is hampered by inadequate knowledge of the atmosphere diffusivity in the cross-flow direction, the strength of pollutant sources, pollutant transformations, as well as the influence of planetary boundary layer (PBL) dynamics, and vertical motions at distances exceeding 1000km.

The modelling of such processes has shown a continuous and remarkable growth in the last three decades (Batterman, 1997). There is a definite need to develop appropriate air pollutant transport and diffusion models capable of giving accurate quantitative estimates of the pollution from different type of sources (industries, mobile sources, domestic households, accidental releases) at various time-space scales. It is generally accepted that air pollution models are important tools, not only for assessing emission reduction strategies, but also for establishing the maximum permissible concentration exposures, and for investigating economical aspects of air pollution (Zannetti, 1990). Moreover, there is a trend towards the increased role of air pollution models in decision-making processes (Batterman, 1997).

Pollution is a global phenomenon, and elimination of risks to humans (health and ecosystems functioning) is a task of paramount importance.

This study is aimed at extending the existing knowledge of air pollution, with special emphasis on atmospheric chemistry and mathematical model development that can be used to predict the future impact of air pollutants under southern African conditions. The results will provide useful information for possible future implementation of emission regulations, control strategies and policy decisions.

1.2 OBJECTIVES AND ENVISAGED OUTPUT

The focus of this study was the developing a fit-for-purpose long-range atmospheric transport and diffusion model applicable to meso- and macro scale problems at any time interval. The year 2000 was chosen as a reference year for all input parameters utilized in the model, in order to assist in testing and evaluation of the developed model. This was linked to a field campaign, called the Southern African Fire-Atmosphere Research Initiative (SAFARI), that was undertaken during 2000 to improve our understanding of trace gas emissions over the southern African subcontinent. The SAFARI 2000 multidiciplinary research plan included the development of a long-range transport model, which allows integration of knowledge and data from the various field experiments. Therefore, the period for which the model should produce reliable results is predetermined to be 2000. The objectives of the study included the development of:

1. Air quality model suitable for modelling the long-range transport and transformation of air pollutants over the southern African region;
2. Atmospheric boundary layer dynamics module for use in the model (Syrakov *et. al.*, 1983);
3. Methodology for calculating event and averaged (monthly, seasonal and annual) atmospheric concentration and deposition fields;
4. Methodology for calculating emitter-receiver matrixes to be used for the transboundary air pollution problems in the southern African countries.

The model includes a chemical transformation module that consists of:

1. Inorganic mechanism for the oxidation of the primary atmospheric pollutants, i.e. sulphur and nitrogen components;
2. Modules for the modelling of sulphur and nitrogen deposition (wet and dry) processes;
3. Module for the calculation of the pH value of wet deposition.

The model results may further contribute to facilitate sound-decision making during air pollution abatement policies, to predict the future impacts of air pollutants under southern African conditions and to assess the appropriate environmental legislation.

Results from this study have been presented at two international air quality modelling conferences during 2004 and 2005 respectively. It is expected that results from the developed model will be published in accredited journals to extend the existing knowledge of air pollution and the transformation during atmospheric processes.

Chapter 2

LITERATURE SURVEY

In this Chapter...

An overview of the relevant literature is detailed. An introduction to air pollution and the atmospheric cycle (Section 2.1) is provided. Sections 2.2 to 2.5 focuses on the environmental aspects and implications of the individual sections of the atmospheric cycle. Section 2.6 focuses on the mathematical modelling of atmospheric processes. Section 2.7 concludes the chapter by highlighting the importance of air pollution modelling in a complete air quality management system.

2.1 INTRODUCTION

Ambient air composition over the earth has undergone several changes throughout history, and early living species have either disappeared as a consequence of these changes, or adapted. Anthropogenic activities, especially since the 14^{th} century, when coal began to replace wood as the primary source of energy, have provided a clear disturbance of the earth's environmental balance. In the atmosphere, these anthropogenic pollutants have often generated locally unhealthy air quality and, sometimes, lethal air pollution concentrations, as during the well-known London episode of December 1952. In addition to short-term effects, atmospheric pollutants are known to generate long-term adverse effects which are, however, difficult to forecast (Zannetti, 1990).

The emergence of petroleum products and the internal combustion engine in the last century gave impetus to the second industrial revolution, and at the same time brought with it new air pollution challenges. In 1945, it was recognized that petroleum products are responsible for a new type of "smog", a photochemical summertime smog, first discovered in the Los Angeles area. Photochemical smog is quite different from the traditional wintertime sulphur smog (the "London" smog) typically generated by the combustion of sulphur-containing fuels, such as coal.

The last decade has been characterized by a growing interest in long-range air pollution transport phenomena and global effects. First in northern Europe and then later in eastern North America, it has been shown that large emissions of "primary" pollutants, such as sulphur dioxide (SO_2), undergo chemical transformations in the atmosphere. These transformations generate new chemical species known as "secondary" pollutants, such as sulphates (SO_4^{2-}), hundreds or thousands of kilometres downwind. These secondary species are re-

sponsible for new adverse effects, such as acidic deposition (or, as commonly and improperly termed in the media, acid rain) (Zannetti, 1990).

Two "global" issues have recently become a major concern: (1) the "green-house" effect, which is believed to be causing an increase of the earth's average temperature as a consequence of increasing concentrations of green house gases, notably carbon dioxide (CO_2), a species that has never been considered a "pollutant" and whose huge emissions have never been controlled; and (2) the possible depletion of the stratospheric ozone layer, a natural protective "blanket" from harmful solar radiation, by certain species emitted by anthropogenic activities (Zannetti, 1990).

It has often been pointed out that government pollution control actions have seldom (or perhaps never) anticipated adverse effects and that only large-scale disasters or environmental deterioration have provided stimuli for effective action and preventative measures. In recent years public awareness with regard to environmental issues has increased, particularly in developed societies. Public opinion has been largely responsible for mounting pressure on Government and industry for major preventative control actions, and for implementation of emergency/accident contingency plans (Zannetti, 1990).

2.1.1 What is an air pollutant?

Which substances must be considered air pollutants? Or better, which substances, emitted into the atmosphere, can be considered safe, non-polluting compounds? The answer is certainly not a straightforward one, since the term "air pollution" may have many definitions.

Williamson (1973) gave a satisfactory clarification of this problem by elaborating the difference between a "pollutant" and a "contaminant". A contaminant was defined as "anything added to the environment that causes a deviation from the geochemical mean composition". On the other hand, a pollutant, to be considered as such, must be a contaminant responsible for causing some adverse effect on the environment.

According to Alloway and Ayres (1997), a widely used definition of pollution is "the introduction by man into the environment of substances or energy liable to cause hazards to human health, harm to living resources and ecological systems, damage to structures or amenity, or interference with legitimate uses of the environment".

However, the same approach to define air pollution, making a clear distinction between contamination and pollution as Williamson does, is also used by Alloway. Contamination is used for situations where a substance is present in the environment, but does not cause any obvious harm, while pollution is reserved for cases where harmful effects are apparent (Alloway and Ayres, 1997).

Clearly, this distinction between pollutants and contaminants is based on our limited understanding of short-term and long-term adverse effects of each chemical compound. Moreover, this evaluation is complicated by chemical reactions that can transform a contaminant into a pollutant. We can therefore say that any contaminant is a potential pollutant and that in many cases, the two words are synonymous.

An example of the above difference is given by CO_2 gas that is abundantly emitted into the atmosphere from anthropogenic combustion processes. CO_2 does not have significant immediate adverse effects to living organisms, and was therefore considered only as a contaminant. Measurements have shown however, that ambient CO_2 concentrations throughout the world are constantly increasing, thus revealing an accumulation in the atmosphere of a considerable fraction of the CO_2 emitted by anthropogenic activities. Since further CO_2 concentration

increases as expected to induce an increase in the average temperature of the earth, CO_2 should be considered, in this respect, as a pollutant.

According to Zannetti (1990) air pollutants are found in the form of:

- gases, e.g. sulphur dioxide (SO_2);
- particulate matter, e.g. fine dust.

These air pollutants are injected into the atmosphere from:

- natural sources (biogenic sources), e.g. volcanoes, ocean spray, pollen, volatile organic compounds (VOC's);
- anthropogenic sources, e.g. industrial, commercial, agricultural, transportation activities.

These "primary" pollutants (i.e. those directly emitted from the source) undergo chemical reactions (often between less harmful precursors within the environment) that result in the subsequent formation of other species, i.e., "secondary" pollutants, in the form of:

- gases, e.g. ozone (O_3);
- aerosols/particulate matter, e.g. sulphates (SO_4^{2-}).

One of the most important factors characterizing the atmospheric particulate matter is the size (e.g. the diameter) of the particles. Particles are called:

- coarse particles, when their diameter is larger than 2.5 μm;
- fine particles (or respirable particulate matter, RPM), when their diameter is less than 2.5 μm; fine particles can also be divided into two modes: the nuclei mode, with a diameter below 0.1 μm, and the accumulation mode, with a diameter greater than 0.1 μm;
- inhalable particles (or inhalable particulate matter, IPM), when their diameter is less than 10 μm.

Coarse particles are generally less important, since their large mass causes fast gravitational removal from the ambient air, and are less harmful to the human species, because they are easily removed by the upper respiratory system. Fine particles are more important because of their visibility and adverse effects on human health.

Particles in the atmosphere can also be classified, independently from their size, as:

- viable particles (e.g. pollen, fungi, bacteria);
- nonviable particles (e.g. inert materials).

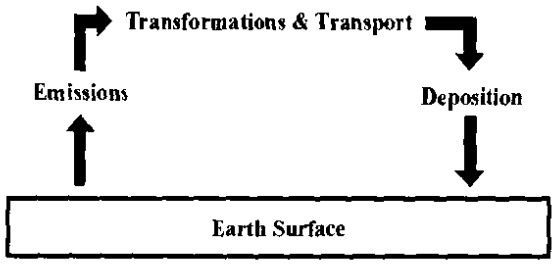

Figure 2.1: Schematic presentation of the atmospheric cycle and its component processes

Atmospheric constituents follow a series of steps or processes from the time of their introduction into the atmosphere until their eventual removal from it. This atmospheric pathway is but one portion of the overall biogeochemical cycle that links the origins and fates of all environmental chemical species. The main processes that comprise the atmospheric pathway are emissions, transformation, transport and deposition (Figure 2.1). Understanding the atmospheric pathways of important species and quantifying the flux of material along these pathways is fundamental to the study of air pollution (Fourie, 2002).

The transport section of the complete atmospheric pathway (Figure 2.1) consists of those processes that mix atmospheric species emitted/released from the earth into the troposphere, and occasionally even the stratosphere. The transport section therefore carries material from where it is introduced into the atmosphere (emissions) to where it is eventually deposited on the earth's surface. The initial mixing of emitted pollutants, vertical-exchange processes, clouds, and advection are important aspects of this part of the atmospheric cycle. The importance of these various physical processes that influence transport depends on the spatial scale of the transport process.

The influence of a chemical species emitted into the atmosphere on the receiving environment depends on both the atmospheric residence time of the species and the prevailing meteorological conditions. Chemical species may reside in the atmosphere for times ranging from a second to as long as several centuries. In the context of acid deposition, the important contributors, that is, gaseous sulphur dioxide, nitric oxide, and ammonia, tend to have relatively short residence times in the order of days, and thus meteorology is crucial in their distribution over tens to thousands of kilometres. Oxidation products, such as particulate sulphate and nitrate or sulphuric acid and nitric acid, have longer residence times of a few days up to weeks. The range of influence of a species with a short residence time depends on wind speed and atmospheric stability near the source. A species with a longer residence time can be distributed over hundreds and thousands of kilometres by large-scale meteorology. Atmospheric constituents are finally removed from the atmospheric cycle by various deposition processes returning to the earth's surface (Fourie, 2002).

As previously mentioned, understanding these atmospheric pathways of important species and quantifying the flux of material along these pathways is fundamental to the study of air pollution and atmospheric science.

Air pollution modelling is an attempt to describe the interrelation between emissions, atmospheric concentrations, and deposition (the abovementioned atmospheric cycle). Air pollution measurements give quantitative information about concentrations and deposition, but they can only give the levels at specific locations. In principle, air pollution modelling can

give a more complete and consistent description, including an analysis of the causes- emission sources, meteorological processes, physical and chemical transformations- that have led to these concentrations/deposition (Fourie, 2002).

Air pollution models play an important role in science, because of its capability to assess the importance of the relevant processes. Air pollution models are the only method that quantifies the relationship between emissions and the concentrations/depositions, including the consequences of future scenarios and determination of the effectiveness of abatement strategies. Numerical modelling will be discussed in Section 2.6 of this Chapter.

A detailed description of the environmental aspects of the individual sections of the atmospheric cycle will be discussed in the following sections, with emphasis on the implications of these sectors in context of the Southern African region.

2.1.2 Air quality legislation

Several countries in the world have established air pollution laws and regulations, and have implemented air quality and/or emission standards. The United States in particular, has developed a large and complex body of air quality laws directed towards the goals of progressive air quality improvement in those regions characterised by unhealthy pollutant levels, and environmental preservation in regions with clean air (e.g. national parks). Moreover, the US regulations have incorporated the use of several air quality dispersion models as official regulatory tools (e.g. to be used for the authorization of new emissions of air pollutants).

Air quality legislation (or the lack of it) has affected the development of air pollution modelling techniques in different countries. In the US, the air quality regulations, together with the existence of a free market typically oriented toward consulting business activities, have created the proper conditions for the development of "practical" techniques, sometimes very sophisticated ones, but still based on methods that rely upon available data and limited computational resources. In general, U.S. studies have benefited from public and private funding sources, and have focused on specific problems with a clear goal-orientated inclination.

European studies and research activities in this field have been carried out mainly by public organizations, i.e. universities and research centres. Research centres of private industries have also provided valuable contributions. European research, performed without the pressure of specific legislative goal orientated objectives, has covered with success interesting and advanced topics. These activities, however, have not yet culminated into a set of transferable computer packages like those in the Unites States.

With regard to long-range transport, national legislation is not sufficient and international rules and agreements need to be found. This seems to be a sensitive issue in the north-eastern North America, where Canada is blaming the United States for a large fraction of their acidic deposition, and in Europe, where many countries are blaming each other for the same issue. The Chernobyl accident has shown everyone that air pollution, unlike people, can freely emigrate from one country to another, and affect even countries like Italy, which many meteorologists believed well-protected by the Alpine mountain range.

In spite of progress toward economical and political unity in Europe over the last two decades, common environmental legislation on recommended numerical models are still lacking. The recent common trend of increasing the average height of industrial emissions (especially power plants) is certainly improving the near-field air quality, but is expanding the effects of long-range transport and acidic deposition all over Europe.

The South African scenario is quite different. The Air Pollution and Prevention Act

(APPA), was promulgated in 1965 in South Africa. APPA, No.45 of 1965 (as amended) is primarily based on the permitting of scheduled processes emitting to the atmosphere, and does not include any ambient air quality standards (guidelines for criteria pollutants are included), or regulation on the long-range transport of air pollutants. Another major shortcoming in APPA is that the act makes no provision for any vehicular emission standards.

Based on these shortcomings, new air quality legislation for South Africa was promulgated during September 2005 in South Africa. The National Environmental Management: Air Quality Act, 2004 (Act No. 39 of 2004) is a total paradigm shift from permitting scheduled processes (although still included in the new act) to ambient air quality standards. Specific ambient concentration standards were set down by the Department of Environmental Affairs and Tourism (DEAT)for specific pollutants, and the latter should not be exceeded. Specific ambient air quality monitoring would thus be an integral part of compliance to the new act.

Moreover, Chapter 6 of the National Environmental Management: Air Quality Act, 2004 in South Africa deals specifically with the issue of International Air Quality Management and transboundary air pollution.

Air pollution modelling will thus be a fundamental tool in assessing the impact and contribution of specific emissions to the ambient air quality. It is foreseen that regulations will incorporate the use of several air quality dispersion models as official regulatory tools.

2.2 EMISSIONS AND SOURCES OF POLLUTION

Africa is largely an underdeveloped continent with concentrations of intensive industrial activity occurring in isolated regions. In general the main sources emitting gases and aerosols into the atmosphere include aeolian crustal material consisting of mineral soil dust, marine aerosols from the two adjacent oceans, biomass burning particles and gases occurring mainly north of 20 $^{\circ}$ S, aerosols from industrial emissions and finally emissions from the biosphere (Piketh and Walton, 2004).

The first part of the atmospheric cycle encompasses emissions from the earth's surface. Surface in this context can also be defined as releases/emissions elevated by hundreds of meters above the earth's surface. These emissions can roughly be divided into two main categories: biogenic (natural) or, anthropogenic (man made/industrial) emissions.

Anthropogenic and biogenic emissions are of interest to scientists as well as policy makers. Central and Southern Africa has undergone and continues to undergo large social, economic and political changes that contribute to large-scale modifications of land use and land cover. Anthropogenic influences, along with a strong source of biogenic emissions and a large natural variability in both regional climate and ecosystem processes, combine to effect changes in the biogeochemical cycling of the region and lead to increased pollution. The mounting burden of air pollution and the deposition of pollutants has serious implications for human health, ecosystem functioning and corrosion of materials.

The most significant anthropogenic trace gas emitted into the atmosphere over Southern Africa is sulphur dioxide (SO_2). Particulate sulphate (SO_4^{2-}) is also emitted. Sulphur emissions are concentrated in two major source regions, the Mpumalanga Highveld of South Africa and the Zambian copperbelt. In addition, there are several large isolated point sources. Siversten *et. al.* (1995) have compiled a comprehensive inventory for sulphur emissions, covering southern Africa south of 17 $^{\circ}$ S. According to Siversten *et. al.* (1995), of the total of 1.1 million tons of suplhur emitted into the regional atmosphere annually (excluding Zambia),

66% originates in South Africa and of this about 90% comes from the Mpumalanga Highveld. This is the region of the country where most of the major coal-fired power plants are situated. More than 90% of South Africa's electricity is generated from the combustion of coal, which contains approximately 1.2% sulphur and up to 45% ash (eia.dov.gov, 2004). Power production in South Africa accounts for 55% of the total emissions for sulphur in southern Africa. The Zambian copperbelt is also an important emitter of SO_2. Currently it is thought that the SO_2 emissions from these anthropogenic sources are up to 2.24 million tons per annum. Globally approximately 74 million tons of SO_2 are emitted into the atmosphere per annum (Piketh and Walton, 2004).

Large-scale air pollution has traditionally been associated with anthropogenic activities in industrialized parts of the world, primarily in the northern hemisphere. However, recent satellite measurements of tropospheric ozone (O_3) have shown that, in addition to district plumes emanating from North America, Asia and Europe, large quantities of O_3 emanates from tropical Africa. This source is reported as being most prominent during September (later during a dry season). Since the industrial inputs to the atmosphere from this region were believed to be small, it was thought that the ozone was formed by gaseous precursors derived from biomass burning (Otter *et. al.*, 2001). Biomass burning, both natural and anthropogenic, has been identified as a significant source of radiatively and chemically active atmospheric gases and pariticulates. Savanna fires are the single largest source of biomass burning emissions worldwide, and account for about 75% of all fire related emissions (Andreae *et. al.*, 1996) (Lacaux *et. al.*, 1993). Savanna fires account for about 57% of the total biomass burnt on the African continent (Piketh *et. al.*, 1996). Biomass burning is a seasonal source with the highest intensity between June and October. In the non-burning season (November to May) few fires are detected south of 20 ° S (central Zimbabwe). During the southern African burning months (June to October), large numbers of fires are detected north of 20 ° S with the highest intensity being in September (Scholes *et. al*, 1996). Biomass emissions include CO_2, CH_4, CO, O_3, NO_x (NO + NO_2), non-methane hydrocarbons (NMHC's) and particulate matter.

A field campaign, called the Southern African Fire-Atmosphere Research Initiative (SAFARI), was undertaken in 1992 and 2000 to improve our understanding of trace gas emissions on the subcontinent, particularly from biomass burning. This project showed that although bush fires are a large source of aerosols and trace gases (which can contribute to the high ozone levels), they were not the only source (Otter *et. al.*, 2001).

Another source of trace gases and aerosols is the burning of wood for energy. Although bush fires have been investigated, research on the use of domestic fuels is minimal. A single household fire might be small, but collectively they provide a continuous supply of by-products into the atmosphere throughout the year. Although fossil fuels, hydropower and nuclear power supply most of our direct energy needs, the majority of the developing world's population relies principally on fuelwood, animal dung and crop residues for domestic heating. These traditional fuels are used mainly for cooking and space heating. These emissions are difficult to distinguish from biomass burning and are less seasonal. In view of its widespread occurrence, particularly in the developing world, there is growing concern about the impact that biofuel burning might have on the environment. Marufu *et. al.* (2000) have estimated that these emissions account for at least as much as biomass burning and industrial emissions. Ludwig *et. al.* (2003) reported that the source strength of biomass domestic burning is in the order of 1500 Tg CO_2-C yr^{-1}, 140 Tg CO-C yr^{-1}, and 2.5 Tg NO-N yr^{-1}. These magnitudes represent contributions of about 7 to 20% to the global budget of these gases.

Besides emissions from burning, there are also biogenic sources of hydrocarbons, CO, CO_2, NO, N_2O and aerosols. Microbial activity in the soil is the main biological source of NO; soil emissions of NO are equal to or greater than those from lightning, and much larger than any other biological source. The global NO budget was estimated by Logan (1983) to be between 25 and 99 Tg NO-N yr^{-1} with the microbial activity in soil contributing in the range of 4 - 20.2 Tg N yr^{-1} (Davidson, 1991) (Potter *et. al.*, 1996). These figures, as well as flux rates reported in more recent studies (0.1-13.3 ng NO-N $m^2.s^{-1}$) (Serca *et. al.*, 1994, Serca *et. al.* 1998), indicate that the biogenic component is comparable to the global NO_x emissions from fossil-fuel combustion (Levine *et. al.*, 1997) (Scholes and Andreae, 2000). Non-methane hydrocarbons are emitted from vegetation, which is estimated to be the source of 90% of the global NMHC budget, with tropical savannas producing an estimated 46.4 Tg yr^{-1} as isoprene, 15.6 Tg C yr^{-1} as monoterpenes and 12% as other reactive volatile organic compounds (Guenther *et. al.*, 1995). The total global emission rate of biogenic volatile organic carbons is 1150 Tg C yr^{-1}, which is more than 10 times that of the estimated annual global anthropogenic emission rate of 100 Tg C yr^{-1} (Hough and Johnson, 1991; Muller, 1992). Biogenic emissions of CH_4 contribute approximately 37% (25% from natural wetlands, 12% from rice paddies) to the global CH_4 budget (Conrad, 1997). Other sources of CH_4 included termites, oceans, landfills, sewage, manure and ruminants (Otter *et. al.*, 2001). Furthermore, savannas and grasslands are considered to be CH_4 sinks, but the few measured fluxes in such regions differ by more than an order of magnitude because CH_4 is emitted as well as consumed. The flux of CH_4 (emission and consumption) in tropical savannas and grasslands needs to be more accurately estimated because, owing to the large area covered, these ecosystems could significantly affect the global CH_4 budget (Otter, *et. al.*, 2001).

An atmospheric pollutant often neglected is wind-blown dust. Emissions of crustal aeolian dust material, often termed aeolian or mineral dust, is caused primarily by the surface winds acting on dry soils where vegetation cover is or has become sparse. The term mineral dust refers to a large range of species that are highly variable in their chemical composition, and include such diverse compounds as quartz, clay, calcite, gypsum, haematite and others (Piketh and Walton, 2004).

2.3 TRANSPORT OF POLLUTANTS

The transport section of the atmospheric pathway consists of those processes that mix material through the troposphere or occasionally even into the stratosphere, and that carry material from where it is emitted/released into the atmosphere, to where it is eventually deposited on the earth's surface.

Southern Africa is situated geographically beneath the planetary-scale, Southern hemisphere descending limb of the Hadley circulation throughout much of the year (Piketh and Walton, 2004). The general circulation of the atmosphere over Southern Africa determines the transport of aerosols and trace gases over the region. Four major synoptic circulation types are responsible for most of the atmospheric transport of aerosols and gaseous pollutants over southern Africa: the semi-permanent subtropical continental anticyclones, transient mid-latitude ridging anticyclones, westerly baroclinic turbances and barotropic quasi-stationary tropical easterly disturbances (Schulze, 1965; Tyson, *et. al.*, 1996; Preston-Whyte and Tyson, 1977). The frequency of occurrence of each of these circulation patterns varies seasonally. The most frequent synoptic-scale circulation type over southern Africa is the continental anticy-

clonic circulation which occurs up to 70% of the time during winter and 20% of the time in summer (Tyson,*et. al.*, 1996). Anticyclonic circulation and westerly disturbances result in air transport from Africa to the southeast over the Indian Ocean in the Natal plume. This anticyclonic flow results in considerable recirculation, which may either be confined to the continent or extend over and return from the Indian Ocean. Easterly wave conditions favour transport to the west over the tropical Atlantic Ocean in the Angolan plume. Transient mid-latitude ridging anticyclones result in maximum transport originating in the mid-latitudes and flowing towards the southern Atlantic Ocean (Piketh and Walton, 2004). The general flow over southern Africa is summarized in Figure 2.2.

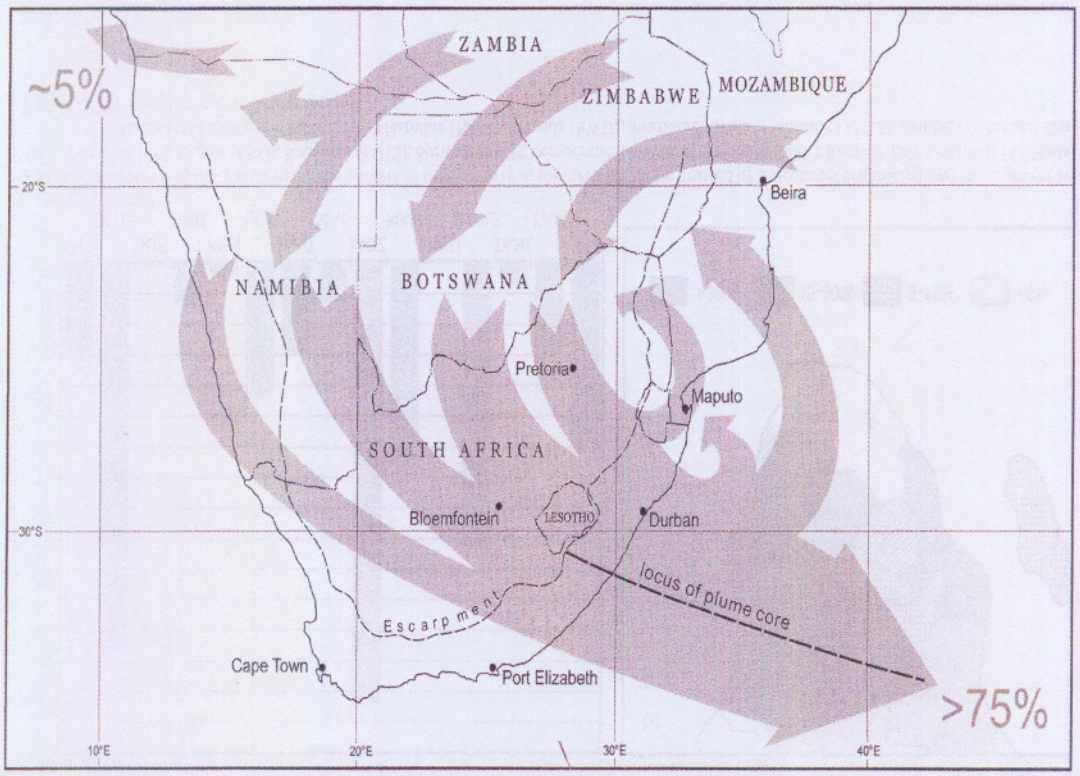

Figure 2.2: Average transport or air over southern Africa. The flow patterns have been summarized from all transport trajectory climatologies undertaken for this part of the continent (Piketh and Walton, 2004)

The northward and southward displacement of the Indian Ocean high pressure cell results in a significant seasonal variation of the boundary layer winds over the Highveld region. During winter (June to August), air flow into the lower boundary layer over the Mpumalanga Highveld, characterized by the 800 hPa wind circulation (about 350 m above ground level), is dominated by the Indian Ocean anticyclone, which extends inland over the northern region of the subcontinent, resulting in dominant westerly and west-north-westerly winds over Gauteng and the industrial region of Mpumalanga (Held, *et. al.*, 1996), as shown in Figure 2.3. However, during summer (December to February), due to the southward migration of the high pressure belt, the circulation is characterised by a weak northerly-component air flow over

the region. These winds then veer progressively towards north-north-east with the approach of February and thereafter tend to back to westerly at the onset of autumn (March to May), due to the gradual northward migration of the pressure belts (Held, *et. al.*, 1996; Tosen and Jury, 1986).

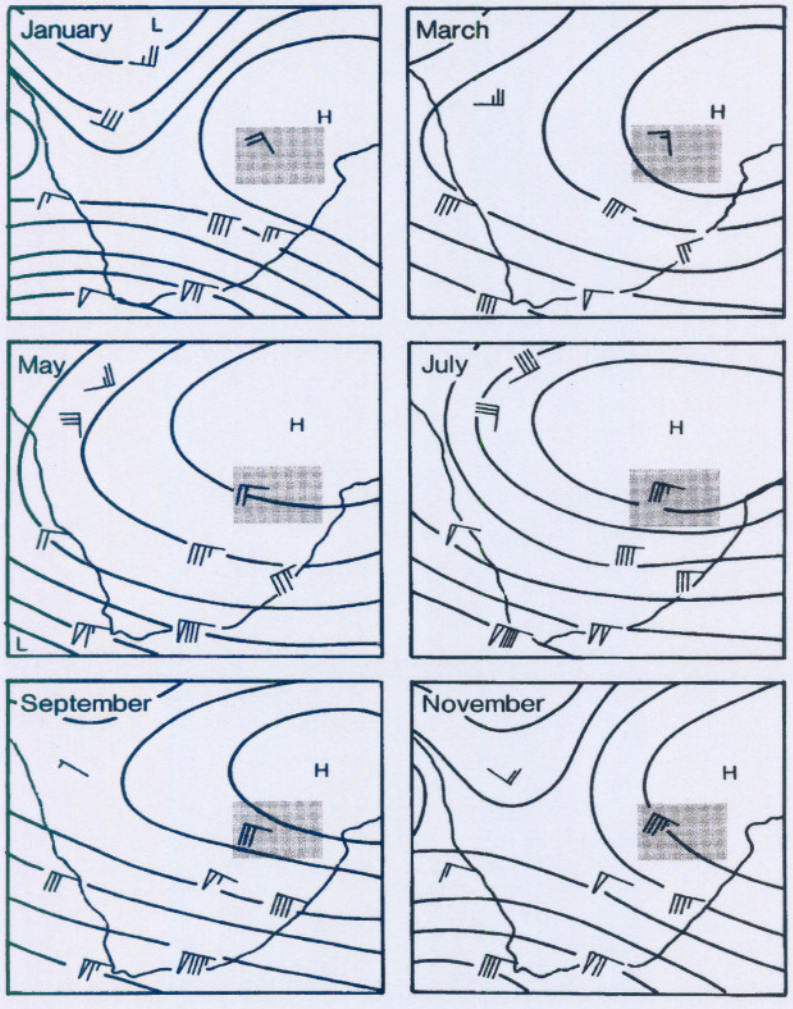

Figure 2.3: Mean monthly circulation at 800 hPa over Southern Africa for the period 1969-1977 (after Tosen and Jury, 1988). The grey-shaded rectangle indicates the industrial Highveld region

Following up on the above observations, a five-year backward- and forward trajectory climatology of air transports from the industrial Highveld region of South Africa was compiled (Piketh and Prangley, 1998). Five major transport pathways of air moving from the highveld were identified (Indian Ocean Plume: 48%, Recirculation: 32%, Southern African Plume: 12%, Central African Plume: 6% and Cape Plume: 1%). The percentages refer to the frequency of occurrence of the various pathways for an initiation level of the trajectories at 750 hPa (about 1000 m above ground level). Figures 2.4a to 2.4e illustrates these transport pathways schematically. It highlights that polluted air does not simply move out over the Indian

Ocean, but up to 50% of the time either circulates over South Africa or flows northwards over Africa, possibly affecting neighbouring countries in various degrees. In terms of seasonal variation it was found that the Indian Ocean Plume is very dominant during the austral winter and autumn, while during summer and spring its frequency is of the same magnitude as that of Recirculation (Piketh and Prangley, 1998), which is in accordance with the mean monthly circulations discussed above.

The southern African plume was identified as air parcels moving in a northerly direction but remaining below 10 ° S. The Central African plume, on the other hand, included all trajectories that moved above 10 ° S. A trajectory was classified as having recirculated once, if it left and returned to southern Africa. According to this study, the Indian Ocean plume consists of all the trajectories that moved quickly in the westerly winds. They may have started to move eastward initially but began to move westward, before leaving South Africa, and continued to do so. The Cape plume consisted of those trajectories whose paths moved south for as long as they were tracked. Those moving south-eastward were placed into the Indian Ocean plume. Each category is shown individually in Figure 2.4a to 2.4e.

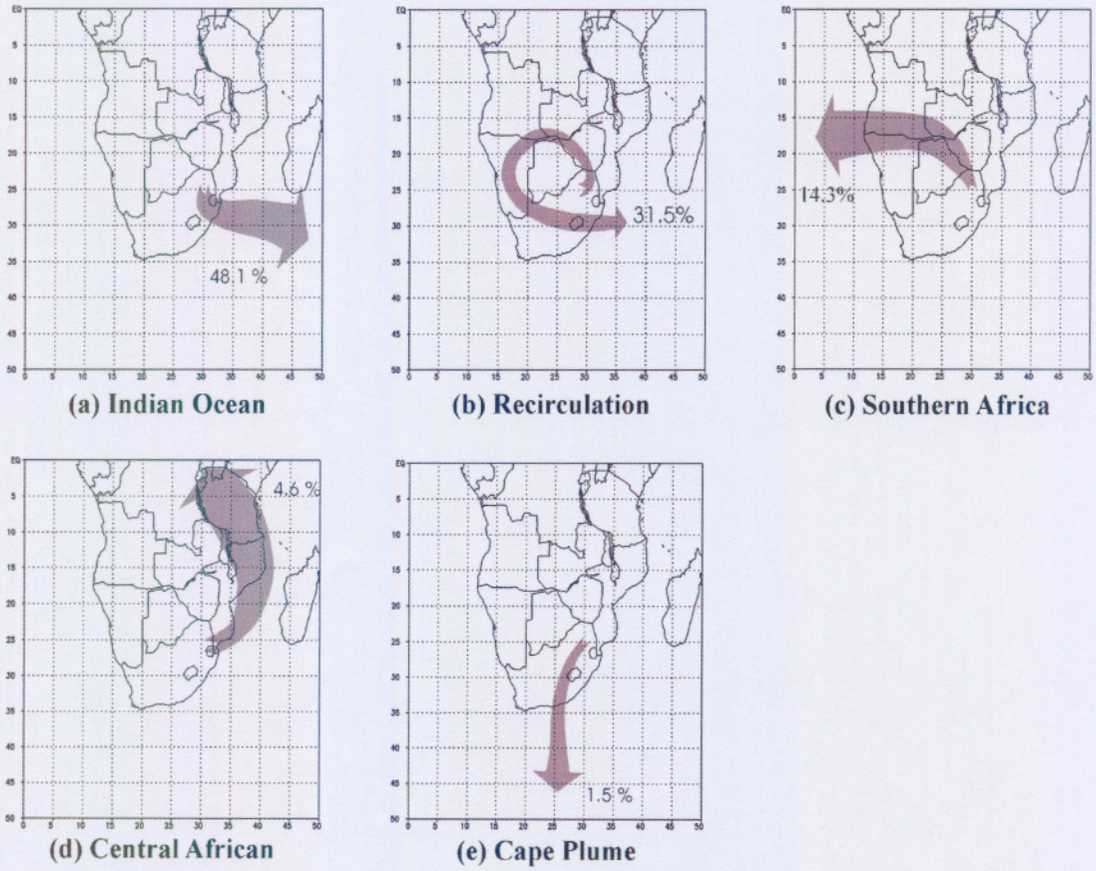

(a) Indian Ocean (b) Recirculation (c) Southern Africa

(d) Central African (e) Cape Plume

Figure 2.4: Five transport pathways from the industrialized Highveld region. Percentages represent the annual persentage of flow from the five-year period (Piketh and Prangley, 1998)

Indian Ocean plume: Almost 50% of air parcels moved directly off the subcontinent

over the Indian ocean (Figure 2.4a). This confirms the direct advection of material off the highveld over the Indian ocean as proposed by Tyson *et. al.*, (1988).

Recirculation: Recirculation over South Africa occurs 32% of the time from within the Highveld (Figure 2.4b). An air parcel was considered to be recirculating if it showed any tendency to turn back on its initial pathway over southern Africa. The different recirculation patterns occurred at a range of scales as they were described in detail by Garstang *et. al.*, (1996). The vast majority of the recirculating air parcels exited the subcontinent on the east coast of South Africa (Piketh, *et. al.*, 1998).

Southern African Plume: Slightly more than 14% of flow was transported northward but remains below 10 degrees south (Figure 2.4c). This included all flows that remained over southern Africa which, in the main, were ultimately transported towards the west or the Atlantic Ocean. This flow included that which was described by Garstang *et. al.*, (1996) to be transported over the Atlantic ocean and which was termed easterly transport. On average, in view of the southern African climatology this type of flow occurred for 24% of the time from the surface to 800 hPa and for 13% of the time from 700 to 500 hPa for all synoptic circulation types (Tyson *et. al.*, 1996). The flow typically took between seven and ten days to reach the west coast of southern Africa.

Central African Plume: Although the schematic in Figure 2.4d shows flow mainly to the eastern equatorial Africa, the flow also reached the western parts of central Africa. Only 4.5% of the trajectories travelled into central Africa above 10 ° S. Although as a percentage of the total flow from the highveld this is a relatively low frequency of occurrence, it does extend the possible impacts of highveld-generated pollutants over a significantly larger area than any of the other flows.

Cape Plume: The least frequent of the transport pathways from the Highveld was the Cape plume (Figure 2.4e). This occurred for only 1.5 % of the time. The transport towards the south off the subcontinent was rapid and rarely exceeded three days. The plumes typically exited the subcontinent at approximately 25 ° E at a height of about 3000 m (700 hPa). The transport along this pathway was therefore consistently below the level of the 700 hPa absolutely stable layer.

A fairly diverse climate prevails over the geographic regions of southern Africa. Most commonly the prominent mountain ranges constitute the main climatic divides. Any generalizations made to cover the entire region would not encompass all the features present in each region. Schulze (1974) points out that there is no truth in the myth that South Africa is drying up. Due to the climatic diversity, one geographic region of the country could experience an above-normal rainfall whilst a drought may prevail in another area. More than 75% of the rainfall received in the subcontinent is concentrated in the areas which lie to the east of the great escarpment while less that 15% of the rainfall occurs over the interior plateau.

In summer low air pressure conditions prevail over the interior of South Africa and conditions are generally unstable promoting dispersal and removal of pollutants whilst the southern and western parts experience dry, stable conditions which do not favour the dispersal and removal of pollutants. However, the regular passage of southbound, high speed winds ensure that no severe build-up of pollutants occurs in these regions. During the winter however, stable conditions with low wind speeds prevail over most parts of the country and the dispersion and removal of pollutants is not favoured. The wind in the upper atmosphere blows predominantly from a westerly direction and thus a large part of the pollutants are ultimately transported to the Indian Ocean.

Held *et. al.* (1996) state that the maximum heights of the mixing layer, i.e. the layer which

acts as a lid on the lower troposphere, vary between 1000 m and 2000 m above ground level at midday during winter, and could exceed 2500 m above ground level during summer. Since gaseous pollutants are generally trapped below this layer, their concentrations can vary even though significant amounts of pollutants may not have been emitted into or removed from the atmosphere. Hence caution must be exercised when interpreting pollutant concentrations. Inversion layers also restrict the vertical mixing of the atmosphere and this phenomenon also influences the concentrations of gaseous pollutants (Annegarn *et. al.*, 1996).

Since the sun's heat is absorbed and dissipated by the earth's surface, the temperature decreases with increasing altitude within the lowest 12 km of the atmosphere and the temperature of the environment drops at a lapse rate of 0.6 ° C per 100 m. When an air parcel from high altitude descends to a region of higher pressure under adiabatic conditions, it warms up at the dry adiabatic temperature lapse rate of around 1 ° C per 100 m. A substantial temperature change can take place if the air parcel descended a long distance and the resulting "Berg Winds" are often responsible for grassland fires in the Mpumalanga Lowveld.

Although surface wind speed is an indicator of the atmosphere's dilution potential, high wind speeds can also lead to stack down-drafting if inversions are present above the effective stack height. This causes a build-up of pollutants in the lower troposphere. Pollutants may be carried long distances from the emission source in relatively undiluted form if light winds and strong surface inversions prevail when stable conditions are present with no vertical motion.

During the SAFARI-92 (southern African Fire-Atmospheric Research Initiative) experiment, it was seen that aerosols could be transported as far as 24000 km from the African sources, reaching across the Indian and Pacific Oceans, as well as the Atlantic Ocean into the Amazon Basin, in just 10 days (Garstang *et. al.*, 1995). Held *et. al.* (1994) have observed mesoscale recirculation patterns in several geographic regions, leading to an accumulation of pollutants at a rate far higher than would have been emitted by local sources. It was also discovered that air being recirculated had undergone maritime modifications.

2.4 TRANSFORMATION OF POLLUTANTS

Early air pollution modelling studies dealt with the challenging problem of correctly simulating atmospheric diffusion and, in particular, the maximum ground-level impact of elevated emissions of primary pollutants, such as sulphur dioxide (SO_2). Two major factors, however, focused attention on atmospheric chemistry: 1) photochemical smog, a new, different smog associated with high-temperature "summertime" conditions, and first recognized in the Los Angeles basin in the 1940s; and 2) long-range transport phenomena, clearly identified in the 1970s, that lead to the study of multiday transport scenario's of industrial and urban plumes and, consequently, to the simulation of the formation of secondary gases and particles in the plume.

Atmospheric chemistry deals essentially with four major issues (Seigneur, 1987):

1. Photochemical smog in sunny, urban areas, such as Los Angeles and Mexico City;
2. Aerosol chemistry;
3. Acidic deposition by dry and wet deposition phenomena;
4. Air toxins.

An important factor that regulates the effect of a particular pollutant is its atmospheric lifetime. Clearly, a species that is present for only a few seconds in sufficient concentrations before it is either dispersed/diluted out to such an extent that it exists in negligible quantities, or undergoes complete decomposition, would not be expected to cause significant effects. The kinetics of chemical species is such that at higher altitudes, lower temperatures result in increased lifetimes of pollutants. Hence a more even global distribution is achieved if pollutants migrate vertically. Depending on the species and the minimum amount of it that needs to be present before a measurable effect is noticed, (threshold level) this phenomenon can be viewed as a dilution of a hazardous compound or the seepage of such a compound into other geographic regions.

Important atmospheric reactions, which need to be considered, occur in the gas phase (homogeneous) and in the aqueous and particulate phases (heterogeneous). In this section, the main chemical reactions for sulphur dioxide and nitrogen dioxide are described qualitatively.

2.4.1 Sulphur dioxide chemistry

Once emitted, SO_2 may be oxidized to sulphates, which may form sulphuric acid aerosols by reactions occurring in the gas phase, in the liquid phase, on solid surfaces or combinations of these three. SO_2 is quite readily dry-deposited, but is relatively insoluble in cloud water, as dissolved SO_2 comes to an equilibrium which depends on its Henry Law's constant, and thus the cloud water acidity (Campbell, 1997). However, photochemical conversion of the gas to soluble sulphate aerosol and chemical reactions within cloud droplets, result in wet deposition being an important process. The photochemical oxidation in the gas phase is driven by the $HO^{\cdot}$ radical. Calvert *et. al.* (1978) have demonstrated that oxidation of SO_2 by photo oxidation is not a predominant mechanism, but the major pathway is rather through the reaction of SO_2 with the $HO^{\cdot}$ radical. On a cloudless summer day, in a relatively clean tropospheric air mass, a 24-hour averaged SO_2 oxidation rate of 0.7% per hour has been estimated (Seinfeld and Pandis, 1998).

From a thermodynamic point of view, SO_2 has a strong tendency to react with oxygen in the air. However, the rate of the reaction is so slow under catalyst-free conditions in the gas phase, that it can be totally neglected as a source of SO_3 (Seinfeld and Pandis, 1998). If formed, SO_3 reacts rapidly with water vapor to form H_2SO_4, so that any processes, in which gaseous SO_3 is formed in a moist atmosphere, can be considered equivalent to the direct formation of H_2SO_4.

The oxidation of SO_2 to SO_3 in the atmosphere has been found to proceed mainly along the following pathway:

$$HO^{\cdot} + SO_2 \rightarrow HOSO_2^{\cdot} \tag{2.1}$$

$$HOSO_2^{\cdot} + O_2 \rightarrow HO_2^{\cdot} + SO_3 \tag{2.2}$$

$$SO_3 + H_2O \rightarrow H_2SO_4 \tag{2.3}$$

Sulphuric acid formed in Reaction 2.3 can be neutralized by NH_3 forming $(NH_4)_2SO_4$ or NH_4HSO_4. Rates of conversion generally seem to be higher during the day than at night, and in summer compared to winter (Seinfeld and Pandis, 1998). This is due to the fact that $HO^{\cdot}$ is higher in daytime and in summer. The presence of liquid water in aerosols, cloud and fog is

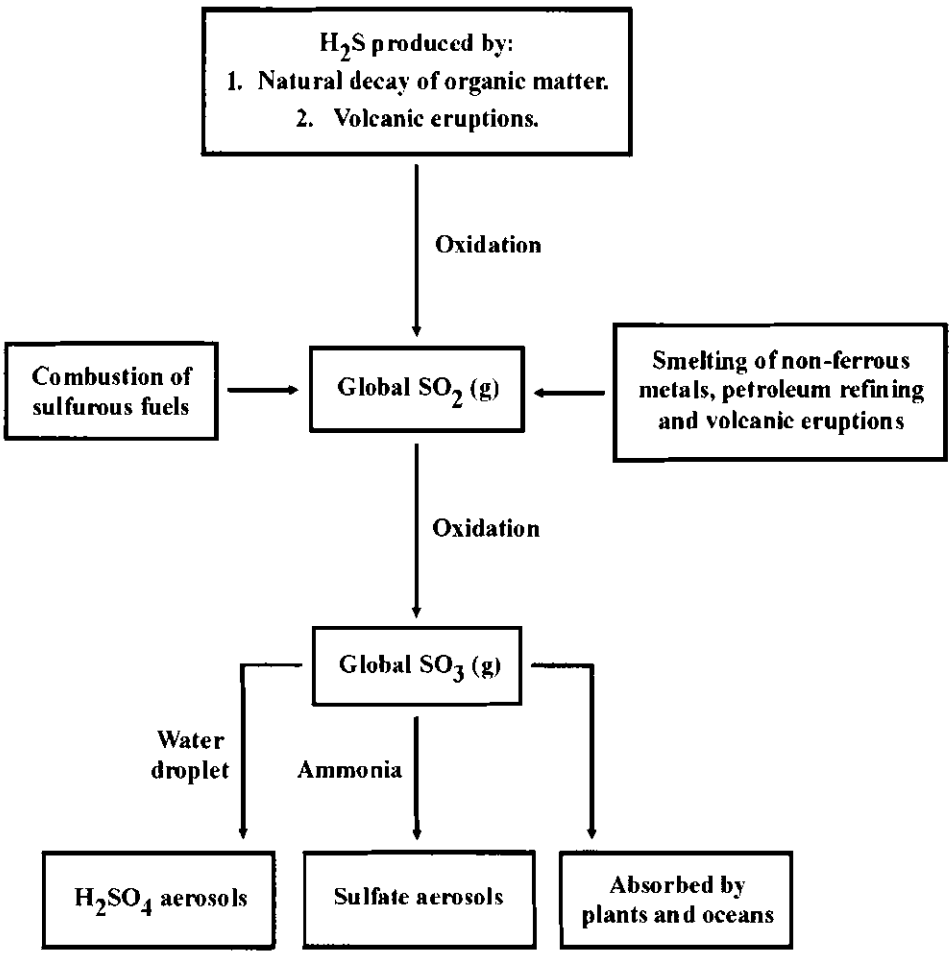

Figure 2.5: Production and dispersion of atmospheric sulfur dioxide gas (Meetham, 1981)

found to be an important factor in determining the rate of conversion of SO_2 (Finlayson-Pitts and Pitts, 1986). Furthermore, the reaction rate in liquids is influenced by the pH, metallic catalysts and oxidizing pollutants (O_2, O_3, H_2O_2) (Whelpdale and Kaiser, 1996). Thus, the intensity of sunlight, the presence of oxidants and/or oxidant precursors, relative humidity and the presence of fog and clouds all appear to affect conversion rates.

Many oxidizing agents (O_3, H_2O_2, PAN, methylhydroperoxide and peroxyacetic acid), formed in the gas-phase, do not react with gaseous SO_2 at measurable rates. However, in aqueous-phase reactions of SO_2, when these species are dissolved in cloud water, they readily oxidize dissolved SO_2 (Helas and Pienaar, 1996).

SO_2 can be oxidized to sulphate in heterogeneous reactions on fly ash (Cohen *et. al.*, 1981), ferric oxide particles and free fall atmospheric dust (Rani *et. al.*, 1992). However, Burger (1993) has demonstrated that ferric oxide, silicon dioxide and activated carbon or fly ash do not enhance the oxidation of SO_2 in the gas-phase or in acidic aqueous solutions.

2.4.2 Nitrogen dioxide chemistry

The atmospheric chemistry of oxidized nitrogen compounds is complicated because they may be converted into a number of different chemical forms (Erisman and Draaijers, 1995). Nitrogen oxides are produced in the troposphere primarily in the form of NO. Nitric oxide reacts rapidly with ozone to form nitrogen dioxide. Unlike sulphur dioxide, which is converted irreversibly into sulphate (in solution or as a particle), the oxides of nitrogen may be chemically transformed through a number of different compounds, before eventual deposition at the earth's surface (Campbell, 1997). There are three main pathways by which NO_2 can be converted into nitric acid and nitrate.

Gas phase oxidation

NO and NO_2 are oxidized to the nitrate radical ($NO_3^{\cdot}$) by reaction with ozone (O_3).

$$NO + O_3 \rightarrow NO_2 + O_2 \tag{2.4}$$

$$NO_2 + O_3 \rightarrow NO_3^{\cdot} + O_2 \tag{2.5}$$

In daylight, Reaction 2.5 is rapidly reversed as the $NO_3^{\cdot}$ radical is photolyzed by sunlight, but in the dark, $NO_3^{\cdot}$ reacts further with NO_2 to give dinitrogen pentoxide (N_2O_5).

$$NO_3^{\cdot} + NO_2 \rightarrow N_2O_5 \tag{2.6}$$

The $NO_3^{\cdot}$ is rapidly removed if unreacted NO is present in the atmosphere.

$$NO + NO_3^{\cdot} \rightarrow 2NO_2 \tag{2.7}$$

Reaction 2.6 is readily reversible, forming an equilibrium in the atmosphere. The N_2O_5 formed may react further with the water vapour to form nitric acid (HNO_3).

$$N_2O_5 + H_2O \rightarrow 2HNO_3 \tag{2.8}$$

However, this reaction only occurs at a surface, for example, the surface of a cloud droplet or aerosol particle. NO_2 may also be oxidized directly to gaseous HNO_3 by reaction with $HO^{\cdot}$.

$$NO_2 + HO^{\cdot} \rightarrow HNO_3 \tag{2.9}$$

The nitric acid formed in this way may then dissolve in cloud or rain or be deposited directly at the earth's surface or react with ammonia to form ammonium nitrate particles. In a similar manner, nitrous acid (HONO) may be produced by the reaction of NO and $HO^{\cdot}$.

$$NO + HO^{\cdot} \rightarrow HNO_2 \tag{2.10}$$

Aqueous phase oxidation

HONO may also be produced by the reaction of NO and NO_2 with water.

$$NO_2 + NO + H_2O \rightarrow 2HONO \tag{2.11}$$

Or by reaction of two molecules of NO_2 with water.

$$2NO_2 + H_2O \rightarrow HONO + HNO_3 \tag{2.12}$$

These reactions can be a source of gas phase HONO in a surface-catalyzed reaction, but the NO and NO_2, despite their low solubility in pure water, can also dissolve in and react with cloud water. The rate of reaction is, however, very slow unless catalyzed by the presence of other solutes.

In solution, HONO and NO_2^- (nitrite) ions may be oxidised to give nitrate (NO_3^-) ions by reaction with oxidants such as hydrogen peroxide (H_2O_2).

$$NO_2^- + H_2O_2 \rightarrow NO_3^- + H_2O \tag{2.13}$$

Although other aqueous phase pathways have been suggested for the oxidation of nitrogen oxides to nitrate, no strong evidence exists to assess their importance (Campbell, 1997). Hydrolysis and reaction of organic nitrates can occur, and there may also be aqueous phase reactions, which lead to the production of organic nitrates.

Nitrate aerosols

The third route, and one of the most important ones, for the incorporation of nitrate into cloud and rain droplets and ultimately into wet deposition, is through the action of nitrate aerosol as cloud condensation nuclei (Campbell, 1997). The various mechanisms by which gas-phase NO_y (all oxidised nitrogen compounds, i.e., NO_x, nitric acid, nitrate particle) may be converted into nitrate aerosol. Gaseous NO_y compounds can react on the surfaces of sea salt aerosols to form sodium nitrate aerosol, with the liberation of chlorine-containing gases.

$$HNO_3 + NaCl \rightarrow NaNO_3 + HCl \tag{2.14}$$

$$NaCl + N_2O_5 \rightarrow ClNO_2 + NaNO_3 \tag{2.15}$$

Where HNO_3 and N_2O_5 are the main product of the daytime and night-time oxidation reactions of NO_x, respectively. Nitrogen dioxide may also take part in reactions with sea salt aerosol.

$$2NO_2 + NaCl \rightarrow ClNO + NaNO_3 \tag{2.16}$$

Nitric acid reacts with soil-derived particles to produce soluble nitrate aerosol.

$$2HNO_3 + CaCO_3 \rightarrow Ca(NO_3)_2 + CO_2 + H_2O \tag{2.17}$$

Nitric acid also reacts with gaseous ammonia forming ammonia nitrate, which may be taken up on pre-existing atmospheric aerosol species, due to its relatively low volatility.

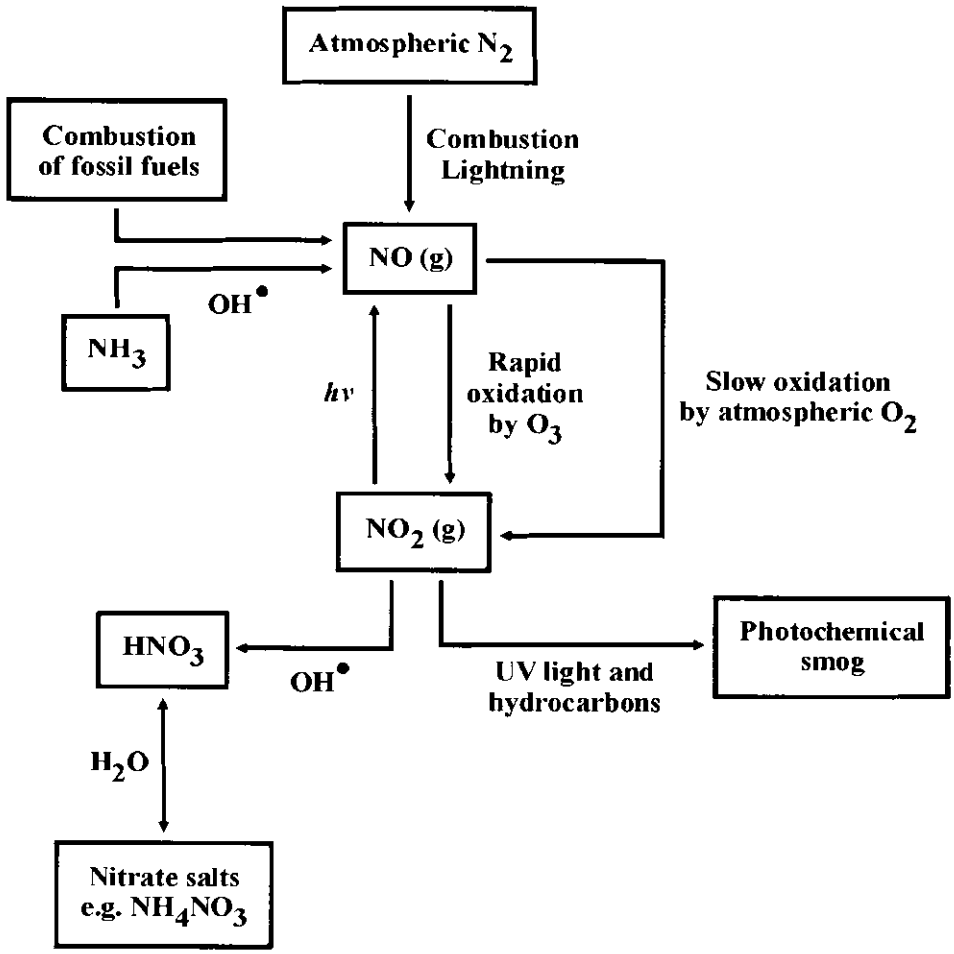

Figure 2.6: Major processes involved in the NO_2 cycle (Seinfeld and Pandis, 1998)

2.5 ATMOSPHERIC DEPOSITION

Deposition phenomena are the physical and chemical processes in which the atmosphere cleans itself by depositing pollutants on the surface of the earth. There are two pathways according to which chemical species are removed from the atmosphere: wet deposition and dry deposition. Wet deposition is the removal by precipitation scavenging and, to a lesser extent, impaction of fog or cloud droplets on vegetation. Dry deposition includes the direct adsorption or deposition of gases on the surface of particles, and the settling and impaction of particles. On a global scale, precipitation scavenging and dry deposition are by far the most efficient methods. Fog and droplet deposition can be locally important, especially in cloudy, high elevation regions in South Africa (WMO, 1996).

Acid deposition and accompanying effects were first noticed as a large-scale environmental problem at the end of the 1960's. During the 25 years since it was originally observed, acidification effects have occurred in many ways and in various ecosystems. Early observations of acidification effects in lakes and streams were followed by later observations of groundwater acidification and, later still, soil acidification. Acid deposition had a considerable negative

impact on materials (WMO, 1996).

Acidification effects are primarily associated with the atmospheric deposition of sulphur and nitrogen compounds. Deposition may occur in the form of strong acids (sulphuric acid, nitric acid, and infrequently hydrochloric acid) or compounds, which, after deposition, may be converted to strong acids (e.g. sulphur dioxide and nitrogen dioxide). In this context ammonia is also a potentially strong acid. In soils it may be converted to nitric acid and thus cause acidification. In tropical areas organic-acid deposition may contribute as much as 50% of the deposition of acids in precipitation. It is, however, assumed that these acids are absorbed or oxidized in soil and will not contribute to soil acidification (McDowell, 1988).

Acid deposition has been of interest not only for its role in acidification but also for effects associated with the deposition of nitrogen as a nutrient. Also, direct effects from sulphur dioxide and nitrogen oxides have sometimes been considered as acidification effects. It is, however, important to note that in many areas of the world, concentrations of sulphur and nitrogen oxides exceed ambient air quality standards, and considerable emission reductions are necessary to protect human health. Sulphur and nitrogen compounds may also affect physical and chemical properties of the atmosphere (Isaksen and Hov, 1987; Langner *et. al.*, 1992).

2.5.1 Wet deposition

Wet scavenging is defined as the natural process by which atmospheric pollutants are attached to and dissolved in the cloud and precipitation droplets (or particles), and subsequently deposited on the earth's surface (Erisman and Draaijers, 1995). Precipitation scavenging is an effective mechanism for removing soluble trace gases and small particles from the troposphere. The gases and particles are incorporated into cloud droplets and falling rain drops in several ways. Those trace particles in the atmosphere that act as ice-forming nuclei or condensation nuclei can be incorporated into hydrometers during the nucleation process itself. This is the process that generates cloud droplets from which raindrops form. In many parts of the world, sulphate particles are the most commonly found condensation nuclei in the atmosphere (Whelpdale and Kaiser, 1996). The cloud droplets that are generated continue to scavenge gases and particles in cloud as they grow in size. As they grow, the droplets fall faster until they leave the cloud base and are deposited as rain, carrying all of the scavenged pollutants with them. It is not only particulate sulphate that is scavenged in this way, gaseous sulphur dioxide can also be dissolved in cloud droplets, whereupon it can be oxidized to sulphate by means of aqueous-phase chemical reactions (Summers, 1992).

Clearly, the actual wet-deposition flux of chemical species to the surface depends on many factors. The most important ones are precipitation form (rain, snow, etc.) and precipitation rate, both of which are strongly related to cloud type, as well as ambient air concentrations within and below a cloud. These complex physicochemical processes can be integrated into several parameters such as scavenging ratio, scavenging efficiency, and scavenging rate. These quantities have varying degrees of applicability, depending on the kind of precipitation system that is considered, but all of them can be formulated from observations giving the "bulk" characteristics of precipitating weather systems. For example, the mass scavenging ratio (S_R) is defined as the concentration of the dissolved chemical species per unit mass of cloud water or rain (C_r) divided by the total concentration of the same species (or its precursor) per unit mass of ambient air, including the mass water in the air (C_a):

$$S_R = C_r/C_a \tag{2.18}$$

The typical liquid water content of precipitating clouds is 1 g of water per 1 m^3 of air at standard temperature and pressure (25 ° C and 101 kPa) (STP) (but it ranges from 0.1 to 5.0). Since 1 m^3 of air weighs approximately 1 kg (STP), if all the trace species in 1 m^3 of air were dissolved in the cloud water (i.e., 100% scavenging efficiency), the species concentration in the rain would be magnified by a factor of 1000 and the scavenging ratio would be 1000. In practice, the efficiency of removal of either pollutants or of water itself is not 100%, and hence the scavenging ratio can vary greatly. At a few locations in North America (Barrie, 1988) and Europe where concentrations of sulphur and nitrogen species have been simultaneously measured in the air and precipitation, values of S_R varied from 100 to a few thousand (Barrie, 1988).

The wet-deposition rate (D_W) is given by the precipitation rate (R) times the species concentration in the rain (C_r):

$$D_W = C_r R = S_R R C_a \tag{2.19}$$

The ratio $S_R R$ is thus analogous to the dry-deposition velocity in the formulation of the dry-deposition flux. However, for wet deposition, C_a refers to the air concentrations at various atmospheric elevations where the species are being incorporated into cloud- and rainwater, whereas for dry deposition, C_a refers to the air concentration immediately above the surface (Barrie, 1988).

The wet deposition in a given precipitation event is calculated as the product of the total precipitation (P) and the measured concentration (C_r) of the species within the precipitation. In many regions the day-to-day variation in wet-chemical deposition is controlled more by the precipitation amount than by trace-chemical concentrations (Barrie, 1988).

Wet removal pathways depend on multiple composite processes, involving numerous physical phases, and are influenced by different phenomena on a variety of physical scales. In dealing with wet deposition, one is not only dealing with the usual phases (gas, aerosol and aqueous), but in addition, the aqueous phase can be present in several forms (cloud water, rain, snow, ice crystal, hail), all of which have a size resolution between 10^{-2} m and 10^{-6} m. To complicate matters even further, processes operating inside a cloud differ from those below cloud base. The complexity of wet deposition removal processes lead early investigators to attempt a quantification of the relationship between airborne species concentrations, meteorological conditions and wet deposition rates by lumping the effects of these processes into a few parameters.

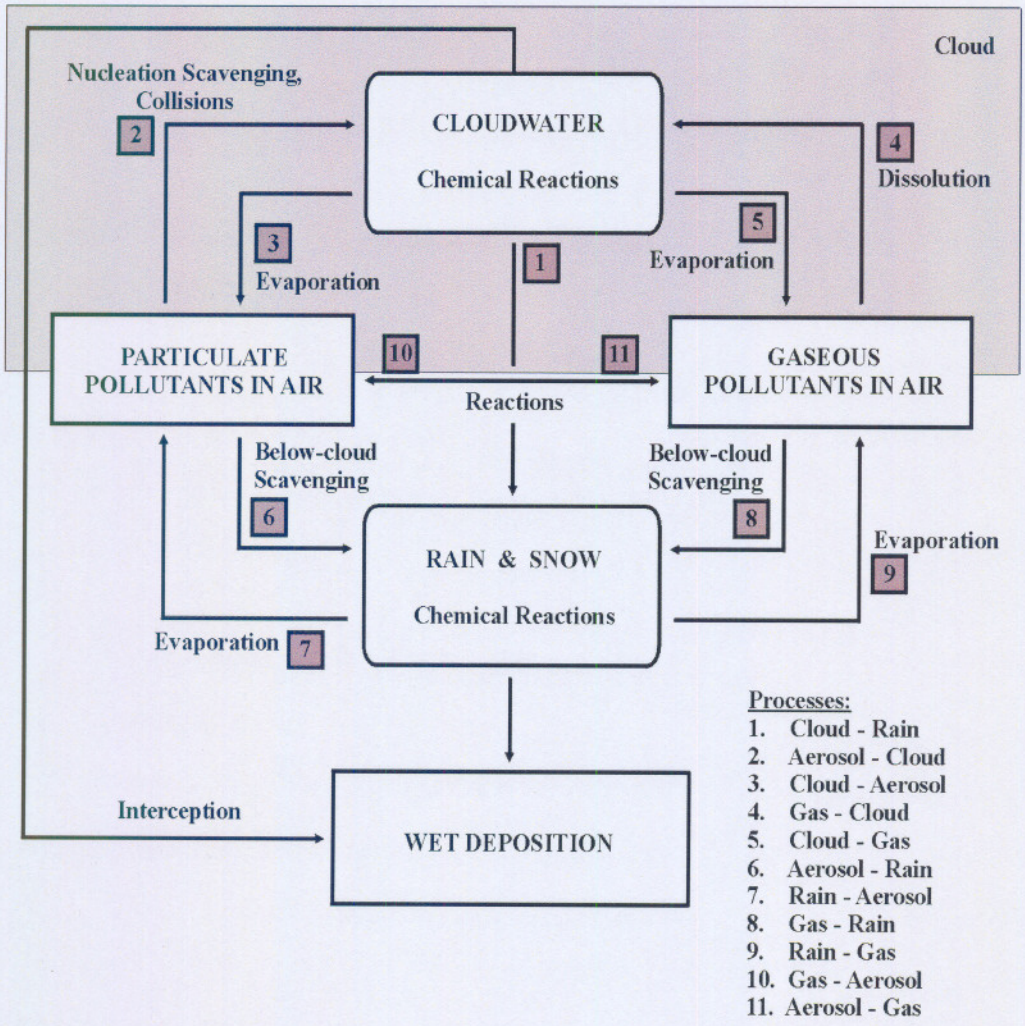

Figure 2.7: Conceptual framework of the wet deposition process (from Seinfeld and Pandis, 1998)

The wet-deposition flux is given by the product of the measured concentration of the species of interest in the rain and the precipitation rate:

$$F = CP \tag{2.20}$$

Where F = wet flux (mol.m^{-2}.yr^{-1}), C = measured concentration in precipitation (mol.m^{-3}), P= precipitation rate (mm.yr^{-1}).

One overwhelming characteristic of wet deposition is how much the total wet deposition of one chemical species can vary from one event to another. Precipitation itself is a highly intermittent phenomenon occurring about 5% of the time in the mid-latitude cyclonic belt, with amounts varying for a given trace with several centimeters from one event to the next; the concentration of a chemical species can vary by an order of magnitude. The largest difference between events occurs on the periphery of industrial regions where emission rates are high. There, depending on air-mass trajectories, the air can be clean or heavily polluted.

Within regions with high emissions and in remote areas, the concentrations vary less. Thus, in southeast Canada and southern Scandinavia, wet-deposition episodicity is the highest, with less than 10% of the wet days accounting for 50% or more of the annual wet deposition of sulphate being typical. In extreme cases a single precipitation event can contribute up to 30% of the annual chemical deposition (Summers, 1992).

2.5.2 Dry deposition

Dry deposition must always be considered in any calculation of total deposition of an acidifying compound, whether it is related to a specified receptor surface or to a large area. The dry deposition of gases and particles from the atmosphere to a receptor surface is governed by the concentration in air and the turbulent transport processes in the boundary layer, as well as by the chemical and physical nature of the depositing species and the capability of the surface to capture or absorb gases and particles. The dry-deposition process involves close interaction between the atmosphere and the surface in which the characteristics of individual underlying surfaces often determine the mass-transfer rates. The transport of gases and particles from the atmosphere to the vicinity of the receptor surface is governed by the level of atmospheric turbulence, generated by both wind shear and buoyancy. The higher the level of atmospheric turbulence, the more efficiently gases and particles are transported to a given receptor surface. Depending on the characteristics of the surface, the ability to "capture" pollutants from the air may vary by more than an order of magnitude, causing highly varied dry-deposition rates even over small areas. Forests, especially coniferous forests, normally receive relatively high dry deposition of acidifying compounds, whereas lake surfaces receive much lower ones. Deposition extremes are often observed at forest edges or in forests on mountain slopes (Hicks *et. al.*, 1987).

Around the source, dry deposition is determined primarily by the configuration of the sources, the type of sources and the pollutant's mixing in the atmosphere. For high-level sources, the deposition near to the source is small and increases with downwind distance from it, until it reaches a maximum and decreases again. However, for ground-level sources, dry deposition takes place in the immediate vicinity of the source, where concentrations are highest and then gradually decreases downwind. At some distance, the influence of the source on the concentration gradient is diminished. At this point, the pollutant is mixed throughout the boundary layer and the concentration gradient is determined primarily by dry deposition processes (Erisman and Draaijers, 1995).

Two layers can be distinguished in the boundary layer for transport of pollutants to a receptor: the fully turbulent layer and the quasi-laminar layer. The quasi-laminar layer is introduced to quantify the way in which pollutant transfer differs from momentum transfer in the immediate vicinity of the surface (Hicks *et. al.*, 1987). In this layer, the transport to the receptor is dominated by molecular diffusion. Once at the receptor surface, the chemical, biological and physical nature of the surface determines the capture or absorbency of the gases and particles. For gases, surface uptake is frequently controlled by the ability of the surface to adsorb the specific chemical species.

In any circumstance dry-deposition rates are proportional to the concentrations of air immediately above (or surrounding) the receptor under consideration. The "constant" of proportionality is referred to as a deposition velocity (V_d) which depends on factors mainly associated with turbulence and related to characteristics of the air near the surface, as well as the composition of the surface itself. Depending on the chemical in question, different factors

assume important roles in determining the magnitude of V_d. In the case of sulphur dioxide, for example, the surface moisture and the photosynthetic activity of vegetation are important factors. The dominant terrestrial surface sink of sulphur dioxide is via open stomata into plant mesophyllic tissue. Actively respiring vegetation presents a good sink for SO_2, whereas the same vegetation suffering under water stress does not (Sheih *et. al.*, 1979).

In practice, using a standardized deposition velocity in numerical models is an engineering approximation that is particularly attractive in relation to large-scale simulations because it combines the effects of many complex processes into a single term (Wesely and Hicks, 1977).

In conclusion, we note that the use of a deposition velocity approach in large-scale numerical models is a simplification of complicated processes that result in substantial computational convenience. This is in contrast to the complexity with which chemical reactions are addressed in advanced Eulerian models. If deposition processes were described with the detail permitted by current understanding, much greater surface detail would be required and computation time would be increased considerably (WMO, 1996).

2.6 MATHEMATICAL MODELLING

2.6.1 Introduction

It is becoming common in the environmental sciences to describe complex systems of interacting physical, chemical, and biological processes through the design of numerical "models". These models consist of sets of mathematical equations that attempt to describe processes observed in nature, allowing scientists to create replicas of natural systems with a computer, so that the causes and effects of system behaviour may be better understood. Although we can study individual interactions within a system by using laboratory simulations or, under favourable conditions, by directly observing nature, the complexity of the Earth's system processes makes the use of these mathematical models necessary, in order to comprehend the behaviour of the system as a whole (Graedel and Crutzen, 1997).

Once scientists are sufficiently convinced of a model's validity, they begin to use the model to predict future conditions arising from changes in important variables within the system such as natural processes, solar activity, volcanic eruptions, anthropogenic factors, and emissions of industrially produced trace gases. Models can also be used to study the past, which in turn provides additional opportunities for testing the models or for learning more about past processes. It is the ability of models to explore situations remote from current conditions and unavailable in reality, as well as their ability to allow numerical experiments aimed at the question, "what would happen if...?", that makes them potentially valuable (Graedel and Crutzen, 1997).

Numerical atmospheric models differ greatly in complexity, especially in their degree of spatial and temporal resolution. Ideally, a model should be able to generate predictions specific to large and small geographical areas and for long and short time intervals. In practice, though, the information required to perform the calculation may not be available, or the capabilities of computers may be insufficient. All computer modelling efforts at best represent trade-offs: scientists must choose spatial and temporal resolution at the expense of physical, chemical, and meteorological detail, or vice versa. For example, smog chemistry may be calculated in great detail, but only for a small localized area (e.g. single city), or climatological features could be calculated for a century, but only for continents instead of

individual regions. Each choice has its uses and limitations; no single model can serve all needs (Graedel and Crutzen, 1997).

A wide range of different models have been published in scientific papers, and an even larger number of unpublished models and special model versions exist. Models can be distinguished on many grounds: e.g. the underlying physical concepts, the temporal and spatial scale, and the type of component involved. Contemporary air pollution models deal with "conventional" primary pollutants (mainly SO_2, CO, NO_x and VOC's). At present the need is recognized for extending the models to include heavy metals and persistent organic pollutants (POP's). Modelling of visibility, particulate concentrations (particulate matter with a size distribution smaller than 10 μm (PM_{10})) and aquatic phase chemistry are among the most important current model developmental trends (Moussiopoulos *et. al.*, 1996).

There are a wide variety of air quality models that have been developed for different pollution sources, meteorology, downwind distances, and other factors that affect how pollutants are dispersed in the atmosphere. In general, however, all of these models require two types of data: information about the source being modelled, including the pollutant emission rate, and information about the dispersing characteristics of the meteorology surrounding the source, such as atmospheric stability, wind speed and direction. The model uses this information to mathematically simulate the pollutant's downwind dispersion in order to derive estimates of concentration at a specified location. Some models even simulate the chemical transformations and removal processes that can occur along the transport path (Zannetti, 1990).

According to Zannetti (1990) four groups of application areas are defined for air pollution models: *regulatory purposes, policy support, public information and scientific research*. Moreover, operational forecast and emergency preparedness models are emerging model application areas in the last decade.

A sound air quality management strategy is necessary to address all emissions and their relative impact on the environment. Air pollution modelling is an integral part of such a sound air quality management program, with the aim to determine the relative impact of industries on the receiving environment (Fourie, 2000).

Mathematical models provide the necessary framework for integration of our understanding of individual atmospheric processes and study of their interactions. A combination of state-of-the-art measurements with state-of-the-art models is the best approach for making real progress toward understanding the atmosphere.

In urban and regional air quality studies, one has often to address questions such as the following:

- What is the contribution of Source A to the concentration of pollutants at Site B?
- What is the most cost-effective strategy for reducing pollutant concentrations below an air quality standard?
- What will be the effect on air quality of the addition or reduction of a specific air pollutant emission flux?
- Where should one place a future source (industrial complex, freeway, etc.) to minimize its environmental impacts?
- What will be the air quality tomorrow or the day after?

Addressing the above questions requires understanding of the relationships between emission fluxes and ambient concentrations. A model involving descriptions of emission patterns, meteorology, chemical transformations, and removal processes is the essential tool for establishing such relationships. Such a model provides a link between emission changes from source control measures and resulting changes in airborne concentrations (Seinfeld and Pandis, 1998).

2.6.2 Why air quality modelling?

According to Seinfeld (1975) air quality models are unique tools for:

- establishing emission control legislation: i.e. determining the maximum allowable emission rates that will meet fixed air quality standards;
- evaluating proposed emission control techniques and strategies; i.e. evaluating the impact of future abatement and mitigation control options;
- selecting locations of future sources of air pollutants, in order to minimise their environmental impacts;
- planning the control of air pollution episodes; i.e. defining immediate intervention strategies, (i.e. warning systems and real-time short-term emission reduction strategies) to avoid severe air pollution episodes in a certain region;
- assessing responsibility for existing air pollution levels; i.e. evaluating present source-receptor relationships.

It is important to clarify what air quality modelling is and what it is not. Air quality modelling is an indispensable tool for all of the above analyses. It is however, only a tool. Modelling, like monitoring, is not the solution of the air pollution problem, even though each is sometimes presented as such. Monitoring and modelling studies constitute only a relative inexpensive activity whose results, in the best case, provide useful information for possible future implementations of much more expensive emission mitigation and abatement strategies (Zannetti, 1990).

It is also important to clarify the real role of modelling versus monitoring efforts. It is not unusual to hear qualified scientists making statements such as "Why do we need to model that? Let's measure it; that's all we need," "Models do not work," etc. These statements imply unscientific thinking. Science involves the development of theories (or "models") based on (1) the empirical interpretation of experimental data, (2) the generalization of experimental relationships, or (3) pure speculative thinking subsequently confirmed by experimental results. The advancement of science is not the consequence of monitoring activities, even though the collection of good, reliable experimental data is often (but not always) a necessary (but not sufficient) condition to it (Seinfeld and Pandis, 1998).

The above concepts, which are well-established in most scientific circles, are sometimes alien to the environmental community, where, for example, it is commonly believed that environmental measurements are the "real world". They are indeed not. Monitoring data are indispensable for inferring theories or parameters and calibration or validating computer simulation packages. Their spatial and temporal resolution, however, is generally insufficient to quantify them as the real world. Only a well-tested and well-validated simulation model can be a good representation of the real world, its dynamics and its responses to perturbations.

Close interaction among ambient monitoring, laboratory experiments, and modelling should take place. Monitoring (routine or intensive) identifies the state of the atmosphere and provides data needed for use and evaluation of atmospheric models. Laboratory studies generally focus on a single atmospheric process, providing parameters needed by atmospheric models. Models are the tools that integrate our understanding of atmospheric processes. Evaluation of models often points out gaps in our understanding, leading to more laboratory and field measurements and then further model development (Seinfeld and Pandis, 1998).

Although measurements form an important aspect of monitoring, measurements alone are rarely sufficient to determine the impact of air pollution on the environment. Models are often needed to establish larger scale average exposure and deposition fields, which cannot easily be derived from measurements. The reason is simply that observations are made at a few locations only and may therefore not be very representative of larger areas. Substantial uncertainty can be introduced if measured data are extrapolated or interpolated into larger domains. Models are therefore used to generate best estimates in situations where measurements are lacking or cannot be made. Models are also necessary if the relative impact of various sources (source categories, emissions from different regions or countries) or emission scenarios have to be investigated. A consistent mass budget of emission, transport and deposition can only be obtained by means of employing models (Fourie, 2002).

2.6.3 Modelling topics

Numerical modelling techniques can be applied to all aspects of the air pollution problem, but the most widely use of models is to describe phenomena that take place in the atmosphere. These include:

- atmospheric transport;
- turbulent atmospheric diffusion;
- atmospheric chemical and photochemical reactions;
- ground deposition.

2.6.4 Suitability of models

The extent to which a specific air quality model is suitable for the evaluation of source impact depends upon several factors. These include: (1) The meteorological and topographic complexities of the area; (2) the level of detail and accuracy needed for the analysis; (3) the technical competence of those undertaking such simulation modelling; (4) the resources available; and (5) the detail and accuracy of the data base, i.e. emissions inventory, meteorological data, and air quality data. Appropriate data should be available before any attempt is made to apply a model. A model that requires detailed, precise input data should not be used when such data is unavailable. However, assuming the data is adequate, the greater the detail with which a model considers the spatial and temporal variations in emissions and meteorological conditions, the greater the ability to evaluate the source impact and to distinguish the effects of various control strategies (Seinfeld and Pandis, 1998).

Air quality models have been applied with the most accuracy or the least degree of uncertainty to simulations of long-term averages in areas with relatively simple topography. Areas

subject to major topographic influences experience meteorological complexities that are extremely difficult to simulate. Although models are available for such circumstances, they are frequently site specific and resource intensive. In the absence of a model capable of simulating such complexities, only a preliminary approximation may be feasible until such time as better models and databases become available.

Models are highly specialized tools. Competent and experienced personnel are an essential prerequisite to the successful application of simulation models. The need for specialists is critical when more sophisticated models are used or the area being investigated has complicated meteorological or topographic features. A model applied improperly, or with inappropriately chosen data, can lead to serious misjudgements regarding the source impact or the effectiveness of a control strategy (Fourie, 2002).

The resource demands generated by use of air quality models vary widely depending on the specific application. The resources required depend on the nature of the model and its complexity, the detail of the database, the difficulty of the application, and the amount and level of expertise required. The costs of manpower and computational facilities may also be important factors in the selection and use of a model for a specific analysis. However, it should be recognized that under some sets of physical circumstances and accuracy requirements, no present model may be appropriate. Thus, consideration of these factors should not lead to selection of an inappropriate model (Seinfeld and Pandis, 1998).

According to Zannetti (1990) three major categories of information are required to formulate inputs into models: air quality, emissions, and meteorology. Consequently, it is appropriate to think in terms of a modelling system, as illustrated in Figure 2.8 and not only an air quality model. Emissions and meteorological information, as well as boundary and initial conditions must be supplied to the air quality model, as shown by the flows in the figure.

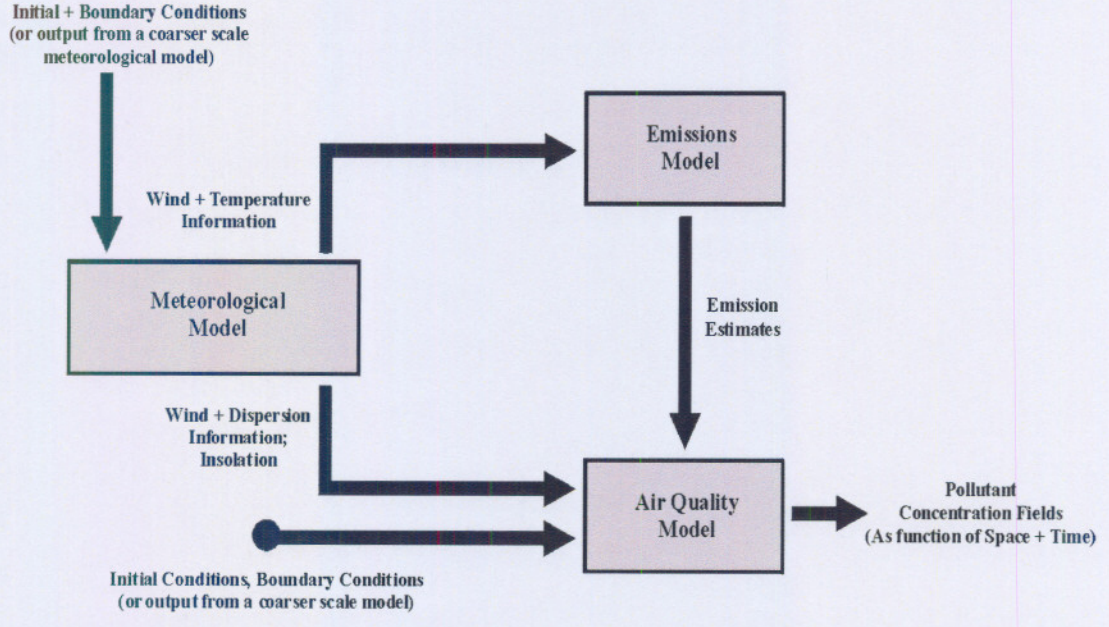

Figure 2.8: The air quality modelling system (Zannetti, 1990)

A detailed scheme of individual components included in an atmospheric chemical transport

model is depicted in Figure 2.9 (Seinfeld and Pandis, 1998).

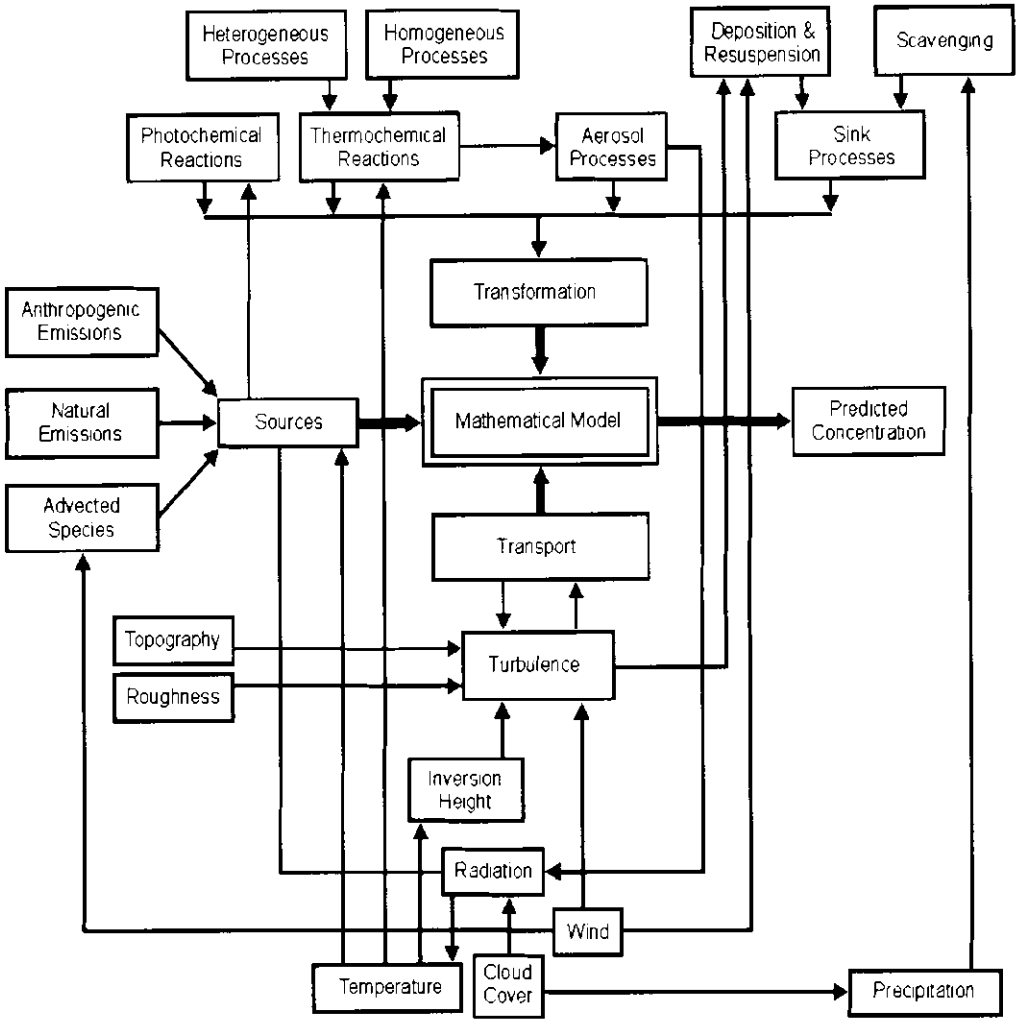

Figure 2.9: Elements of a mathematical atmospheric chemical transport model (Seinfeld and Pandis, 1998)

2.6.5 Spatial scales of models

Air pollution transport phenomena are decisively influenced by atmospheric processes, which are commonly classified with regard to their spatial scale. The latter is in turn related to the characteristic time of the individual process. Orlanski (1975) recommends distinguishing between the following atmospheric scales:

- Macroscale (characteristic lengths exceeding 1,000 km); at this scale, the atmospheric flow is mainly associated with synoptic phenomena, that is, the geographical distribution of pressure systems. Such phenomena are mainly due to large-scale inhomogeneties of the surface energy balance. Global dispersion phenomena (as well as the majority of

regional-to-continental scale) are related to macroscale atmospheric processes, for which the hydrostatic approximation can be considered as valid.

- Mesoscale (characteristic lengths between 1 and 1000 km); the flow configuration in the mesoscale is dependent both on hydrodynamic effects (e.g. flow channelling, roughness effects) and inhomogeneties of the energy balance (mainly due to the spatial variation of area characteristics (e.g. land use, vegetation, water), but also as a consequence of terrain orientation and slope. From the air pollution point of view, thermal effects are the most interesting, as they are of particular importance at times of weak synoptic forcing, that is, bad ventilation conditions. As a minimum requirement mesoscale meteorological models should be capable of simulating local circulation systems, for instance sea and land breezes. Mesoscale atmospheric processes affect primarily local-to-regional scale dispersion phenomena, of which urban studies are the most important examples. The description of such phenomena requires, even for practical applications, the utilisation of fairly complex modelling tools.

- Microscale (characteristic lengths below 1 km); in general, air flow is exceedingly complex at this scale, as it depends strongly on detailed surface characteristics (that is, form of buildings, their orientation with regard to the wind direction, etc). Although thermal effects may contribute to the generation of these flows, they are mainly determined by hydrodynamic effects (e.g. flow channeling, roughness effects) which have to be described well in an appropriate simulation model. In view of the complex nature of such effects, local scale dispersion phenomena (which are to a large extent associated with microscale atmospheric processes) are mainly described with robust "simple" models in the case of practical applications, such as street canyon models, etc.

However Zannetti (1990) made a distinction between the different scales of dispersion phenomena as follows:

- Near-field phenomena ($<$ 1 km from the source); e.g. downwash effects of plume caused by building aerodynamics.

- Short-range transport ($<$ 10 km from the source); e.g. the area in which the maximum ground-level impact of primary pollutants from an elevated source is generally found.

- Intermediate transport (between 10 km and 100 km); e.g. the area in which chemical reactions become important and must be taken into account.

- Long-range (or regional or interstate) transport ($>$ 100 km); e.g. the area in which large-scale meteorological effects, deposition and transformation rates play key roles.

- Global effects; i.e. phenomena affecting the entire earth atmosphere; e.g. CO_2 accumulation.

2.6.6 Classes of models

Models describing the dispersion and transport of air pollutants in the atmosphere can be distinguished on many grounds, for example:

- The spatial scale (global, regional-to-continental, local-to-regional and local).

- The temporal scale (episodic models, statistical and long-term models).
- The treatment of transport equations (Eulerian and Lagrangian models).
- The treatment of various processes (chemistry, wet and dry deposition).
- Ensemble models.
- The complexity of the approach.

Air quality modelling procedures discussed can be categorized into four generic classes: (1) Gaussian, (2) numerical, (3) statistical or empirical, and (4) physical. Within these classes, especially Gaussian and numerical models, a large number of individual "computational algorithms" may exist, each with its own specific applications. While each of the algorithms may have the same generic basis, e.g. Gaussian, it is accepted practice to refer to them individually as models. For example, the Industrial Source Complex (ISC) model is commonly referred to as individual models. In fact, they are both variations of a basic Gaussian model. In many cases the only real difference between models within the different classes is the degree of detail considered in the input or output data (Zannetti, 1990).

1. Gaussian models. Gaussian plume models are the most widely used techniques for estimating the impact of non-reactive pollutants, or pollutants being treated as non-reactive. It is based on the assumption that the plume concentration at each downwind distance has independent Gaussian distributions both in the horizontal and in the vertical axis, thus the Gaussian formula will describe a three dimensional concentration field generated by a point source under stationary meteorological and emission conditions. Almost all the models recommended by the EPA are Gaussian. Gaussian models have been modified to incorporate special dispersion cases. A simplified version of the Gaussian model, the Gaussian climatological model, can be used to calculate long-term averages (e.g. annual values).

2. Numerical models may be more appropriate than Gaussian models for area source urban and industrial applications that involve reactive pollutants, but they require much more extensive input databases and resources and therefore are not as widely applied. According to Zannetti (1993), the following numerical types can be distinguished:

    - Plume-rise models. In most cases, pollutants injected into ambient air are at a higher temperature than the surrounding air. Most industrial pollutants, moreover, are emitted from smoke stacks or chimneys, and therefore possess an initial vertical momentum. Both factors (thermal buoyancy and vertical momentum) contribute to increasing the effective stack height. Plume-rise models calculate the vertical displacement and general behaviour of the plume in this initial dispersion phase. Both semi-empirical and advanced plume-rise formulations are available.
    - Eulerian models. The transport of inert air pollutants may be conveniently simulated by the aid of these models which numerically solve the atmospheric diffusion equation, that is, the equation for conservation of mass of the pollutant (Eulerian approach). Such models are usually embedded in prognostic meteorological models. Advanced Eulerian models include refined sub-models for the description of turbulence (e.g. second-order closure models and large-eddy simulation models).

- Lagrangian models. As an alternative to Eulerian models, the Lagrangian approach consists of describing fluid elements that follow the instantaneous flow of air. They include all models in which plumes are broken up into elements such as segments, puffs, or particles. Lagrangian models use a certain number of fictitious particles to simulate the dynamics of a selected physical parameter. Particle motion can be produced by both deterministic velocities and semi-random pseudo-velocities generated using Monte Carlo techniques. Hence, transport caused by both the average wind and the turbulent terms due to wind fluctuations is taken into account.
- Chemical modules. Several air pollution models include modules for the calculation of chemical transformation. The complexity of these modules ranges from those including a simple, first-order reaction (e.g. transformation of sulphur dioxide into sulphates) to those describing complex photochemical reactions. Several reaction schemes have been proposed for simulating the dynamics of interacting chemical species. These schemes have been implemented into both Langrangian and Eulerian photochemical models. In Eulerian photochemical models, a three-dimensional grid is superimposed to cover the entire computational domain, and all chemical reactions are simulated in each cell at each time step. In the Langrangian photochemical models a single cell (or a column of cells or a wall of cells) is advected according to the main wind in a way that allows the injection of the emissions encountered along the cell trajectory.

3. Semi-empirical / Statistical models. This category consists of several types of models that were developed mainly for practical applications. In spite of considerable conceptual differences within the category, all these models are characterized by drastic simplifications and a high degree of empirical parameterizations. Among the members of this model category are box models and various kinds of parametric models. Statistical or empirical techniques are frequently employed in situations where incomplete scientific understanding of the physical and chemical processes, or lack of the required databases make the use of a Gaussian or numerical model impractical.

4. Physical modelling, the fourth generic type, involves the use of wind tunnel or other fluid modelling facilities. This class of modelling is a complex process requiring a high level of technical expertise, as well as access to the necessary facilities. Nevertheless, physical modelling may be useful for complex flow situations, such as building, terrain or stack downwash conditions, plume impact on elevated terrain, diffusion in an urban environment, or diffusion in complex terrain. It is particularly applicable to such situations for a source or group of sources in a geographic area limited to a few square kilometers. If physical modelling is available and its applicability demonstrated, it might be the best technique.

5. Receptor models, in contrast to dispersion models (which compute the contribution of a source to a receptor as the product of the emission rate multiplied by a dispersion coefficient), receptor models start with observed concentrations within a receptor and seek to apportion the observed concentrations at a sampling point among several source types. This is done based on the known chemical composition of source and receptor materials. Receptor models are based on mass-balance equations and are intrinsically statistical in the sense that they do not include a deterministic relationship between

emissions and concentrations. However, mixed dispersion-receptor modelling methodologies have been developed recently and are very promising. Table 2.1 gives a summary of each scale of dispersion phenomenon.

2.6.7 Levels of sophistication of models

In addition to the various classes of models, there are two levels of sophistication. The first level consists of general, relatively simple estimation techniques that provide conservative estimates of the air quality impact of a specific source, or source category. These are screening techniques or screening models. The purpose of such techniques is to eliminate the need for further more detailed modelling for those sources that clearly will not cause or contribute to ambient concentrations in excess of either the National Ambient Air Quality Standards (NAAQS) or the allowable prevention of significant deterioration (PSD) concentration increments. If a screening technique indicates that the concentration contributed by the source exceeds the PSD increment or the increment remaining to just meet the NAAQS, then the second level of more sophisticated models should be applied.

The second level consists of those analytical techniques that provide more detailed treatment of physical and chemical atmospheric processes, require more detailed and precise input data, and provide more specialized concentration estimates. As a result they provide a more refined and, at least theoretically, a more accurate estimate of source impact and the effectiveness of control strategies. These are referred to as refined models.

The use of screening techniques followed by a more refined analysis is always desirable. However, there are situations where the screening techniques are practically and technically the only viable option for estimating source impact. In such cases, an attempt should be made to acquire or improve the necessary databases and to develop appropriate analytical techniques.

2.6.8 Practical modelling considerations

Practical application of air quality models requires:

- analysis of the problem;
- selection of the appropriate model(s);
- application of the selected model(s) (Zannetti, 1990).

According to Zannetti (1990), the analysis of the problem requires, as a minimum, the identification of:

- the type of pollutant (reactive or non-reactive);
- the averaging time of interest (e.g. instantaneous concentrations for odour problems; one-hour averages for short term cases; or annual averages for long term analysis);
- the characteristics of the domain (e.g. simple flat terrain cases or complex topography);
- the computational limitations (e.g. simple assumptions or more complex formulations, depending on the available computational facilities).

Model selection should be performed by taking into account the above factors, as illustrated in Figure 2.10.

Table 2.1: Summary of each scale of dispersion phenomenon: 1. Regulatory purposes; 2. Policy support; 3. Public information and 4. Scientific research (Zannetti, 1993)

Scale of atmospheric process	Microscale	Mesoscale	Macroscale	
Scale of dispersion phenomenon	Local	Local-to-regional	Regional-to-continental	Global
Model type				
Plume-rise	1,2,4			
Gaussian	1,2,4	1,2		
Semi-empirical / Statistical	1,2,3,4	1,2,4		
Eulerian	1,2,4	2,3,4	2,4	2,4
Lagrangian	4	4	2,4	
Chemical	1,2,4	2,3,4	2,4	2,4
Receptor		2,4		

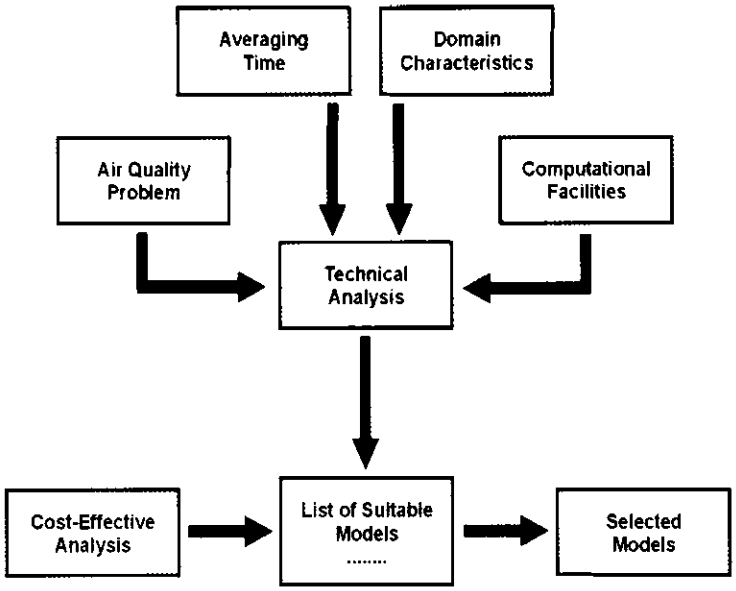

Figure 2.10: The model selection process (Zannetti, 1990)

2.6.9 Model evaluation

Finally, the optimal application of a numerical model for control strategy analysis should incorporate its calibration and evaluation with local quality monitoring data, in order to determine its applicability and minimize forecasting errors, as illustrated in Figure 2.11. Only models that have been verified by past data should be used for future forecasting. Calibration and evaluation are, however, difficult in many cases, when sufficient air quality and meteorological data is not available, and impossible in others, when, for example, models are used to simulate the impacts of possible future new sources (Zannetti, 1990).

Analyzing the potential for the practical use of mathematical models for air quality assessments implies investigating the following aspects:

- Which kind of statements can be made by the aid of models (qualitative approach).
- The accuracy of these statements (quantitative approach).

It appears that the former approach is easier, because it only requires knowledge of the characteristics and the application range of a model. In addition to this, quantification of the accuracy of the model results presupposes insights into the following:

- Input data accuracy, and how the latter affects the accuracy of model results.
- Uncertainties in model assumptions and parameterizations.
- Methodologies for judging to which extent model results represent reality.

As a consequence of the above, model validation (typically with the aid of available analytical solutions) should be considered as an indispensable part of the model development process, whereas a model which has been validated already, should be subject to a more

thorough evaluation procedure in order to ensure that potential users can assess the degree of reliability and accuracy inherent in the given model. High quality field data which is needed for evaluation purposes is, however, very rare (Moussiopoulos *et. al.*, 1996).

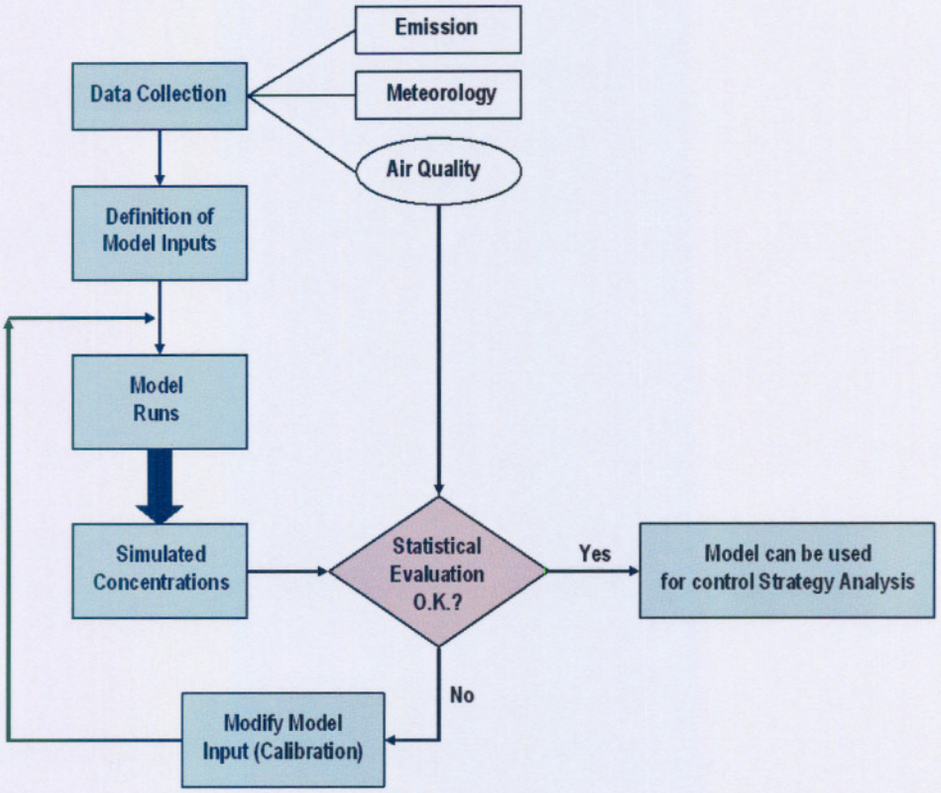

Figure 2.11: Optimal model application (Zannetti, 1990)

The way to evaluate air pollution models seems to be straightforward: model predictions are compared against appropriate measurements and identified deviations are statistically analyzed to allow for quantification of model uncertainties. In spite of the simplicity of this method, there are considerable difficulties both in defining the evaluation procedure and in interpreting its results. These are listed below:

- Different evaluation procedures should be applied to the various model categories. In other words, the experimental data set needed to evaluate the models in addition to the evaluation of software, should be tailored for the specific application.
- Deviations between model results and observations may be caused by a variety of reasons such as: shortcomings in model assumptions and parameterisations, errors and inaccuracies in input data (particularly emission data and meteorological data), uncertainties related to the stochastic nature of atmospheric processes, uncertainties in observations, uncertainties in the representativeness of both observed and modelled data, etc.

2.6.10 Atmospheric modelling - A South African perspective

Modelling efforts in South Africa have mainly focused on the short range transport (dispersion less than 50 km) of air pollutants during the last two decades. Gaussian plume models were utilized, and in limited cases Gaussian puff models were used for impact assessment studies. The models utilized in many cases were obtained from US and EU sources, and seldomly developed or modified for South African conditions.

Currently no long-range transport model is available for southern African conditions, to simulate the transboundary and long-range movement of emissions over the southern African region.

It is forseen that the role of air quality models in decision-making processes and impact studies will increase as a result of the new National Environmental Management: Air Quality Act, 2004 (Act No. 39 of 2004) implemented in South Africa. Air quality models are the only tool to relate emissions to ambient air concentrations (impacts), which forms the basis for the new act.

2.7 CONCLUSIONS

A sound air quality management strategy is necessary to address all emissions and their relative impact on the environment. Air quality modelling is an integral part of such a sound air quality management program, with the aim to determine the relative impact of emissions on the receiving environment. Moreover, there is a trend towards the increased role of air pollution models in decision-making processes.

Since ideal model application conditions are seldomly found, air quality models are often used beyond their theoretical and practical limits of applicability, increasing uncertainties. Correct input data into the models is imperative in order to minimize uncertainties and assumptions.

Plenty of models (knowledge) are available in the global modelling domain, but many gaps are still eminent.

Chapter 3

LED MODEL DEVELOPMENT

In this Chapter...

Section 3.1 to gives a detailed description of the atmospheric diffusion theories implemented in this study. Section 3.2 focuses on the theoretical development of the long-range air pollutant transport and chemistry model, highlighting the different aspects pertaining to the theoretical model, while Section 3.3 discusses the development of the numerical LED model. Section 3.4 concludes the chapter by summarizing and pointing out possible areas of application and improvement of the developed LED model.

3.1 ATMOSPHERIC DIFFUSION THEORIES

A major goal in studying the atmospheric aspects of air pollution is to describe mathematically the spatial and temporal distribution of contaminants released into the atmosphere. It is common to refer to the behaviour of gases and particles in turbulent flow as turbulent "diffusion" or, in this case, as atmospheric "diffusion", although the processes responsible for the observed spreading or dispersion in turbulence are not the same as those acting in ordinary molecular diffusion. A more precise term would perhaps be atmospheric dispersion, but to conform to the common terminology the term atmospheric diffusion will be used. This section is devoted primarily to the description of the two basic ways for studying turbulent diffusion. The first is the Eulerian approach in which the behaviour of species is described relative to a fixed coordinate system. The Eulerian description is the common way of treating heat and mass transfer phenomena. The second approach is the Lagrangian in which concentration changes are described relative to the moving fluid (Garatt, 1992).

3.1.1 Eulerian approach

Let us consider N species in a fluid. The concentration of each must, at each instant, satisfy a material balance taken over a volume element. Thus, any accumulation of material over time, when added to the net amount of material convected into the volume element, must be balanced by an equivalent amount of material that is produced by chemical reaction in the element, which is emitted into it by the source, and that enters by molecular diffusion (Djolov, 1991).

Expressed mathematically, the concentration of each species, c_i, must satisfy the mass conservation law, commonly known as the continuity equation:

$$\frac{\partial c_i}{\partial t} + \frac{\partial}{\partial x_j} u_j c_i = D_i \frac{\partial^2 c_i}{\partial x_j \partial x_i} + R_i \left(c_1, ..., c_N, T\right) + S_i \left(\vec{x}, t\right) \tag{3.1}$$

where u_j is the jth component of the fluid velocity, D_i is the molecular diffusivity of species i in the carrier fluid, R_i is the rate of generation of species i by chemical reaction (which depends in general on the fluid temperature T), S_i is the rate of addition of species i at the location $\vec{x} = (x_1, x_2, x_3)$ and time t.

In addition to the requirements that c_i satisfies equation (3.1), the fluid velocities u_j and the temperature T, must satisfy the Navier-Stokes and energy equations, which themselves are coupled through the u_j, c_i and T with the total continuity equation and the ideal gas law. In general, it is necessary to carry out a simultaneous solution of the coupled equations of mass, momentum, and energy conservation to account properly for the changes in u_j, T, and c_i and the effects of the changes of each of these on each other. In dealing with atmospheric pollutions, however, since species occur at parts-per-million concentrations, it is quite justifiable to assume that the presence of pollutants does not affect the meteorology to any detectable extent, thus the equation of continuity can be solved independently of the coupled momentum and energy equations. Consequently, the fluid velocities u_j and the temperature T can be considered independent of the c_i. From this point onwards we will not explicitly indicate the dependence of R_i on T (Djolov, 1991).

The advantage of the Eulerian approach is that the turbulent diffusion equation is integrated in a fixed geographical mesh in which the necessary meteorological fields: wind velocity, temperature, precipitations, as well as roughness and emissions are naturally determined by the meteorological network or appropriate meteorological model. Thus the concentration fields are also determined in the same system. In the framework of the Eulerian approach it is easy to determine the properties of the underlying surface, linear and non-linear chemical reactions and other processes. Still there are substantial problems connected with securing proper initial conditions, the approximation of the advective terms, the appearance of fictitious waves at the boundary of the integration region and lack of physical sound theories for modelling the horizontal turbulence for distances larger than hundreds of kilometers (Djolov, 1991).

3.1.2 Lagrangian approach

The Lagrangian approach to turbulent diffusion is concerned with the behavior of representative fluid particles during its motion. We therefore begin by considering a single particle which is located at $\vec{x'}$ at time t' in a turbulent fluid. The subsequent motion of the particle can be described by it's trajectory, $\vec{X}\left[\vec{x'}, t', t\right]$, that is, it's position at any later time, t. Let $\psi\left(x_1, x_2, x_3, t\right) dx_1 dx_2 dx_3 = \psi\left(\vec{x}, t\right) d\vec{x}$ = probability that the particle at time t, to be in volume element x_1 to $x_1 + dx_1$, x_2 to dx_2, and x_3 to dx_3, that is that $x_1 \leq X_1 < x_1 + dx_1$, and so on. Thus, $\psi\left(\vec{x}. t\right)$ is the probability density function (pdf) for a particle's location at time t. By the definition of a probability density function:

$$\int_{-\infty}^{\infty} \int_{-\infty}^{\infty} \int_{-\infty}^{\infty} \psi\left(\vec{x}, t\right) dx = 1$$

According to Djolov (1991) the probability density of finding the particle at $\vec{x}$ at t can also be expressed as the product of two other probability densities:

(1) The probability density that if the particle is at $\vec{x'}$ at t' it will undergo a displacement to $\vec{x}$ at t. Denote this probability density $Q(\vec{x},t|\vec{x'},t)$ and call it the *transition probability density* for the particle.

(2) The probability density that the particle was at $\vec{x'}$ at t', $(\vec{x'},t')$, integrated over all possible starting points $\vec{x'}$. Thus,

$$\psi(x,t) = \int_{-\infty}^{\infty}\int_{-\infty}^{\infty}\int_{-\infty}^{\infty} Q(\vec{x},t|\vec{x'},t')\psi(\vec{x'},t')d\vec{x'} \tag{3.2}$$

The density function $\psi(\vec{x},t)$ has been defined with respect to a single particle. If, however, an arbitrary number m of particles are initially present and the position of the ith particle is given by the density function $\psi_i(\vec{x},t)$ it can be shown that the ensemble mean concentration at the point $\vec{x}$ is given by:

$$\langle c(\vec{x},t)\rangle = \sum_{i=1}^{m} \psi_i(\vec{x},t)\langle c(\vec{x_0},t_0)\rangle \tag{3.3}$$

By expressing the pdf $\psi_1(\vec{x},t)$ in equation (3.2) in terms of the initial particle distribution and the spatial temporal distribution of particle sources $S(\vec{x},t)$, say in units of particles per volume per time, and then substituting the resulting expression into equation (3.3), we obtain the following general formula for the mean concentration:

$$\begin{aligned}\langle c(\vec{x},t)\rangle = &\int_{-\infty}^{\infty}\int_{-\infty}^{\infty}\int_{-\infty}^{\infty} Q(\vec{x},t|\vec{x_0'},t_0')\langle c(\vec{x_0},t_0)\rangle d\vec{x_0'} \\ &+ \int_{-\infty}^{\infty}\int_{-\infty}^{\infty}\int_{-\infty}^{\infty}\int_{t_0}^{t} Q(\vec{x},t|\vec{x'},t')S(\vec{x'},t')dt'd\vec{x'}\end{aligned} \tag{3.4}$$

The first term on the right-hand side represents those particles present at t and the second term on the right-hand side accounts for particles added from sources between t' and t.

Equation (3.4) is the fundamental Lagrangian relation for the mean concentration of species in turbulent fluid. The determination of $\langle c(\vec{x},t)\rangle$, given $\langle c(\vec{x_0},t)\rangle$ and $S(\vec{x},t)$, rests with the evaluation of the transition probability $Q(\vec{x},t|\vec{x'},t')$. If Q were known for $\vec{x}$, $\vec{x'}$, t, and t', the mean concentration $\langle c(\vec{x},t)\rangle$ could be computed by simply evaluating equation (3.4). However, there are two substantial problems with using equation (3.4). First, it holds only when the particles are not undergoing chemical reactions. Second, such complete knowledge of the turbulence properties as would be needed to know Q is generally unavailable except in the simplest of circumstances. The major advantage of the Lagrangian method is the easy integration along the particles trajectory thus avoiding the difficulties with the numerical modeling of the advective terms in the turbulent diffusion equation (Djolov, 1991).

3.1.3 A combined Eulerian-Lagrangian description of the turbulent diffusion

The analysis of the two basic fluid dynamics approaches for the description of flow properties clearly reveals their advantages and shortcomings. There is, however, hope that some appropriate unification of the Eulerian and Lagrangian approaches may enhance our ability to tackle the problem of accurate solution of the long-range air pollutant equations. The basis of this idea stems from the experimental fact that the turbulence in vertical direction

is small scale, and it would be appropriate to use the turbulent diffusion equation, while in horizontal direction the turbulence is large scale, the turbulent eddies are not limited by the earth surface and the diffusion process requires a statistical description in this direction. The theoretical investigations confirmed that in a direction perpendicular to the wind velocity the concentration distribution is Gaussian while in vertical direction there is no appropriate statistical description of the process (Djolov, 1991).

The possibility arise therefore to describe the diffusion process independently in a vertical and horizontal direction, thus making it possible to combine and utilise the advantages of the Eulerian and Lagrangian approaches and to minimize their shortcomings. Therefore the following formula is postulated by Djolov (1991):

$$c^k(x,y,z,t) = \sum^{M} \sum^{N_i} Q_{ij}(t_{ij}) q_h(x, x^c_{ij}, y, y^c_{ij}, t_{ij}) q_z(z, z^c_{ij}, t_{ij}) q_w(t_{ij}) \tag{3.5}$$

where $Q_{ij}(0)$ is the quantity of the k^{th} pollutant in the j^{th} volume (puff) of pollutants emitted by the i^{th} source at the moment $t_{ij}= 0$. M is the number of sources, N_i is the number of puffs, q_z and q_h are the vertical and horizontal pollutant distribution functions, q_w is wet deposition function and t_{ij} is the life time of existence of the individual puffs.

This formula clearly indicates the application of the idea of separate description of the diffusion process in vertical and horizontal direction. Additional support to the general validity of Equation (3.5) is the linearity of the continuity equation, a fact which allows the independent study of the phenomenon along the different coordinates. This linear property of Equation (3.1) is also the basis upon which the splitting numerical method has been developed. It also allows the application of the superposition principle, i.e., the concentration at a given point (x, y, z) to be the sum of the concentration caused by all puffs.

3.2 DEVELOPMENT OF A LONG-RANGE AIR POLLUTANT TRANSPORT AND DIFFUSION MODEL WITH ATMOSPHERIC CHEMISTRY

The basic structural element in developing the model will be a "puff" which allows proper time and space simulation of any type of source. For example, continuous surface and linear sources can be conveniently approximated by instantaneous sources, which are shaped as rotational ellipsoids with a vertical axis and a Gaussian concentration distribution (Syrakov *et. al.*, 1983).

Using the combined Lagrangian-Eulerian approach, it is assumed that the polluted air mass is transported by air currents, which are considered to be external to the model. For simplicity, it is assumed that during its motion the polluted volume does not undergo any dynamical deformation, but only diffuses under the action of the turbulence.

The continuous pollution field is formed by periodically created puffs in the different cells; these puffs are transported by the flow and diffused by the turbulence. The location of the puff is determined by the position of its center, and the displacement velocity is equal to the wind speed at that point. In this case, the coordinates of the puff center change according to:

$$x_c(t) = x_c(t - \Delta t) + u(x_c, y_c, z_c)\Delta t$$

$$y_c(t) = y_c(t - \Delta t) + v(x_c, y_c, z_c)\Delta t \tag{3.6}$$

$$z_c(t) = z_c(t - \Delta t) + w(x_c, y_c, z_c)\Delta t$$

where Δt is a properly chosen time interval. The wind components *u(x,y,z)*, *v(x,y,z)*, *w(x,y,z)* are obtained from the standard meteorological observations or numerical weather forecasting models (Syrakov *et. al.*, 1983). They are assumed to be constant during time interval T_c between two consecutive observations, usually 12 to 24 hours apart.

New puffs are emitted at times equal to T_c, a simplification which is not a principal cause of uncertainty in the model. In order to achieve satisfactorily smooth trajectories, the time interval Δt is taken small in comparison with T_c.

Equation (3.6) clearly demonstrates the elegancy of using the Lagrangian approach in describing the advection process.

3.2.1 Horizontal diffusion

For the determination of the analytical expression for the horizontal diffusion we choose a local Cartesian coordinate system whose origin coincides with the puff center. In the model, it is assumed that the horizontal diffusion process is defined by the equation:

$$\frac{\partial q}{\partial t} = \frac{\partial}{\partial \zeta_1} K_1 \frac{\partial q}{\partial \zeta_1} + \frac{\partial}{\partial \zeta_2} K_2 \frac{\partial q}{\partial \zeta_2} + \frac{\partial}{\partial \zeta_3} K_3 \frac{\partial q}{\partial \zeta_3} \tag{3.7}$$

where $q(\zeta_1, \zeta_2, \zeta_3)$ is the pollutant concentration at a point $(\zeta_1, \zeta_2, \zeta_3)$ and K_1, K_2, K_3 are the turbulent diffusion coefficients (Djolov, 1991).

The turbulent diffusion process in the horizontal direction, in accordance to the experimental evidence, is considered isotropic. If during a time interval Δt, $K_1 = K_2 = K$ and K_3 do not significantly change in time and space, Equation (3.7) describes a Fickian type diffusion, which is nonisotropic in vertical direction. The initial condition is:

$$q(r, \zeta_3, 0) = \begin{cases} A \exp(-\frac{r^2}{a^2} - \frac{\zeta_3^2}{a_3^2}) & |r| \le r_0, \quad \zeta_3 \le \zeta_3^0 \\ 0 & |r| > r_0. \quad \zeta_3 > \zeta_3^0 \end{cases} \tag{3.8}$$

where $r^2 = \zeta_1^2 + \zeta_2^2$; r^0 and ζ_3^0 are the radius and semi-thickness of the volume source; and A is a constant which should be determined from the mass conservation condition (Djolov, 1991).

The solution of Equation (3.7) subject to the initial condition Equation (3.8) and zero boundary condition at infinity can be found in the paper by Djolov and Syrakov (1971). In this paper it is shown that the solution can be rather simplified if the puff is considered infinite. The puff boundary condition is then taken as the surface where the concentration is p%, (usually p = 0.01) of the puff center concentration. This rather accurate approximation is admissible because of the fast exponential decrease of the concentration with the distance from the center. This allows the constant A in the Equation (3.8) to be determined as:

$$A = \frac{Q_0}{\pi^{3/2} a^2 a_3} \tag{3.9}$$

where Q_0 is the total pollutant mass of the source and a, a_3 are dispersions given by:

$$a = \frac{r_0}{\sqrt{-\ln p}} \qquad a_3 = \frac{\zeta_3^0}{\sqrt{-\ln p}} \tag{3.10}$$

The solution of Equation (3.7) has the form:

$$q(r, \zeta_3, t) = \frac{Q_0}{\pi^{3/2}} \frac{\exp\left(-\frac{r^2}{a^2+4Kt} - \frac{\zeta_3^2}{a_3^2+4K_3t}\right)}{(a^2+4Kt)\sqrt{a^2+4K_3t}} \tag{3.11}$$

Equation (3.11) gives the opportunity to consider a puff at any moment t as an infinite volume source with time dependent dispersions. Transforming the results to a fixed coordinate system and assuming that the pollutants are reflected by the earth's surface, the concentration at a given point x,y,z, and time t is given by:

$$q(x, y, z, t) = \frac{Q_0}{\pi^{3/2}} \frac{\exp\left(-\frac{(x-x_c(t))^2+(y-y_c(t))^2}{a^2(t)}\right)\left(\exp\left(-\frac{(z-z_c(t))^2}{a_z^2(t)}\right) + \exp\left(-\frac{(z+z_c(t))^2}{a_z^2(t)}\right)\right)}{a^2(t)\, a_z(t)} \tag{3.12}$$

where

$$a^2(t) = a^2(t-\Delta t) + 4K\Delta t \tag{3.13}$$

$$a_z^2(t) = a_z^2(t-\Delta t) + 4K_z\Delta t$$

In Equations (3.7) and (3.8), $K_z = K_3$, and $a_z = a_3$. The concentration at the earth surface *(z=0)* is:

$$q(x, y, z, t) = \frac{2Q_0}{\pi^{3/2}} \frac{\exp\left(-\frac{(x-x_c(t))^2+(y-y_c(t))^2}{a^2(t)} - \frac{z_c^2(t)}{a_z^2(t)}\right)}{a^2(t)\, a_z(t)} \tag{3.14}$$

3.2.2 Vertical diffusion

The function q_z which describes the vertical pollutants' distribution is determined again in the framework of Eulerian approach in the moving coordinate system with origin at the respective puff center. The diffusion process, which is caused by microscale turbulence in vertical direction, is described by the semi-empirical turbulent diffusion equation:

$$\frac{\partial q_z}{\partial t} = K_Z \frac{\partial^2 q_z}{\partial z^2} \quad , \quad K_z(z) = const. \tag{3.15}$$

which is solved subject to the following initial and boundary conditions:

$$q_z = \delta(z - z^c) \quad , \quad t = 0 \tag{3.16}$$

$$K_z \frac{\partial q_z}{\partial z} = \begin{cases} \beta q_z & , \quad z = 0 \\ 0 & , \quad z = z_i \end{cases} \tag{3.17}$$

where β (deposition velocity) is a constant of interaction between the pollutants and the underlying surface and z_i is the mixing height (Djolov *et. al.*, 1987), and δ is the delta function.

Equations (3.15), (3.16) and (3.17) describe the different cases of possible vertical diffusion in PBL. They are schematically shown in Figure 1.

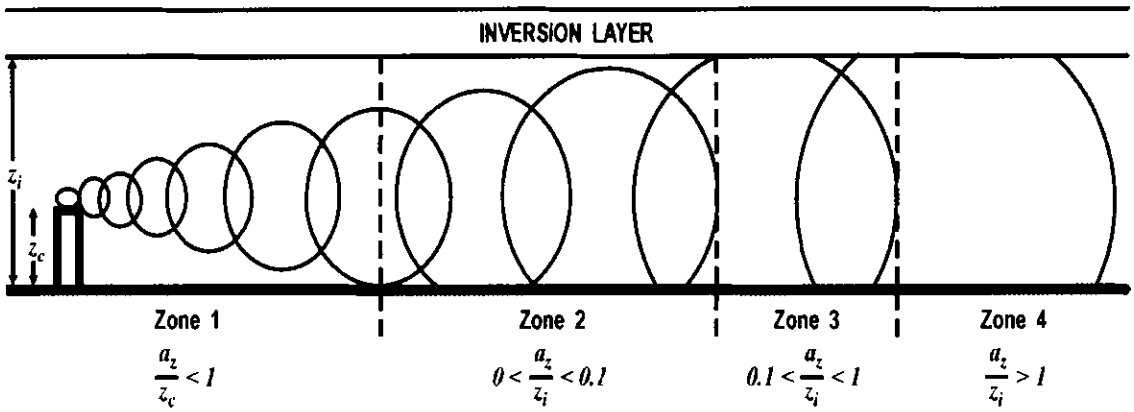

Figure 3.1: Zones with different vertical diffusion conditions possible in the PBL (Djolov *et. al.*, 1987)

In the cases when the puffs have not reached the ground the obvious solution $q_z = 0$. Most frequently, the diffusion process is realized in the conditions shown in Zone 3, i.e., between partially absorbing and reflecting inversion layer at height z_i. The Zone 4 shown in Figure 3.1 corresponds to the expected asymptotic case where at sufficiently large distances the concentration is constant at the different heights due to the continuous action of the vertical turbulent exchange. In Zone 2 the diffusing pollutants interact only with the underlying surface and do not reach the upper reflecting surface ($z_i = \infty$).

The solutions to Equation (3.15), after appropriate integration to determine the volume source solutions from the point sources, for the different zones exhibited in Figure 3.1 at height $z = 0$ (ground level) are according to Djolov *et. al.* (1987), as follows:

Zone 1:

$$q_z = 0 \tag{3.18}$$

Zone 2:

$$q_z = 2\exp\left(-\frac{(z_c)^2}{a_z^2}\right)\left(1 - \sqrt{\pi}\frac{b}{a_z}e^{\eta^2}erfc\,(\eta)\right)/\sqrt{\pi}a_z \tag{3.19}$$

Zone 3:

$$q_z = \frac{1}{z_i}\sum_n \frac{2\cos\alpha_n \cos\alpha_n\,(1 - z_c/z_i)}{(1 + \sin 2\alpha_n)\,/2\alpha_n}\exp\left(-\frac{b^2}{a_z^2\tan\alpha_n}\right) \tag{3.20}$$

where α_n are determined from the equation:

$$\alpha\tan\alpha = \beta\frac{z_i}{K_z} \tag{3.21}$$

Zone 4:

$$q_z = \frac{1}{z_i}\exp\left(-\frac{\delta}{2z_i}\right) \tag{3.22}$$

In the above formulae the following variables corresponding to the chosen simulation are used:

$$a_z^2(t+\Delta t) = a_z^2(t) + 4K_z\Delta t \quad , \quad a_z(0) = 0$$

$$b(t+\Delta t) = b(t) + 2\beta\Delta t \tag{3.23}$$

$$\eta = \frac{(z^c + b)}{a_z}$$

Equations (3.23) allow to take into account the horizontal inhomogeneity of the vertical turbulent exchange coefficient. The function q_z depends on K_z and time through a_z, and the change in the position of the volume in regions with different K_z is reflected by the rate of change of a_z.

3.2.3 Deposition mechanisms and pH determination

A simplistic technique in dealing with the deposition processes in the model is to assume a constant rate of change, λ.

The wet-deposition function (q_w) describes the wash-out of pollutants from the atmosphere due to precipitation. The function (q_w) is calculated from:

$$\frac{\partial q_w}{\partial t} = -\lambda_w t \quad , \quad q_w(0) = 1 \tag{3.24}$$

where λ_w is the wash-out coefficient. Determination of λ_w will be addressed later in this section.

A solution for Equation (3.24) is:

$$q_w(t)\delta_w \exp(-\lambda_w t) \tag{3.25}$$

where $\delta_w = 1$ during the rain and $\delta_w = 0$ without rain.

The dry-deposition is calculated using the boundary condition for the pollutant i (Equation 3.17). The dry deposition parameter β varies between infinity (totally absorbing surface) and zero (totally reflecting surface). The typical interval for the variation of β over land surfaces is between 1 cm.s^{-1} to 15 cm.s^{-1}. Specific interval values used in the LED model are summarized in Table 3.2 for β, and in Table 3.3 for λ_w in the next section.

The dry- and wet quantities deposited on the ground are summed. For each time step, the total concentration of the pollutant in each puff is reduced by the magnitude of the deposited mass.

The development of a model for the calculation of the pH value of precipitation relies on the theoretical understanding of the mechanisms of interaction of pollutants with clouds/rain physics as well as experimental data for the acidity of precipitations.

At the beginning of 1980 special networks for measuring of pH value of precipitations were created, and these networks are already an integral part of GEMS (Global Environmental Monitoring Network).

The extensive data from the pH networks allowed for the establishment of a statistical correlation between the anthropogenic ions of sulfates and nitrates in precipitations and the pH values. The greater part of the variations in the pH values are satisfactorily explained by

the changes in the concentrations of SO_4^{2-} and NO_3^-. In most cases even the variations of the sulfate anions is sufficient to derive reliable semi-empirical relations for the pH calculations.

In the paper by McNaughton (1981) the results of the study on the acidity of precipitations in Northern America are presented. Logarithmic type of regression equations for pH using as predictors the anion of both sulfate and nitrate concentrations in precipitations, or only sulfate concentrations are presented and validated in his work. The use of logarithmic type of equations secures smoothening of the extreme high and low values of pH.

The LED model predicts the concentrations of the SO_4^{2-} and NO_3^- in ambient air. Therefore, there is a need to use all available theoretical and experimental knowledge on the processes of scavenging and wash-out of atmospheric pollutants by atmospheric precipitation. Amongst the several wash-out coefficients the following expression has been adopted:

$$\lambda_w = \frac{[c]_p}{[c]_a}$$

where λ_w denotes wash-out coefficient, $[c]_p$ is the concentration of pollutant in the precipitation, $[c]_a$ is the concentration of pollutant in the air. The advantage of this expression lies in its simplicity, clear physical meaning and easy experimental determination.

The wash-out process in the atmosphere can be considered as a two-stage process. The first in-cloud process describes the role of the pollutants in the creation of hydrometeors (condensation particles). The second deals with the processes during the path of the falling rain drops.

The main mechanisms in the creation of hydrometeors are: 1. molecular diffusion, 2. Brownian diffusion, 3. collision and scavenging, 4. dilution of gases and 5. creation of drops on a particle nuclear. Mechanism 1 is effective for particles with diameter $d < 0.1\,\mu m$. The Brownian diffusion is also effective for these diameters but is a considerably slower process. The collision and scavenging process realizes in the under-cloud areas. It depends on the droplet falling velocity and is effective for particles with diameters $d > \mu$. The main air pollutants SO_2, NO_2, gas phase nitric acid and ammonia dilute well in water, whilst NO has a very limited solubility. The dilution velocity depends on the surface area of the rain droplets, temperature, physical-chemical properties of the particle, and pH value of the droplets. The most important mechanism for the in-cloud stage of pollutant removal is nuclear condensation. The short revue of the main in-cloud mechanisms for pollutant removal demands knowledge on the microphysics of the clouds, the rain systems configuration and flux of pollutants.

In the paper by Scott (1978) three typical types of cloud systems are considered theoretically, which are applicable for Bergeron (winter) clouds, warm clouds and convective clouds. Using the equations for precipitation formation during their free fall, Scott (1978) has obtained the following relationship:

$$\lambda_w = \frac{14000 M_g(0)}{R^{0.88}} + \frac{750(1 - 4.41x10^{-2}R^{0.88})}{(1.56 + 0.44 \ln R)}$$

where R is the precipitation intensity measured in $mm\,h^{-1}$. $M_g(0)$ is the mass of the pollutants associated with the hydrometeors and has the form:

$$M_g = \{0\} \quad \textit{winter clouds}$$

$$M_g = 0.1 \; \textit{warm clouds}$$

$$M_g = 0.75[(4.41x10^{-2} - R^{0.88})(435R^{-0.71} + 1200)/(8450 + 2383 \ln R)] \; \textit{convective clouds}$$

It should be noted that the wash-out coefficient is a function of only one easily measurable precipitation characteristics, namely, the intensity of rain.

Using the log type of regression equations for the pH calculation, the definition of wash-out coefficient and the formula for its calculation proposed by Scott (1978), one can derive the following expression for the pH used in the LED model:

$$pH = a\left[-\log\left\{10^{-6}\lambda_w\left(\frac{2}{96}[SO_4^{2-}] + \frac{1}{62}[NO_3^-] + [background]\right)\right\}\right] + b. \tag{3.26}$$

The regression coefficients a and b for the different types of clouds are taken from the study by McNaughton (1981). The coefficients before the anions in the equation take into account the different valences of the anions, and 10^{-6} results from the conversion of mol/l to mg/m^3. The background value of pH is taken to be the contemporary accepted value of 5.6.

The success of the application of Equation (3.26) depends on the appropriate determination of the wash-out coefficient which varies seasonally. This requires a proper parameterization of the time and space climatic peculiarities of the precipitations taking place in different seasons for the specific region of study.

3.2.4 Atmospheric chemistry

The major anthropogenic pollutants present in the atmosphere are sulphur, nitrogen and hydrocarbon compounds as discussed in Chapter 2. In this model only sulphur and nitrogen oxide chemical transformations are modelled, because their abundance and relatively long residence times in the atmosphere are the major reason for the formation of acidic deposition.

The most important mechanism for the formation of acid deposition is the direct transformation of sulphur dioxide to sulphate:

$$SO_2 \xrightarrow{k_1} SO_4^{2-} \tag{3.27}$$

where $k_1(t,r)$ is the constant of transformation which is a function of the time and space. The k_1 value can be obtained assuming that it can be written as a sum of homogeneous and heterogeneous components. The rate of homogeneous transformation is taken from Endlich *et. al.* (1984), where it is calculated as a function of the solar insulation using data for a clear atmosphere. The heterogeneous component is chosen on the basis of the review presented by Moller (1980). It should be noted that in Equation (3.27) only the balance of S is preserved.

The chemical transformations which NO and NO_2 undergo are rather complicated. Smog chamber measurements of the typical reactions of NO compounds show that 90% of them result in the formation of NO, NO_2, PAN (Peroxyacetyl nitrate) and NO_3. This allows the chemical transformations of these five components to be included in the model. The equations describing the rate of transformation of the nitrogen compounds due to chemical and physical processes are (Brodzinsky *et. al.*, 1984):

$$\frac{d}{dt}[NO_2] = -k_2[NO_2] + k_4[PAN] \tag{3.28}$$

$$\frac{d}{dt}[PAN] = 0.5k_2[NO_2] - (0.5k_3 + k_4)[PAN] \tag{3.29}$$

$$\frac{d}{dt}[NO_3] = 0.1(k_2[NO_2] + k_3[PAN]) \tag{3.30}$$

$$\frac{d}{dt}[HNO_3] = 0.4(k_2[NO_2] + k_3[PAN]) \tag{3.31}$$

$$0 = [NO_2] - k_5[NO] \tag{3.32}$$

Where k_2, k_3, k_4 and k_5 are the rates of chemical transformation as summarized in Table 3.1. The equilibrium of NO and NO_2 reflects the photolysis of NO_2 to NO and the photo and thermal pathways of NO to NO_2 conversion. The rate equations shown in equations (3.27) to (3.32) are linear. The tranformation constants can be a function of time and space. The chemical reactions in the model are calculated for every puff at every time step after the completion of the transport and diffusion processes.

3.2.5 The planetary boundary layer

The investigation of dynamic processes in the planetary boundary layer (PBL) presents a definite theoretical challenge and plays a growing role in the solution of a number of practical tasks. The improvement of large-scale air quality models depends, to a certain degree, on the proper inclusion of the PBL in the numerical models. Further progress in a number of micro- and mesoscale problems such as: air pollution, development and dispersal of fog, formation of late spring and early fall frosts, wind load on high buildings, convective cloud dynamics, local winds and others, is closely connected with the use of a proper PBL model.

The investigation of PBL dynamics has developed on the basis of sophisticated models which use equations for higher-order moments and appropriate hypothesis for the system equation closure (Deardorff, 1974). This approach allows one to clarify the nature of physical processes taking place in the PBL and secures a basis for further investigations. The use of such models for the solution of practical problems is not feasible because of computer and other difficulties. In a number of cases simpler PBL models can give sufficiently accurate results (Yordanov (1975); du Vachat and Musson-Genon (1982); Arya and Sundarajan (1976); Shir and Bomstein (1977)).

A description of the transport and diffusion of the polluted air volumes requires the wind fields and horizontal and vertical diffusion coefficients. They can be obtained from a proper planetary boundary layer (PBL) model. In this model a simple and reliable PBL model described by Yordanov *et. al.* (1983) and Syrakov *et. al.* (1983) was used.

A usefull feature to LED, amongst the long-range models known to the author, is the use of an appropriate atmospheric boundary layer (ABL) model calculating its dynamics and turbulent characteristics. Usually, long-range models are driven by the output of the best available meso-scale forecast models, or in the diagnostic case by observed meteorological fields. In both cases, however, the ABL dynamics are not properly represented due to the restrictions in the model vertical resolution or insufficient number and distribution of observations. This is a serious simplification since the changes in wind velocity and atmospheric stability occurring in the ABL dramatically influence the transport and diffusion processes.

Thus, for example, the value of the vertical exchange coefficient changes by orders of magnitudes depending on the stability conditions in the ABL. The magnitude and direction of the wind velocity vary considerably with height and the angle between the geostrophic and surface wind can surpass 50-60 degrees. The wind variations in the ABL are even more complicated when baroclinicity effects are present. Turbulent friction convergence creates vertical motions that in spite of their small value, lead to substantial displacement of the polluted air volumes because of their perseverance. Another important consideration is that most of the emissions of pollutants and trace gases are released from sources located near the earth surface up to a few hundred meters. The existence of frequent inversion layers at the top of the ABL forces the diffusion and transport of pollutants to take place in the lower parts of the atmosphere for prolonged periods of time. These facts underline the importance of inclusion of an appropriate ABL model in any turbulent dispersion package aimed at modelling long-range diffusion and transport phenomena.

In the Lagrangian-Eulerian Diffusion (LED) model the two-layer parametric ABL model proposed by Yordanov *et. al.* (1983), is included. The ABL model is driven by the following meteorological variables: 1) the geostrophic wind vector v_g; 2) the potential temperature $\vartheta_H$at the top of the ABL; 3) surface temperature ϑ_s which can be calculated from the energy balance equation or taken from observation or numerical weather forecast model. Note that these are the boundary conditions for the turbulent ABL equations for momentum and heat exchange at arbitrary stratification.

From these external ABL meteorological variables, and the local parameters: the Coriolis parameter - f, the roughness parameterz_0 and the buoyancy parameter$\beta = g/\bar{\vartheta}$, the following non-dimensional external parameters can be composed:

$$Ro = \frac{|v_g|}{fz_0} \tag{3.33}$$

the Rossby number, and

$$S = \frac{\beta(\vartheta_H - \vartheta_s)}{f|v_g|} \tag{3.34}$$

the external stratification parameter.

These parameters uniquely determine the turbulent regime in a horizontally homogeneous ABL. The details of the ABL model are presented in Yordanov *et. al.*, (1983).

3.3 Development of the numerical model

The development of a numerical model for long-range transport and diffusion of air pollutants requires the satisfaction of two, to a certain degree conflicting conditions: an accurate and realistic description of the phenomenon, and minimal computational run-time.

The numerical simulation of the long-range pollutants with atmospheric chemistry requires a proper combination of the models outlined in Section 3.1 and 3.2. The incorporation of the PBL model in the long-range pollutant transport model is presented by Syrakov *et. al.*, (1983).

The input information consists of the time intervals Δt, Δt_c, Δt_i: the time step, the period during which the meteorological conditions are assumed steady, the integration period, the horizontal turbulent exchange coefficient K, the decrease of the concentration p% at the puff boundary, the minimum observable concentration q_{min}; and the source parameters: Q_0, the

total pollutant emitted in a given grid cell $\Delta x \Delta y$ for time Δt; x_c, y_c,z_c, the initial coordinates of the puff center; and ζ_3^0, the vertical semi-thickness of the ellipsoid.

The initial dispersions of the volume source are calculated in accordance with Equation (3.10), where $r^0 = (\Delta x \Delta y/\pi)^{1/2}$. The consecutive location of every puff is determined by Equation (3.6) and the surface concentration field by Equation (3.14). The concentrations are calculated and summed for the points which satisfy the following conditions:

(a) They are located within the puff, i.e., their distances to the point (x_c,y_c) is less or equal to:

$$r_\varphi^2 = -a^2(t) \ln \frac{p(1 + \exp(-4z_c^2(t)/a_z^2(t)))}{2\exp(-z_z^2(t)/a_z^2(t))} \tag{3.35}$$

(b) The concentration is greater or equal to q_{min}. These are the points for which the distance to (x_c,y_c) is less or equal to:

$$r_c^2 = -a^2(t) \ln \frac{q_{min}\pi^{3/2}}{2Q_0} \frac{a^2(t)a_z(t)}{\exp(-z_c^2(t)/a_z^2(t))} \tag{3.36}$$

The combination of equations (3.11) and (3.12) gives the criterion:

$$(x - x_c(t))^2 + (y - y_c(t))^2 \leq min(r_\varphi^2, r_c^2) \tag{3.37}$$

The chemical transformations described by equations (3.27) to (3.32) are calculated for each volume for each time step, following the calculation of transport and diffusion processes of the puff. The equations are integrated using an implicit scheme. The rates of chemical transformations are shown in Table 1.

Table 3.1: The rates of chemical transformation

	$k_1(s^{-1})$	$k_2(s^{-1})$	$k_3(s^{-1})$	$k_4(s^{-1})$	$k_5(s^{-1})$
Day	10^{-6}	2.8 x 10^{-5}	2.8 x 10^{-5}	0	2
Night	10^{-6}	5.6 x 10^{-6}	0	5.6 x 10^{-6}	50

The constraints of dry- and wet deposition for winter time are taken from Endlich *et. al.*, (1984) and Brodzinsky *et. al.*, (1984) and summarized in Tables 2 and 3 as previously mentioned.

Table 3.2: Deposition velocities for selected species (β) / m.s^{-1}

		SO_2	SO_4^{2-}	NO_2	PAN	NO_3^-	HNO_3	NO
Night	**Sea**	0.0035	0.0025	0.0007	0.0007	0.006	0.0007	0.0007
	Land	0.0007	0.0060	0.0007	0.0007	0.006	0.0007	0.0007
Day	**Sea**	0.0055	0.0035	0.002	0.0025	0.006	0.01	0.002
	Land	0.0065	0.0080	0.002	0.0025	0.006	0.01	0.002

Table 3.3: Seasonal wash-out coefficients utilized in LED (λ_w) / h^{-1}

	Pollutant						
Season	**SO_2**	**SO_4^{2-}**	**NO_2**	**PAN**	**NO_3^-**	**HNO_3**	**NO**
Summer	0.32E-04	0.75E-04	0.80E-05	0.16E-04	0.75E-04	0.37E-04	0.80E-05
Autumn/Spring	0.26E-04	0.74E-04	0.66E-05	0.13E-04	0.74E-04	0.37E-04	0.66E-05
Winter	0.19E-04	0.40E-04	0.47E-05	0.94E-05	0.40E-04	0.20E-04	0.47E-05

3.4 SUMMARY

The LED model development discussed in this Chapter meets the demands for studying the long-range transport and turbulent diffusion of atmospheric pollutants and trace gases. It has a strong atmospheric physics basis by recognizing the theoretical understanding and experimental facts of turbulent diffusion, being of micro-scale nature in the vertical direction and large-scale in the horizontal direction. This makes it possible to postulate an appropriate formula and derive analytical solutions that allow the calculation of concentrations in a Lagrangian framework using the emitted puffs as a basic element. The LED model has additional advantages in its flexibility to incorporate new developments in long-range transport and diffusion physics. It has two essential sub-models: planetary boundary layer and chemical species transformation. The PBL model can easily be upgraded to incorporate the new emerging knowledge in non-local turbulent transport phenomenon which is very relevant to the atmospheric conditions of tropical regions. The chemical transformation sub-model can incorporate non-linear chemistry as well as new chemical species relevant to the region. In addition the model for pH calculation provides the advantage to evaluate the impact of acid rains on the fragile ecosystems in the region. Lastly, the Fortran code in which LED has been written makes it user-friendly, allowing its adaptation to different demands relevant to the southern Africa region.

After development and modification of the LED, it can be used to assist in identifying potentially high impact areas. Concentration and deposition fields for specific regions, allow the study of anthropogenic impacts caused by the transport of major air pollutants such as sulphates and nitrogen oxides. The ability to define the relative importance of each source in the total pollution and deposition fields can be used to determine the most effective strategy for decreasing the emissions of a given region.

Chapter 4

LED INPUT PARAMETERS

In this Chapter...

The objective of this chapter is briefly stated (Section 4.1). Section 4.2 gives a detailed description of the modelling domain implemented for this study. Sections 4.3 to 4.6 focuses on the different input parameters utilized by LED for the specific modelling domain. Section 4.7 concludes the chapter by summarizing and pointing out the optimal range of the input parameters utilized in the LED model.

4.1 OBJECTIVES

This section will focus and discuss the input parameters (data) utilized in the LED model, during the various modelling scenarios.

4.2 MODELLING DOMAIN

The modelling domain implemented for this study extends from 10 ° E to 40 ° E and 10 ° S to 35 ° S as illustrated in Figure 4.1. This region covers the southern part of Africa, including Angola, Namibia, Botswana, Zambia, Zimbabwe, Mozambique, Malawi and South Africa.

A Cartesian grid was superimposed on the modelling domain illustrated in Figure 4.1. The 60 x 50 grid (3000 cells) were positioned to conform to a 0.5 ° resolution on the modelling domain. An illustration of the superimposed Cartesian grid is illustrated in Figure 4.2.

The Cartesian grid illustrated in Figure 4.2 was utilized as a reference framework for all simulations in LED.

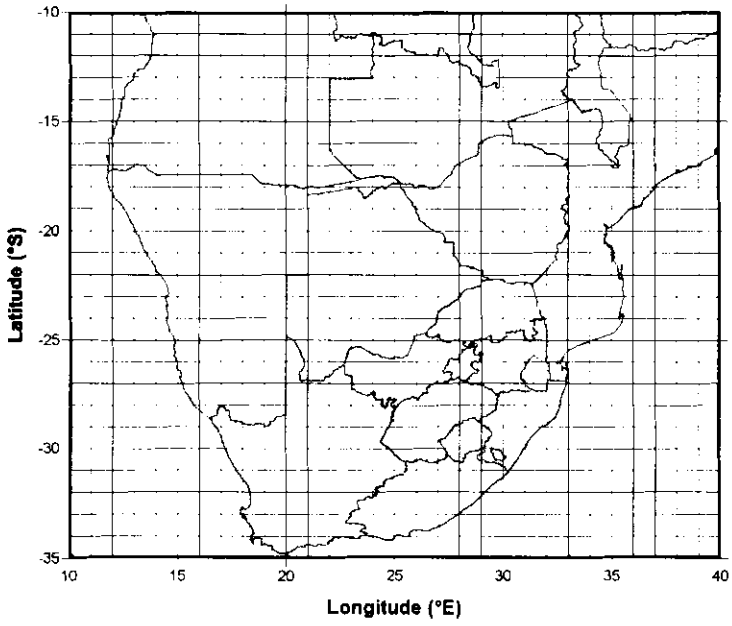

Figure 4.1: Modelling domain implemented for LED

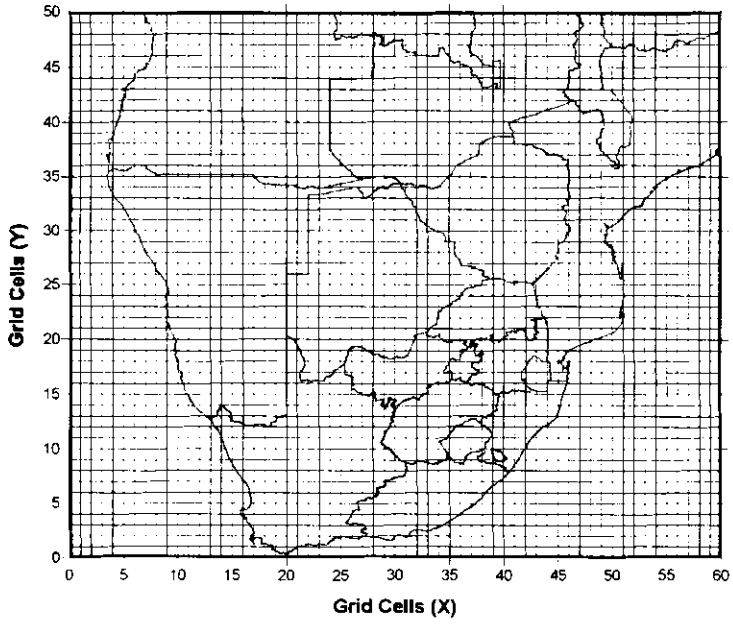

Figure 4.2: Cartesian grid domain implemented for LED

4.3 SURFACE ROUGHNESS

Most surfaces are aerodynamically rough. The surface roughness length (z_0) defines the height at which the wind profile in the absence of buoyancy, extrapolates to a zero wind speed, and is therefore a function of the height of surface roughness elements of the surface. This layer is called the surface roughness layer and defined as the region above the ground in which turbulence is intermitted or not fully developed, as previously mentioned in Chapter 2. z_0 can also be interpreted as the eddie size (turbulence) at the surface.

The surface roughness can be defined as the geometric characteristic of a surface, associated with its efficiency as a momentum sink for the turbulent flow, due to the generation of drag forces and increased vertical wind shear. In micrometeorology, the surface roughness is usually measured by the roughness length, a length scale that arises as an integration constant in the derivation of the logarithmic wind profile relation. In neutral stability the logarithmic wind profile extrapolates to zero wind velocity at a height equal to the surface roughness length. Several formulas exist to parameterize this length scale as a function of the roughness element geometry.

The surface roughness parameters utilized in the LED model conforms to a 0.5 degree spatial resolution Cartesian grid, inferred from the Olson (1992) ecosystem database. The Olson (1992) database describes the global distribution of 72 ecosystem types, then together with satellite remote sensing data of Normalised Difference Vegetation Index (NDVI) infers biomass properties like LAI (Leaf Area Index) and dry matter. Combined with assigned values of canopy height to the ecosystem classes z_0 (meters) (roughness for momentum) are inferred using relationships proposed by Raupach (1992). The roughness parameters (z_0) utilized for the specific modeling domain in LED were generated and obtained from the Max-Planck Institute, Mainz, Germany. A detailed methodology on the generation of the roughness parameters (z_0) can be found in Ganzeveld *et. al.*, 2002.

There is a seasonal cycle in the z_0 values through its dependence on the monthly mean LAI values. This seasonal cycle is clearly distinguishable in Figures 4.3 and 4.4, which illustrate the roughness parameters (z_0) utilized in LED for January and July 2000.

4.4 METEOROLOGY

The meteorological data utilized for input in the LED model is taken from the short-range forecasting ETA model routinely run by the South African Weather Service (SAWS).

The ETA model is a well established and frequently used prognostic meteorological model, which is very similar to the older synoptic-scale Nested Grid Model (NGM), forecasting the same atmospheric variables. The ETA model takes its name from the vertical coordinate η (Greek letter êta), defined by Mesinger, 1984. This coordinate is also known as the step-mountain coordinate because the surfaces are represented in the form of steps whose tops coincide with model layer interfaces. The ETA vertical coordinate system was used in order to remove the large errors that are known to occur when computing the horizontal pressure gradient force, as well as the advection and horizontal diffusion, along a steeply sloped coordinate surface. The ETA coordinate system makes the surfaces quasi-horizontal everywhere as opposed to sigma surfaces which can be steeply sloped. Because the ETA coordinate is pressure based and normalized (i.e. quasi-horizontal), it leads to a much simpler solution of the equations of motion. As a result of using this coordinate system, combined with a higher

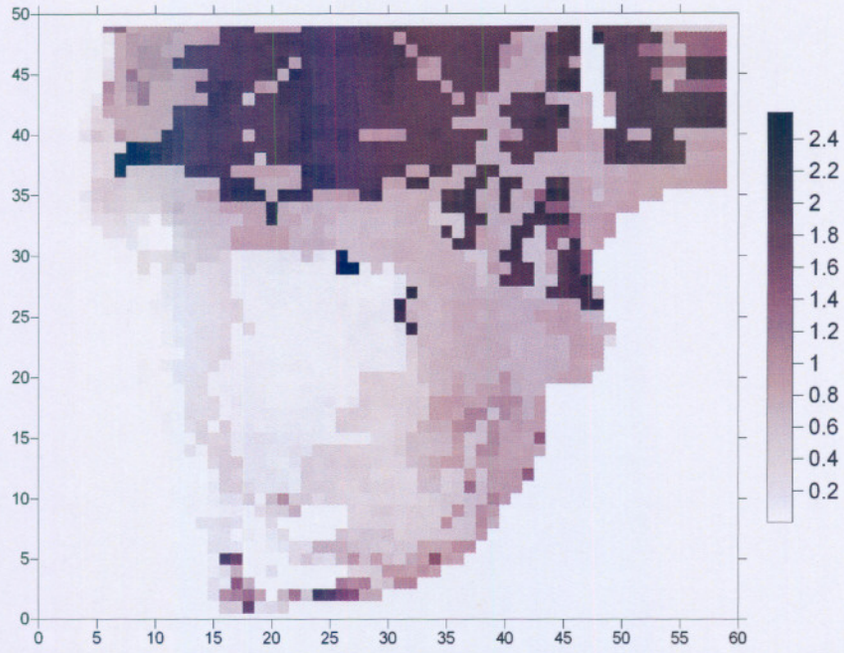

Figure 4.3: Surface Roughness lengths z_0 (meters) for January 2000 for the study domain (Ganzeveld *et. al.*, 2002)

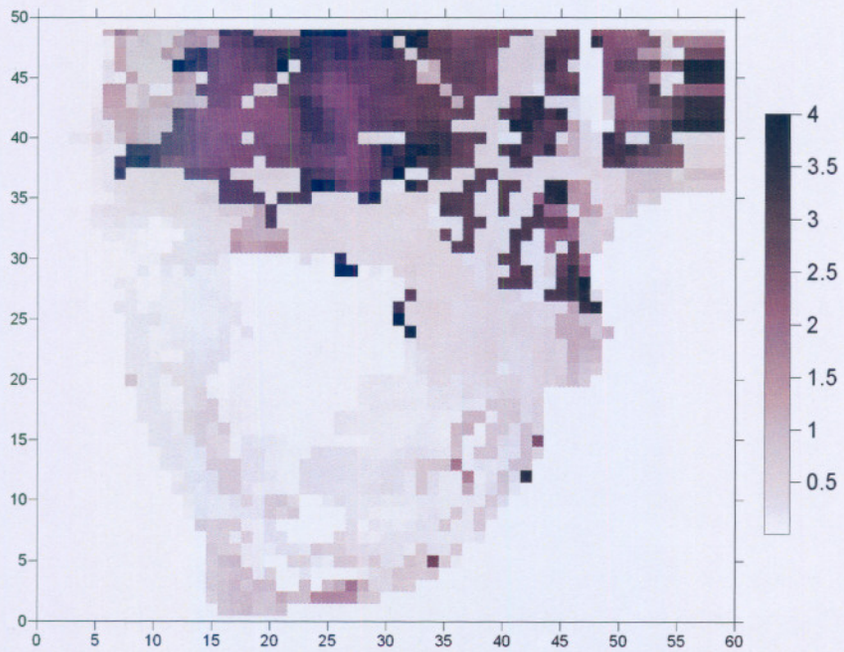

Figure 4.4: Surface Roughness lengths z_0 (meters) for July 2000 for the study domain (Ganzeveld *et. al.*, 2002)

resolution, the ETA model resolves the influence of terrain on the atmospheric dynamics in a better manner.

In the ETA coordinate, the surface terrain heights exist at a discrete set of values or steps. These steps or values are dependent upon the vertical resolution of the model and the height of the mountains. Because of this, terrain appears step-wise rather than smooth and continuous as in the sigma coordinate. Figure 4.5 illustrates the depiction of terrain in the ETA coordinate. For a given range of surface elevations, the êta coordinate allows the terrain to exist on more than one êta surface while in the sigma coordinate, the terrain can only exist on one sigma surface.

Since êta is normalized by a constant value of sea level pressure (1013 hPa) rather than the station pressure, which varies considerably over mountainous terrain, each êta surface is flat when lying over mountains. This allows for more accurate calculation of the horizontal pressure gradient terms because the errors due to elevation changes between adjacent grid points is minimized.

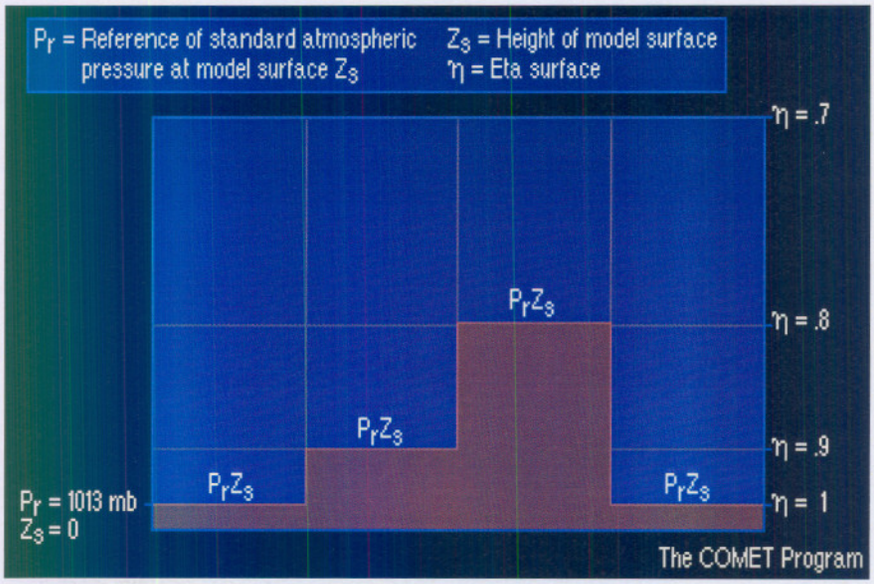

Figure 4.5: ETA Coordinate Depiction of Terrain

In general, model terrain is much smoother than in reality, even in the êta coordinate. Terrain smoothing can be a large source of error in regions affected by small-scale terrain features. However, terrain smoothing is done partly because airflow over complex terrain will otherwise generate small-scale noise in the model that can mask the large-scale signal. For example, vertical motion changes induced by complex terrain can mask the large-scale vertical motion field.

The ETA model uses step-mountain topography in which, after interpolation to the ETA native grid, the step-mountain is raised or lowered to the closest vertical interface. The mountain is represented as discrete steps whose tops coincide exactly with the model layer interfaces. Figure 4.6 illustrates how terrain is handled in the êta coordinate. Points (1) and (2) are raised and lowered respectively to the 0.9 êta surface and point (3) is raised to the 0.8 êta surface.

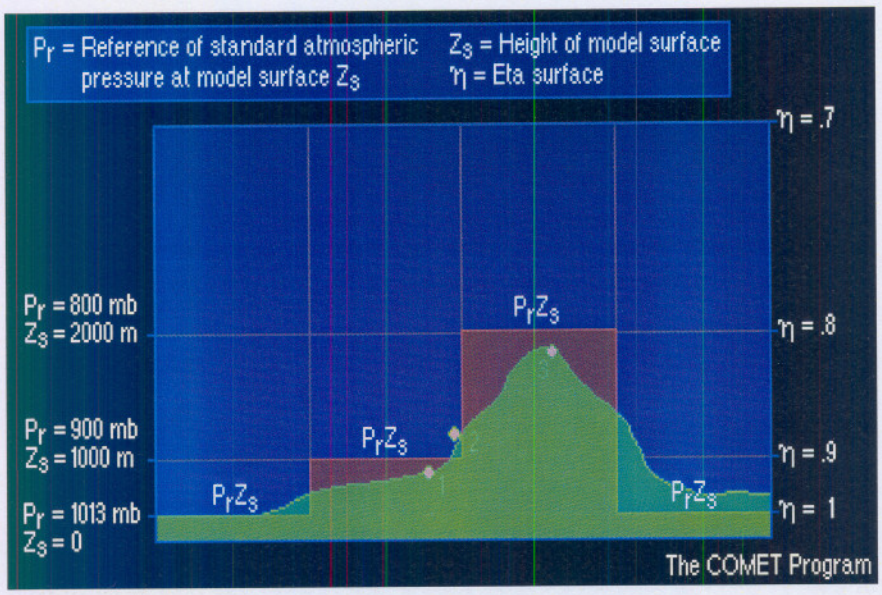

Figure 4.6: ETA Step-Mountain Topography

The US National Center for Environmental Prediction (NCEP) ETA data assimilation and prediction system (Mesinger *et. al.*, 1988; Black, 1994) has been used by the South African Weather Service to provide operational regional forecast guidance since November 1993. SAWS used this model to produce the basic meteorological data for the Southern African Regional Science Initiative (SAFARI) 2000 project. The SAWS ETA model is a hydrostatic model with a horisontal grid spacing of approximately 48 km and 38 vertical levels, with layer depths that range from 20 m in the planetary boundary layer to 2 km at 50 mb. There have been several major ETA Model upgrades at SAWS: in March 1996, August 1998, November 1999, and August 2001. The integrated SAWS domain for the ETA model is southern Africa and surrounding waters, a transformed grid roughly contained in 52 ° S to 1 ° N, 28 ° W to 68 ° E. The vertical coordinates utilized in the model is based on the êta coordinate system, with step-like terrain representation.

The ETA model outputs provided by the SAWS are ASCII map images (0.5 degree) for each of 51 parameters at 12 hour intervals. These ASCII map images are based on a 79 by 133 grid, 53 ° S to 9 ° S, 13 ° W to 53 ° E, half-degree resolution. Parameters available include geopotential height, temperature, potential temperature, dewpoint temperature, specific humidity, relative humidity, u and v wind components, cloud cover and pressure vertical velocity.

Complete data sets for 2000 at 12 hour intervals were obtained from the SAWS, and specific data components utilized by LED were extracted from the main SAWS ETA data sets for the modeling domain discussed in section 4.2. Meteorological parameters utilized by LED include u, v wind components and atmospheric temperature at 700 hPa, as well as atmospheric temperature and precipitable water at the surface. These extracted parameters were combined in appropriate input files for utilization in the LED model for specific modelling scenarios.

Figures 4.7 to 4.10 are graphical illustrations of the resulting u and v wind components

(vectors) at 700 hPa level (about 3000 meters above ground level at the ocean, and 1500 meters above ground level over the Highveld of South Africa) for the 14^{th} of August at 0:00 to the 15^{th} of August at 12:00 at 12-hour intervals superimposed on the LED modelling domain. This series of illustrations clearly illustrate a relatively closed anticyclonic atmospheric recirculation pattern southern Africa experienced during the winter season of 2000. These typical circulation patterns were previously discussed in Chapter 2, Section 2.5.

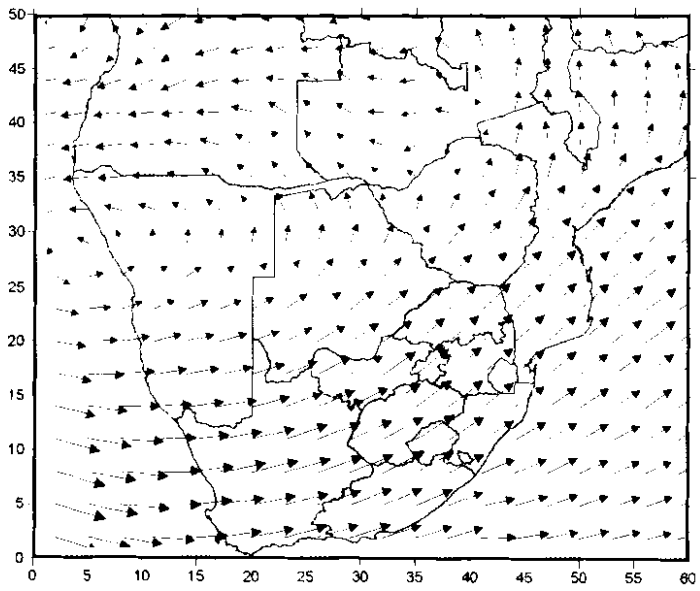

Figure 4.7: Geostrophic wind vectors at 700 hPa for 14 August 2000 at 00:00

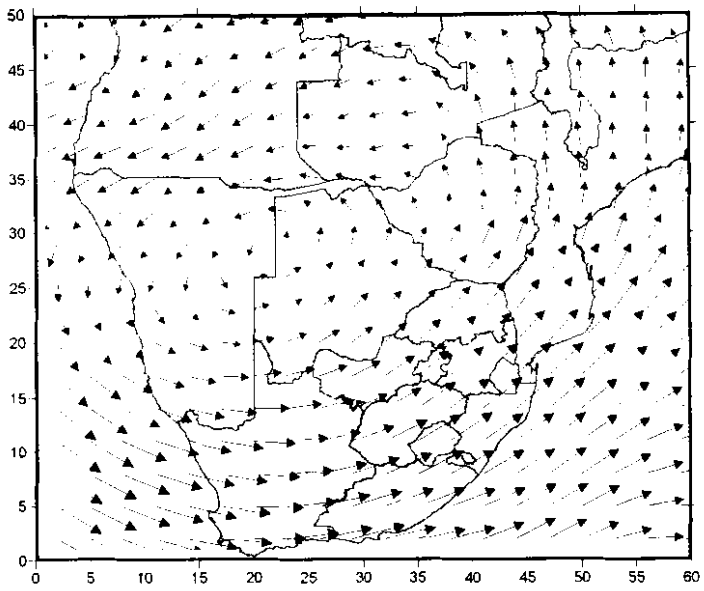

Figure 4.8: Geostrophic wind vectors at 700 hPa for 14 August 2000 at 12:00

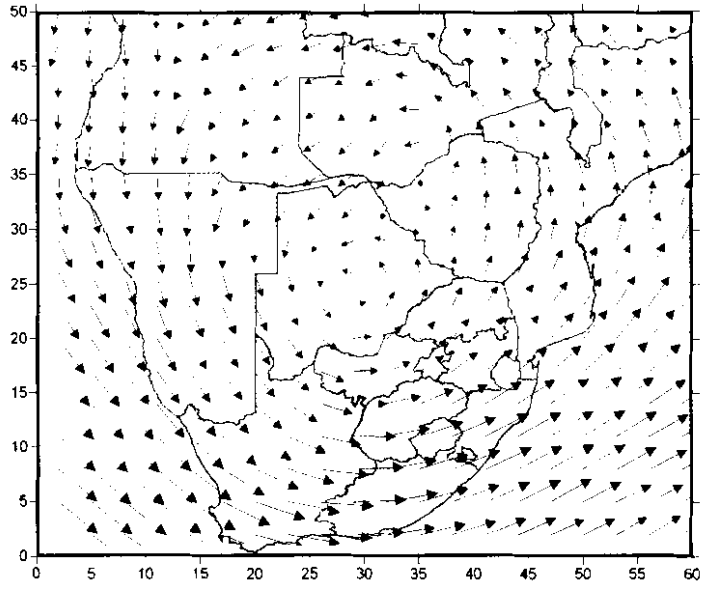

Figure 4.9: Geostrophic wind vectors at 700 hPa for 15 August 2000 at 00:00

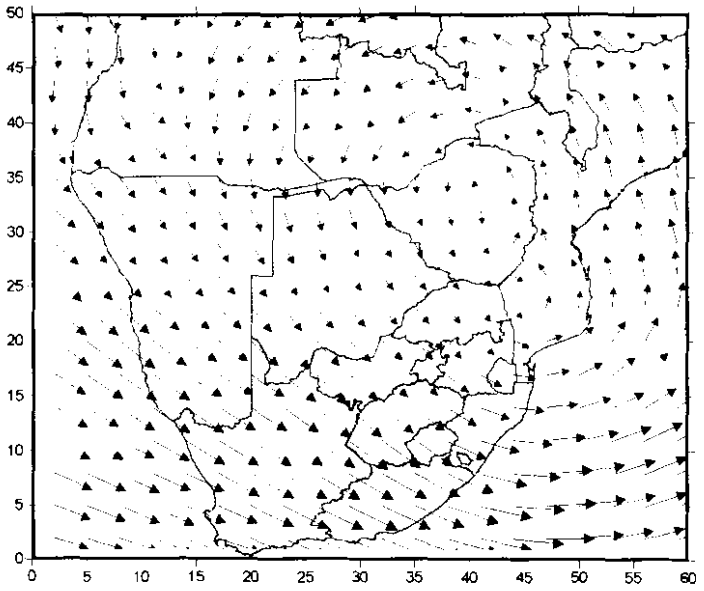

Figure 4.10: Geostrophic wind vectors at 700 hPa for 15 August 2000 at 12:00

4.5 EMISSION DATABASE

The emission database adapted for utilization in the LED model is a customized version of the emissions inventory developed by Fleming and Van der Merwe, 2000, in the framework of the SAFARI 2000 science initiative.

The main aim of the emission project by Fleming and Van der Merwe (2000) was to upgrade and spatially disaggregate 1990 national emissions inventory data to a 20km grid for Africa south of the equator and temporally interpolate them on a monthly basis for the period 1999 to 2001 for the Southern African Regional Science Initiative (SAFARI) 2000 project. The SAFARI 2000 project was an international science initiative aimed at understanding linkages among physical, chemical, biological and anthropogenic processes in southern African systems. A detailed description of the methodology applied for SAFARI 2000 emissions project is available from Fleming and Van der Merwe (2000).

Results from the final emission model by Fleming and Van der Merwe (2000) is structured so that the emissions database can be edited, the driver surfaces be replaced or edited, or annual rates of change are edited, to recreate an output database. While the input of a model run consists of emission values from the database, spatial driver grids and temporal driver values, the output consists of one workspace per emission species that contains grids for every sector, for each year (1990, 1999, 2000, and 2001). The methodology followed and sectors included in the inventory were done according to the guidelines provided by the International Panel on Climate Change (IPCC). All countries that signed and ratified the United Nations Framework Convention on Climate Change (UNFCCC) are required to follow these guidelines in order to compare emissions on an equal basis:

- Energy: Fuel Combustion: Energy Industries
- Energy: Fuel Combustion: Manufacturing Industries

- Energy: Fuel Combustion: Transport
- Energy: Fuel Combustion: Other Sectors (where fuel combustion sources were not included under the abovementioned headings)
- Energy: Fuel Combustion: Other (mining)
- Energy: Fugitive Emissions from Fuels: Solid Fuels (such as charcoal production and coal mining)
- Energy: Fugitive Emissions from Fuels: Oil and Natural Gas (mainly petroleum refining)
- Industrial Processes: Mineral Products (non-energy-related emissions)
- Industrial Processes: Chemical Industry (non-energy-related emissions)
- Industrial Processes: Metal Production (non-energy-related emissions)
- Industrial Processes: Other Production (non-energy-related emissions)
- Solvent and Other Product Use (mainly volatile emissions)

Figure 4.11 shows the total SO_2 emissions summed for all sectors for 2000. The spatial data domain used in the model by Fleming and Van der Merwe (2000) were in 20km^2 grids, registered to the same point and in an Albers projection (central meridian 25 $^\circ$, 1st parallel -30 $^\circ$; 2nd parallel -6 $^\circ$; Cape datum).

As mentioned previously the emission database from Fleming and Van der Merwe (2000) was customized to fit LED. The centre points of all the emission grids from Fleming and Van der Merwe (2000) were converted from the original Albers geographical projection to a latitude/longitude geographical projection for LED. The resulting emission points from the conversion were summed into a 0.5 $^\circ$ resolution latitude/longitude Cartesian grid. Quality assurance and quality control procedures were built into the conversion process to verify final emission values for both emission inventories. Moreover, only the section pertaining to the LED modelling domain was utilized from the final emission inventory grid for LED in all modelling scenarios. Sulfur emissions emanating from the oceans and DMS mechanisms, were not considered in the LED simulations.

Figure 4.12 is a graphical illustration of the final emissions grid for SO_2 for all sources for 2000, utilized in LED for the modelling scenarios, while Figure 4.13 indicate the total NO_X emission for all sources for 2000.

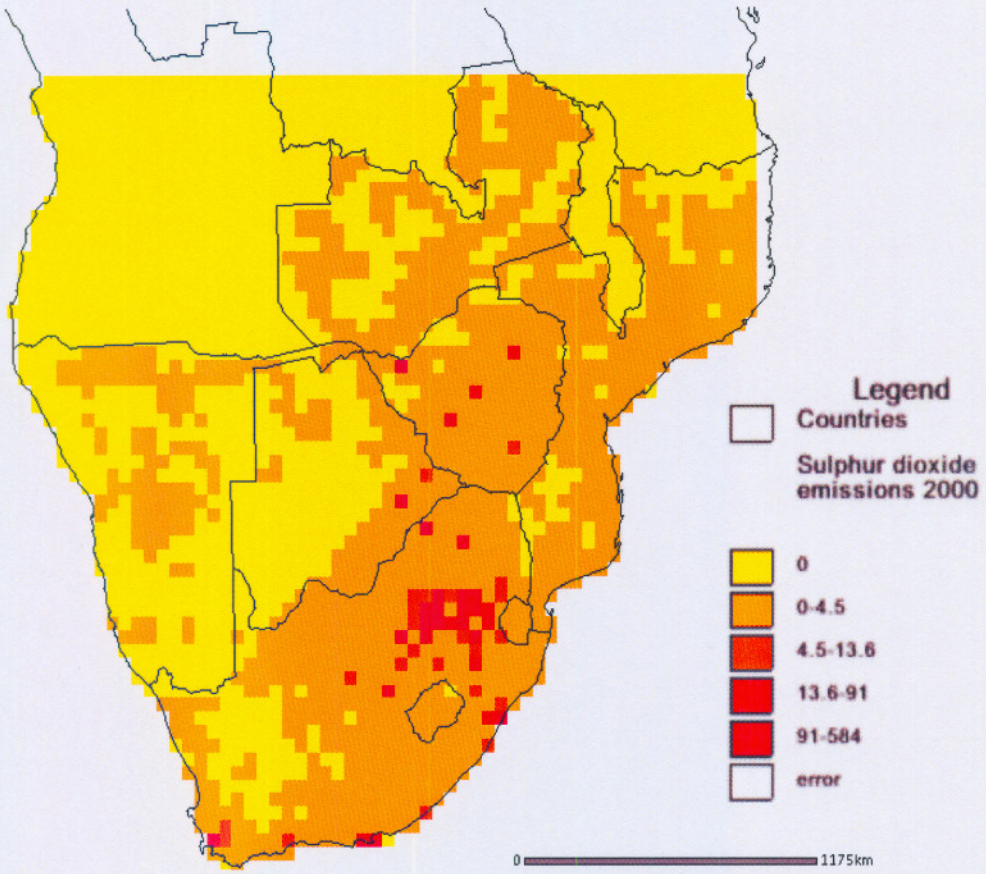

Figure 4.11: Sulphur Dioxide (SO_2) emissions summed over all sectors for 2000. Units in Gg/annum (Fleming and Van der Merwe, 2000)

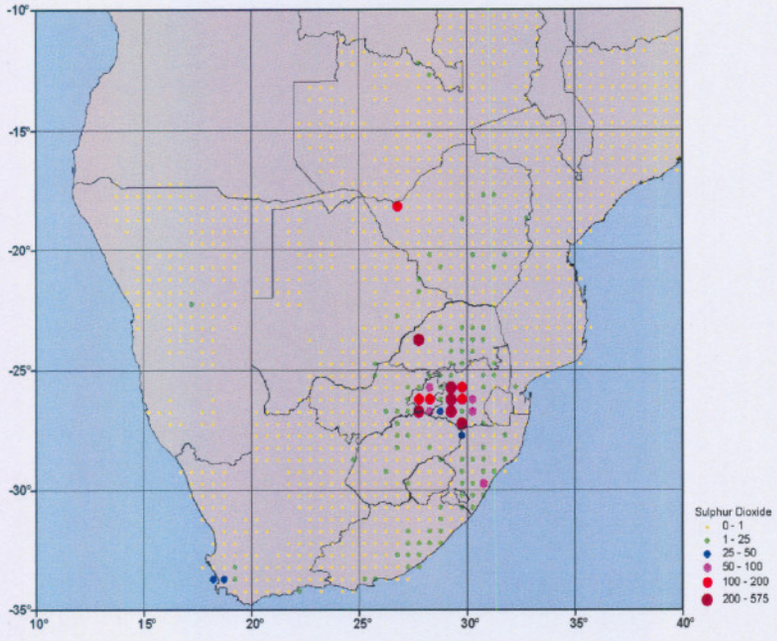

Figure 4.12: Sulphur Dioxide (SO_2) emissions in Gg/annum for the modelling region. (From Fleming and Van der Merwe, 2000)

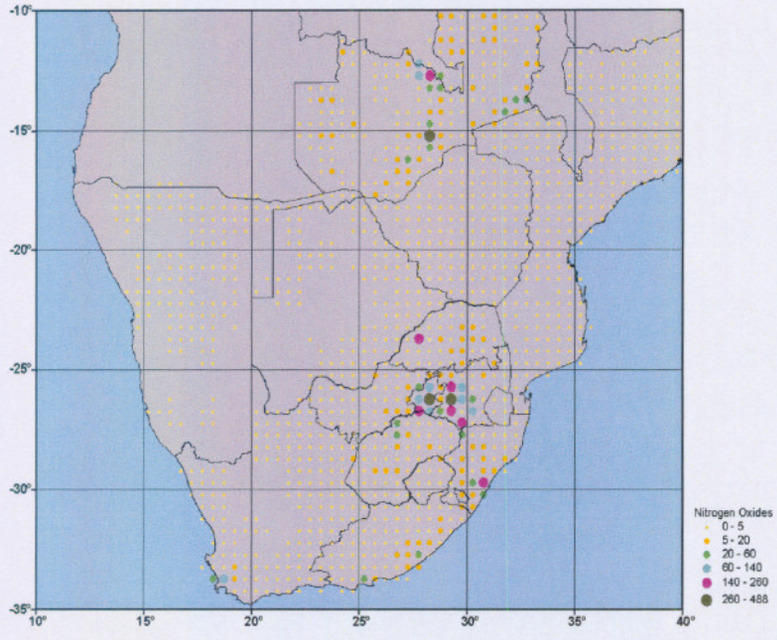

Figure 4.13: Nitrogen Dioxides (NO_x) emissions in Gg/annum for the modelling region. (From Fleming and Van der Merwe, 2000)

4.6 SUMMARY

The acquisition of reliable input parameters presents a definite technical, as well as a research challenge. The first challenge stems from the fact that the comprehensive data sets needed to run LED and other long-range models utilized in other countries is not readily available in South Africa. There is a need for the development of appropriate software capable of extracting data from the existing meteorological data archives/forecasts, available emission datasets, aerodynamic characteristics of the surface and vegetation characteristics. In addition, an essential task of the data acquisition process is to assure its quality.

Essential for the final results of any air pollution model is the reliability of the emission rates. Relevant to the African continent is the need to further investigate and better quantify the emissions from natural biomass burning as well as biomass burning for domestic use. Although in this model, specially designed for the southern African region, the emission data set developed during the international SAFARI 2000 initiative is used, its quality should be compared against international available data sets.

Chapter 5

EVALUATION OF THE LED MODEL

In this Chapter...

The objective of this chapter is briefly stated (Section 5.1). Section 5.2 gives a detailed description of the DEBITS (Deposition of Biogeochemical Important Trace Species) program, and the associated measurement stations used in the LED evaluation process. Section 5.3 focuses on discussions of the results obtained by LED for the year 2000, and the comparison with the SAFARI 2000 initiative observation data. Section 5.4 concludes the chapter by summarizing and pointing out possible reasons for observed discrepancies between the model results and experimental data during the evaluation process.

5.1 OBJECTIVES

Model performance evaluation, or model validation is the process of testing a model's ability to accurately estimate observed measurements of air quality parameters over a range of meteorological conditions and emission scenarios. When conducted thoughtfully and thoroughly, the process of model evaluation will give direction to the continuing cycle of model development, data collection, model testing, diagnostic analysis, refinement, and retesting.

In this chapter the LED's model performance is tested (evaluated) against air quality measurements for the year 2000 over the southern African region. This period coincides with the international SAFARI 2000 science initiative. During this period intensive ground based and remote measurements of the air quality and meteorological parameters were observed.

5.2 DEBITS

The IDAF program (IGAC (International Global Atmospheric Chemistry) /DEBITS/Africa) was initiated in 1994 by French and African scientists within the scope of the DEBITS (Deposition of Biogeochemical Important Trace Species) program, in order to study atmospheric depositions in the tropical regions.

In 2000, the IDAF network was formed with 10 stations situated on the African continent. Each station is representative at the regional scale of a great African ecosystem. The 6 stations of West/Central Africa are under the responsibility of the Laboratory of Aerology

in France, while the 4 South African stations are under the responsibility of the North-West University (gaseous) and ESKOM (wet deposition), Johannesburg.

The DEBITS/IDAF objectives are sustained by a measurement program including:

- rainwater sampling for chemical analysis to estimate wet deposition of identified species;
- measurement of gaseous O_3, SO_2, NO_2, HNO_3, NH_3 concentrations to estimate dry deposition values of these species;
- collection of bulk aerosol samples for chemical analysis to estimate dry deposition fluxes of aerosols.

Monthly mean gaseous measurements at the DEBITS sites are based on the property of molecular diffusion of gases on an impregnated filter, species-specific to each pollutant. Each sampler consists of an impregnated filter or molecular sieve that absorbs the gas to be analyzed, and a diffusion barrier (usually an entrapped air volume) that keeps the sampling rate constant. If the absorption is efficient, the sampling rate can be calculated from the cross-section area perpendicular to the transport direction and the distance over which the gas has to diffuse, using Fick's first law of diffusion. It is essential that the transport occurs only by molecular diffusion and that no gas is lost to the walls of the sampler. The sampling rates, and for that matter, the concentration range of the sampler, is directly proportional to its cross-sectional area and inversely proportional to its length. Passive samplers have been tested and validated since the beginning of 1998 in the IDAF network in 6 African stations (Al Ourabi and Lacaux, 1999; Lacaux, 1999). This technique has also been tested in different tropical and subtropical regions (Ferm and Rodhe, 1997; World Meteorological Organization (WMO), 1997). Diffusive samplers have many advantages in the field such as: no need for calibration, sampling tubing, electricity or technicians. The samplers are small, light, re-usable, cost-efficient and soundless.

5.2.1 Sampling Sites

Figure 5.1 shows the location of the five sampling sites, Amersfoort, Louis Trichardt, Palmer and Elandsfontein, as well as the predominant vegetation of the respective sites. The elevation of the Highveld ranges from about 1400 to 1700 m above mean sea level. The regional climate is typified by hot summers with afternoon thundershowers and cold dry winters with strong thermal stratification near ground level, particularly at night. Approximately 70 % of the area is covered by grassland with the remainder used for crop cultivation and commercial forestry. This region is also the main coal-producing region of South Africa, where currently about 80 % of South Africa's electricity is being generated (Eskom, 2001). The region also houses major petrochemical plants, smaller industries and numerous smouldering colliery discard dumps.

Cape Point

The Cape Point Global Atmosphere Watch Station is located at 34 ° 21' south and 18 ° 29' east, in a nature reserve at the southern end of the Cape Peninsula. The monitoring station is exposed to the sea on top of a cliff 234 m above mean sea level, about 60 km south from the city of Cape Town. Since the dominant wind direction is southeast-south-southwest, the station

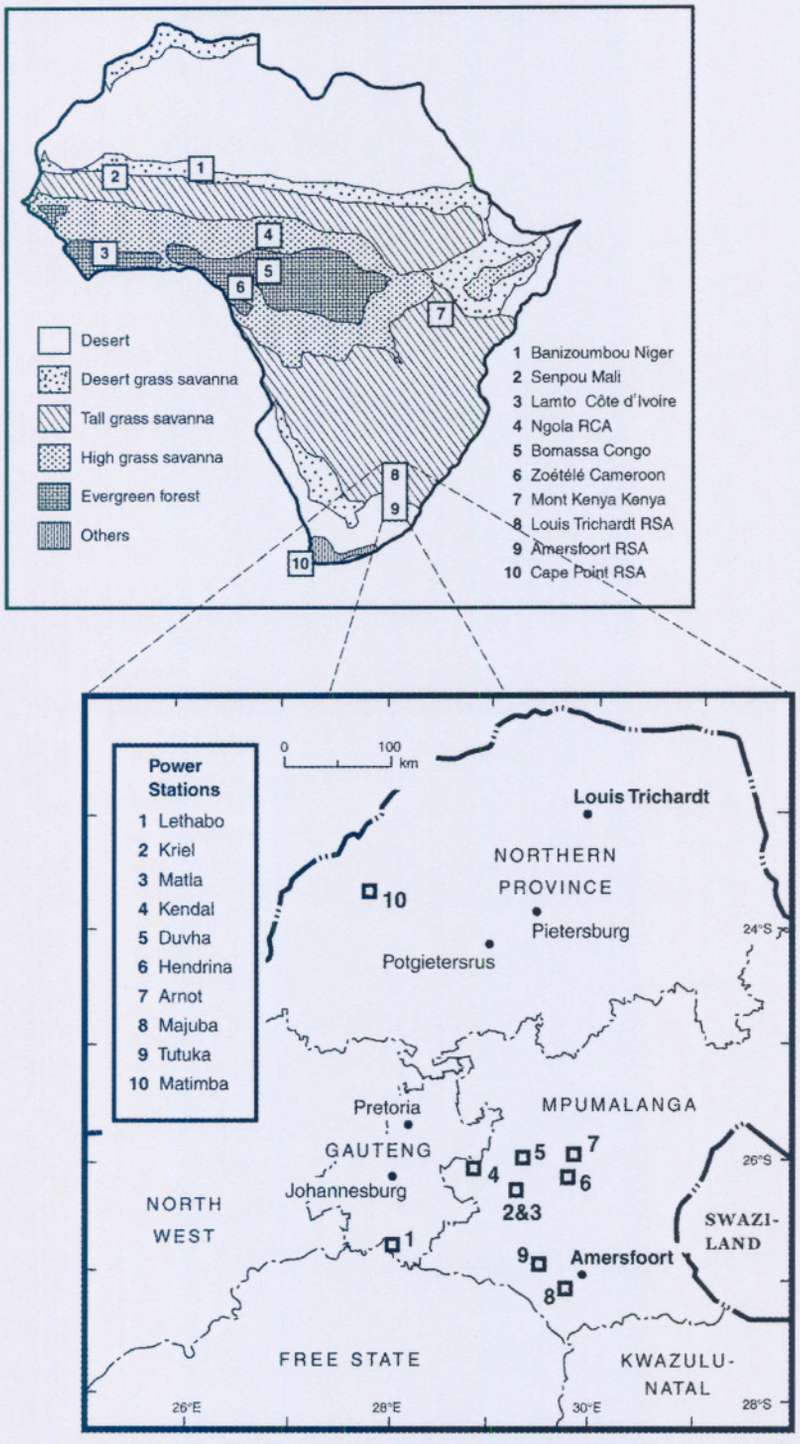

Figure 5.1: Vegetation and location map of the 10 measurement stations of the IDAF network in 2002 (top). The Louis Trichardt and Amersfoort sampling sites, as well as major Power Stations, are shown in the map below (after Galy-Lacaux and Modi, 1998)

is subjected to maritime air from the South Atlantic most of the time. The Cape Peninsula has a Mediterranean-type climate where the summers are generally dry and windy, whilst the winters are cold and wet. Cape Point can approximately be considered as a representative regional air quality station despite the proximity of industrial souces. This is attributed to very frequent high speed wind, characteristic to the site, which leads to rapid ventilation.

Louis Trichardt

The Louis Trichardt site is located at 23 ° 00' south and 30 ° 02' east in the Northern Province (Figure 5.1), 961 m above mean sea level, roughly 400 km to the north-north-east of Johannesburg. Although the mean annual precipitation is very similar (748 mm) to that at Ermelo (representing Amersfoort), the distribution of rain differs, viz. only 83.8 days/year with $\geq$ 0.1 mm are recorded on average, of which 20 days/year receive $\geq$ 10 mm/day. January is the month with the highest mean total (164 mm), while only 8 mm fall during August. From May to September $\leq$ 20 mm/month are recorded on average (SAWB, 1986). Winds show a distinct seasonal variation with a more dominant easterly component during summer, veering through south-east in autumn, to predominantly southerly in winter, followed by slightly more frequent northerly-component winds in spring. Winds rarely blow directly from the industrialized region towards this site. However, the site is ideally located to detect any pollution that has been recirculated within the frequently occurring sub-continental anticyclone system. There are no major cities or towns within a 100 km radius. The area is predominantly used for agricultural purposes, such as maize and cattle farming, and therefore it can be assumed that Louis Trichardt represents a rural site in a semi-arid region.

Amersfoort

The Amersfoort site is located at 27 ° 08' south and 29 ° 49' east, in the south-eastern part of the Mpumalanga Province (Figure 5.1), 1646 m above mean sea level. It is roughly 200 km south-east of Johannesburg and 50-100 km south-east to south-south-east of the major industrial activities, which also include the main centre of electric power generation in the Mpumalanga Highveld area. Amersfoort falls into a climatological transition region between the highveld and the nearby escarpment. The nearest representative long-term climatological observations are from Ermelo, about 90 km north-north-east of Amersfoort (SAWB, 1986). The mean annual precipitation is 755 mm, with January (126 mm) and November (131 mm) having the highest mean monthly rainfall. Rain is recorded on 96.7 days/year ($\geq$ 0.1 mm/day), of which on average 24 days receive $\geq$ 10 mm/day. However, from May to August the average monthly rainfall totals are $\leq$ 20 mm. During winter and spring, most winds in the Amersfoort area blow from westerly directions (south-west to north-west, 78 %, being slightly more south-westerly in autumn, while during summer only 47 % of winds come from the west and 28 % from south-easterly directions. Thus, prevailing winds can be expected to frequently transport pollutants from the metropolitan and industrial regions (Gauteng and Mpumalanga) towards this site. This station is representative of a site strongly influenced by industry in a semi-arid area.

Elandsfontein

Elandsfontein is located at 26 ° 15' south and 29 ° 25' east, about 1950 m above mean sea level, in the south of the Witbank/Middelburg industrial region and in the center of the

Mpumalanga Highveld. It lies 55 km south-south east of Witbank and 150 km east of Johannesburg, approximately 150 m above the surrounding farmland. Possible sources likely to impact this site are urban plumes from either Witbank/Middelburg (northerly winds) or from the Gauteng region (westerly to west-north-westerly winds). Meteorological observations from a nearby weather station (Bethal, 1986; SAWB, 1986) indicate similar climatic characteristics as those described for Amersfoort. Major coal fired power plants are in a close proximity to the observation point. Elandsfontein can therefore be considerd an industrial site, heavily influenced by the local industries.

Palmer

Palmer is located at 25 ° 15' south and 30 ° 04' east, 2000 m above mean sea level and about 100 km north-east of Elandsfontein, near the escarpment, in an area which is thought to be representative of a semi-industrialized region in a semi-arid region, as the air-flow rarely originates from the industrial region (Held *et. al.*, 1996). The climate at Palmer, due to its high elevation, is obviously more extreme than that of the lower-lying plateau, especially in terms of the temperature range and the frequently occurring fog events (on average 43 days per year, compared to only 19 days at Bethal). The average annual rainfall is about 15 % higher than at Amersfoort and Bethal (SAWB, 1986).

5.3 RESULTS AND DISCUSSIONS

The LED model was run for each month during 2000 using the relevant meteorological data, and the converted emission database by Fleming and Van der Merwe (2000) as discussed in Chapter 4.

Diffusive sampler monthly mean results were obtained for selected pollutant species for the year 2000 from the abovementioned DEBITS sites. Special emphasis was given to the SO_x and NO_x species. These monthly mean values were compared to the calculated (modelled) results from the LED model. The error margins of the diffusive samplers utilized at the DEBITS sites are 17.4 % and 3.7 % for SO_2 and NO_2 respectively (DEBITS , 2005).

It should be pointed out that the design of the DEBITS network locations and density was designed (aimed) for obtaining the general regional long term air quality trends in the southern African region. The number of observational points is extremely small, and not all of the observation sites are chosen in accordance to the World Meteorological Organisation (WMO) criteria for long-range observational sites. However, in the absence of any other air quality obervational sites in the modelling region these DEBITS sites are used to approximately evaluate the validity of the calculated concentration and deposition ranges by LED. Keeping in mind that the comparison of the modelled and measured results will be of a general qualitative nature.

Table 5.1 presents a comparison of the annual measured concentrations at the DEBITS sites againts modelled (calculated) results from the LED model for SO_2 for the year 2000, while Table 5.2 presents the same for the monthly quantities. Figures 5.2 to 5.7 give the tabulated results graphically for the same locations respectively. The % difference column in Table 5.1, indicates the persentage difference between the annual mean measured and modelled values for the specific stations respectively.

Table 5.1: Annual mean ambient concentrations for SO_2 in $\mu g.m^{-3}$ (passive data) compared to modelled data for 2000

DEBITS Site	SO_2 / $\mu g.m^{-3}$	Annual mean	% Difference	Minimum monthly mean	Maximum monthly mean
Cape Point	Measured	1.4	-	0.5	2.4
	Modelled	1.5	6.7	1.0	1.8
Amersfoort	Measured	5.4	-	2.4	8.8
	Modelled	5.1	5.9	2.7	10.5
Louis Trichardt	Measured	1.1	-	0.5	1.9
	Modelled	0.6	83.3	0.2	0.9
Elandsfontein	Measured	18.7	-	11.4	30.8
	Modelled	16.5	13.3	8.7	27.2
Palmer	Measured	5.0	-	2.4	11.9
	Modelled	7.2	30.6	3.3	10.5

Table 5.2: Monthly averaged ambient concentrations for SO_2 in $\mu g.m^{-3}$ (passive data) compared to modelled data for 2000

Site		Jan	Feb	Mar	Apr	May	Jun	Jul	Aug	Sep	Oct	Nov	Dec
Cape Point	Measured	1.33	1.59	1.33	0.80	1.59	1.59	1.06	N/A	N/A	1.33	2.39	0.53
	Modelled	1.61	1.64	1.70	1.51	1.88	1.39	1.20	1.14	1.00	1.44	1.47	1.46
Amersfoort	Measured	5.57	3.71	2.39	5.04	5.04	5.57	8.75	6.89	N/A	N/A	5.57	N/A
	Modelled	3.28	2.74	3.04	7.22	2.96	3.88	4.02	6.98	10.50	6.88	4.53	5.06
Louis Trichardt	Measured	1.06	1.86	1.06	0.80	1.33	1.06	1.06	1.59	0.80	0.53	0.80	N/A
	Modelled	0.76	0.15	0.32	0.45	0.84	0.42	0.25	0.71	0.60	0.77	0.94	0.48
Elandsfontein	Measured	13.52	11.40	15.38	15.38	17.24	18.30	30.76	28.50	19.09	22.27	14.05	N/A
	Modelled	15.30	11.10	14.00	23.00	12.80	8.72	12.60	24.50	27.20	17.70	13.50	17.80
Palmer	Measured	3.18	3.45	2.92	5.30	2.92	5.30	11.93	10.08	3.71	3.71	2.39	N/A
	Modelled	9.04	3.28	5.25	9.01	9.12	3.52	4.38	10.5	8.11	8.53	6.61	9.17

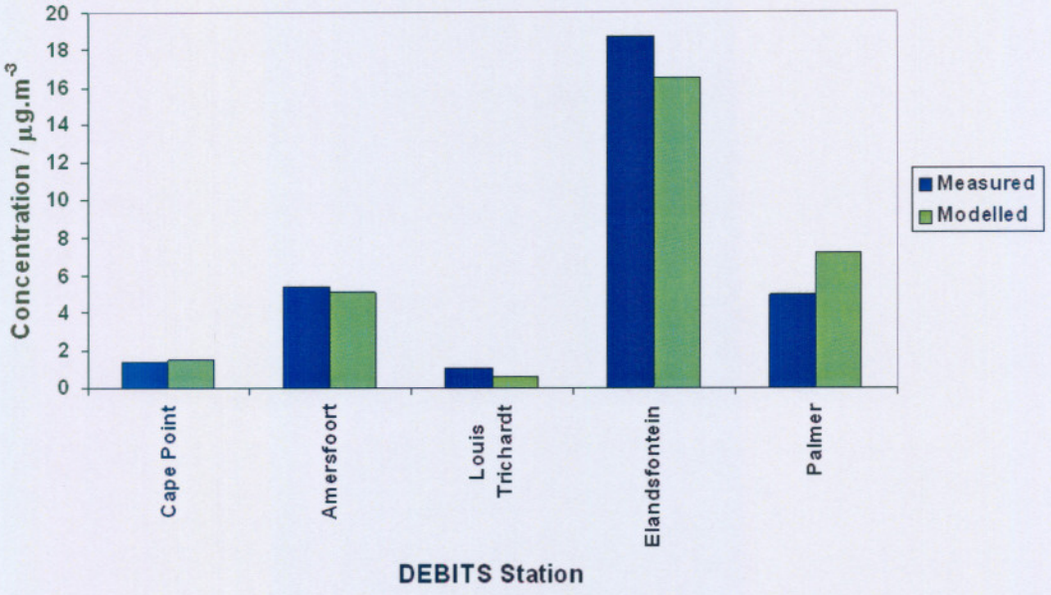

Figure 5.2: An comparison of the annual modelled results versus measured SO_2 results for the DEBITS stations for the year 2000

The analysis of Table 5.1 and Figure 5.2 reveals that both the measured and modelled concentrations clearly discern the sites which partially fulfill the requirement of regional air quality stations, from the stations that are located in industrial areas. The annual concentration in Amersfoort (AF), Elandsfontein (EL) and Palmer (PA) (located in industrial areas) are five to eighteen times higher than the LT and CP stations (partial WMO compliant). This fact gives the first assurance that LED can produce reliable results for the mean annual quantities. This conclusion is further supported by analysis of the minimum and maximum concentrations where the discrepancies between the observed and modelled concentrations are quite acceptable.

One should note however the relatively big discrepancy calculated for the Louis Trichardt site which ammounts to 83%. Possible explanations for this might be sought in the accuracy and reliability of the emission data set utilized in LED scenarios. This point will be further discussed, when comparing the concentration fields produced by the SAFARI 2000 emission data set with the international EDGAR 2000 emission data set.

The application of LED for the region under study is further supported by the graphical results from Figures 5.3 to 5.7. For the majority of the months at all stations, the discrepancies between the measured and modelled results do no exceed 10% to 40%. There is a need for analysis for the few cases where the discrepancies exceed 100%. For example the most noticable discrepancies can be noted for the Louis Trichardt station for the month February.

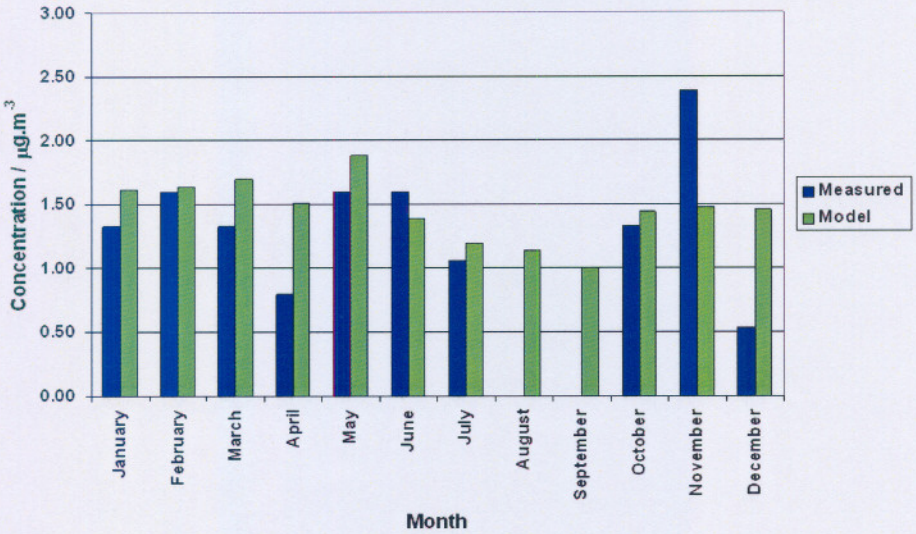

Figure 5.3: A comparison of monthly modelled SO_2 results versus measured SO_2 results for the Cape Point station during 2000 (Note the absence of measurements during August and September during 2000)

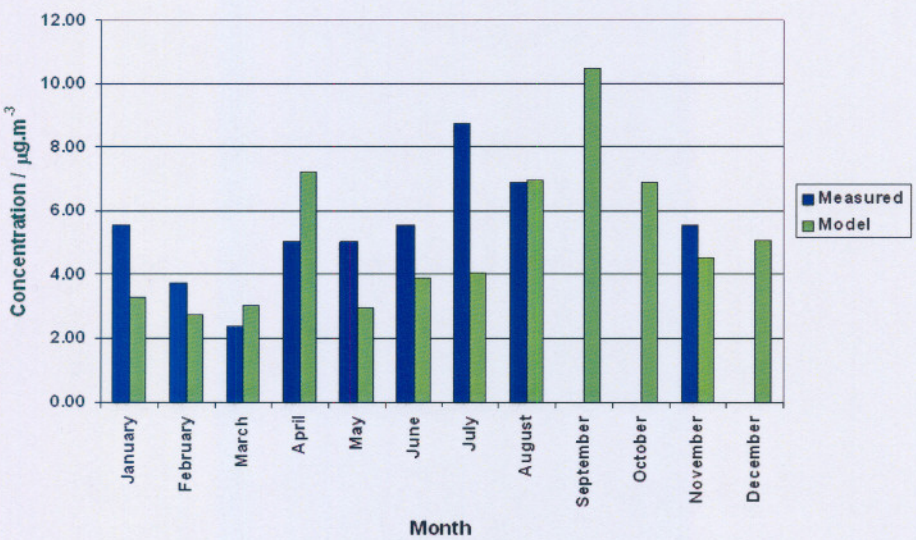

Figure 5.4: A comparison of monthly modelled SO_2 results versus measured SO_2 results for the Amersfoort station during 2000

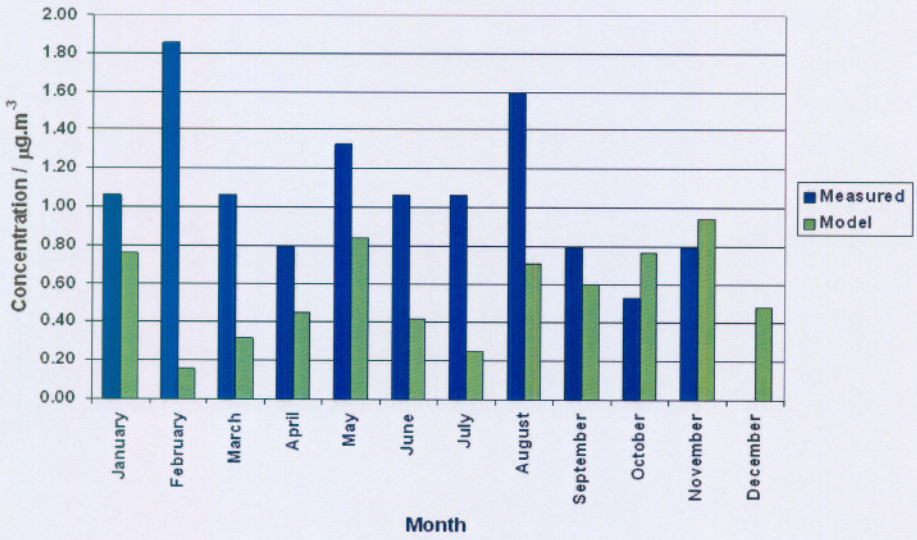

Figure 5.5: A comparison of monthly modelled SO_2 results versus measured SO_2 results for the Louis Trichardt station during 2000

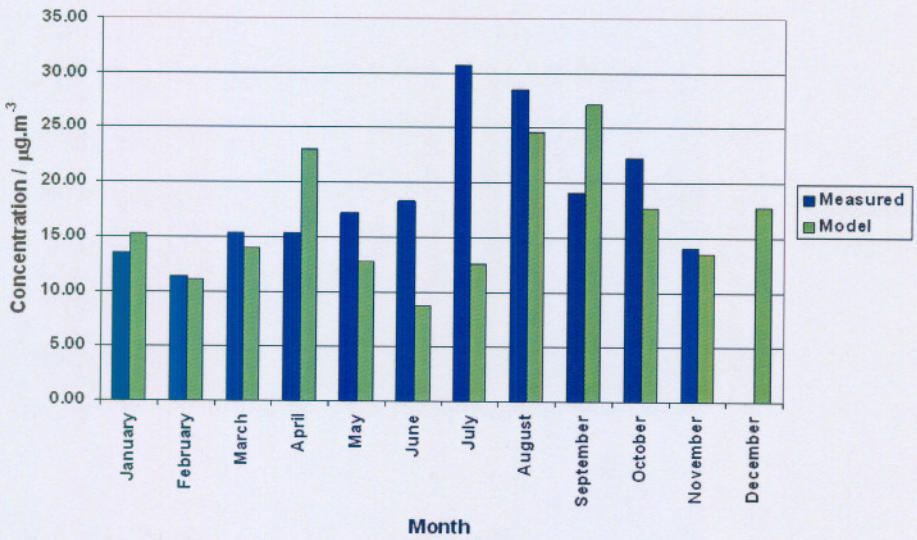

Figure 5.6: A comparison of monthly modelled SO_2 results versus measured SO_2 results for the Elandsfontein station during 2000

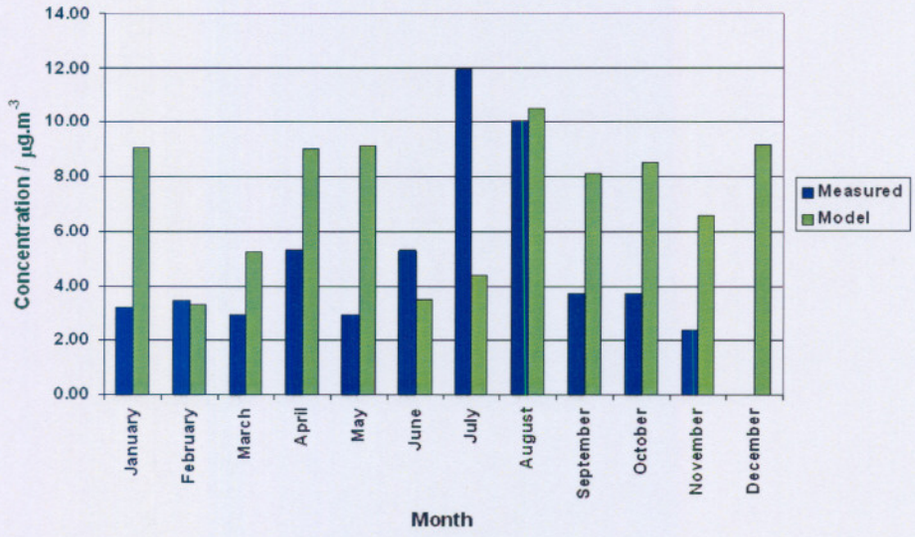

Figure 5.7: A comparison of monthly modelled SO_2 results versus measured SO_2 results for the Palmer station during 2000

Tables 5.3 and 5.4 together with Figures 5.8 to 5.13 represents the results for NO_2 which are compiled in the same manner as SO_2.

Table 5.3: Annual mean ambient concentrations for NO_2 in $\mu g.m^{-3}$ (passive data) compared to modelled data for 2000

DEBITS Site	NO_2 / $\mu g.m^{-3}$	Annual mean	% Difference	Minimum monthly mean	Maximum monthly mean
Cape Point	Measured	1.5	-	0.9	2.3
	Modelled	3.6	58.3	2.4	4.7
Amersfoort	Measured	4.1	-	2.1	5.5
	Modelled	4.3	4.7	2.3	8.2
Louis Trichardt	Measured	0.7	-	0.2	1.0
	Modelled	0.9	22.2	0.3	1.3
Elandsfontein	Measured	7.5	-	5.5	10.1
	Modelled	12.6	40.5	6.8	20.1
Palmer	Measured	3.2	-	1.7	5.1
	Modelled	6.2	48.4	2.7	9.3

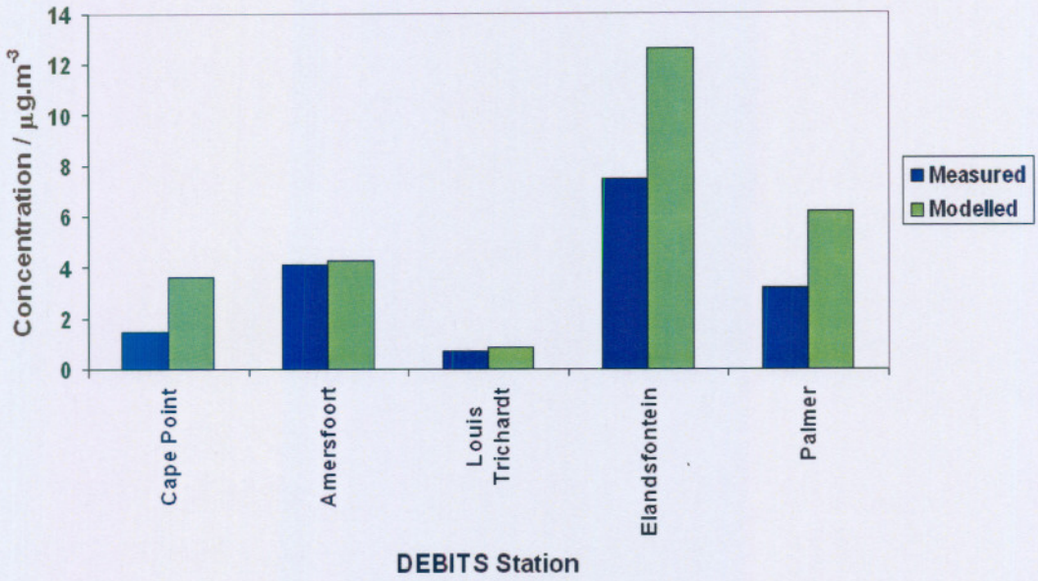

Figure 5.8: A comparison of the annual modelled results versus measured NO_2 results for the DEBITS stations for the year 2000

The LED results for the annual minimum and maximum concentrations (Table 5.3 and Figure 5.8) allow for making the same conclusion as for SO_2, namely that LED reproduce the annual quantities reasonably well. The monthly quantities shown in Figures 5.9 to 5.13 and Table 5.4 reveal the almost consistent overprediction of LED for all observation sites. The magnitute of this overprediction which reaches 100 to 150% for certain months is not unusual in the field of air pollution modelling, but deserves further study. One reason for the overprediction might be in the more complicated chemical transformation mechanisms of nitric species compared to sulphur compounds, as well as deposition mechanisms implemented in LED. It should be noted that LED chemical transformation mechanism is based on linear transformation mechanisms. The refinement of the NO_x chemistry mechanism is also compelled by the need of modelling the tropospheric ozone cycle.

Table 5.5 contains the historical data for seasonally average concentrations for SO_2 and SO_4, as well as NO_2 for the years 1996 to 1998 as taken from Mphepya (2002). The comparison of this set of data with the modelled results for the year 2000 allows one to make only one conclusion, namely that the LED results modelled for 2000 fall within the range for the observed concentrations during the specified time period 1996 to 1998.

Table 5.4: Monthly averaged ambient concentrations for NO_2 in $\mu g.m^{-3}$ (passive data) compared to modelled data for 2000

Site		Jan	Feb	Mar	Apr	May	Jun	Jul	Aug	Sep	Oct	Nov	Dec
Cape Point	Measured	1.72	1.52	1.72	2.10	1.52	1.52	2.29	N/A	N/A	0.95	1.14	0.95
	Modelled	4.18	4.21	4.47	3.88	4.69	3.44	2.86	2.85	2.38	3.44	3.81	3.37
Amersfoort	Measured	2.10	4.76	4.38	4.00	5.15	3.81	5.53	3.24	N/A	N/A	3.81	N/A
	Modelled	2.84	2.34	2.57	5.88	2.49	3.20	3.42	6.38	8.23	5.71	3.75	4.31
Louis Trichardt	Measured	0.95	0.19	0.38	0.57	0.95	0.57	0.95	0.95	0.95	0.57	0.95	N/A
	Modelled	1.13	0.34	0.58	0.75	1.08	0.66	0.46	1.17	0.86	1.01	1.27	0.85
Elandsfontein	Measured	6.67	5.53	6.86	10.10	7.24	6.29	10.10	8.39	6.86	7.24	6.67	N/A
	Modelled	11.40	8.28	10.40	17.60	9.54	6.81	10.10	18.80	20.10	14.30	10.20	13.80
Palmer	Mesured	5.15	2.29	2.29	3.24	2.86	4.96	3.81	3.43	2.86	2.67	1.72	N/A
	Modelled	7.55	2.73	4.33	7.70	7.70	2.95	3.90	9.37	6.75	7.46	5.62	7.91

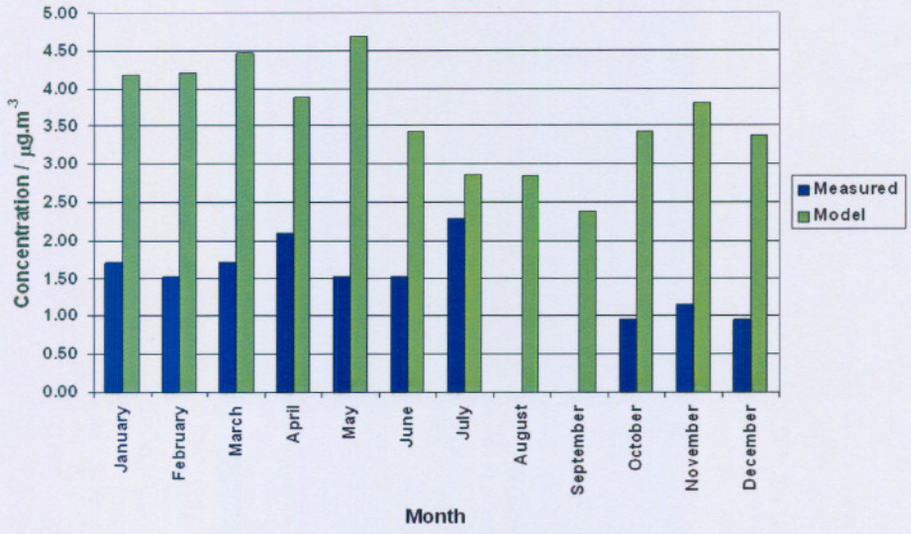

Figure 5.9: A comparison of monthly modelled NO_2 results versus measured NO_2 results for the Cape Point station during 2000

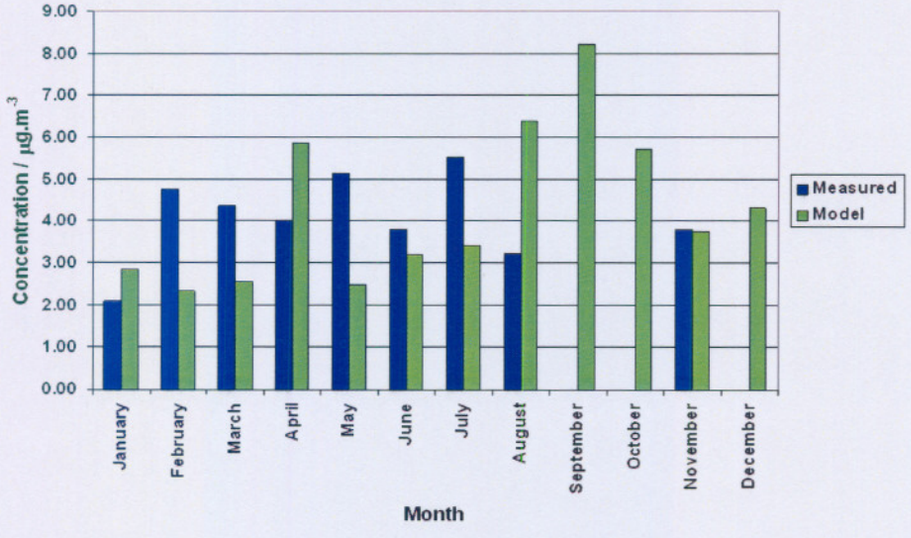

Figure 5.10: A comparison of monthly modelled NO_2 results versus measured NO_2 results for the Amersfoort station during 2000

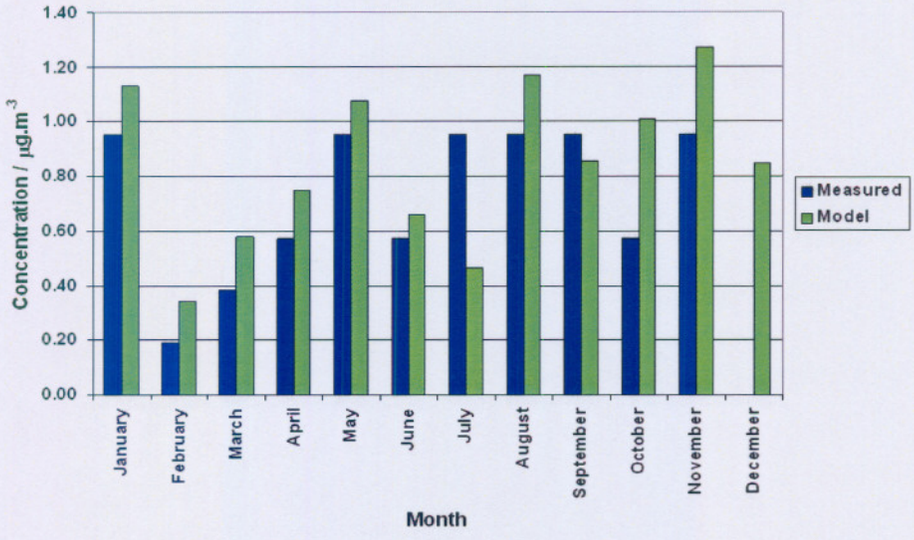

Figure 5.11: A comparison of monthly modelled NO_2 results versus measured NO_2 results for the Louis Trichardt station during 2000

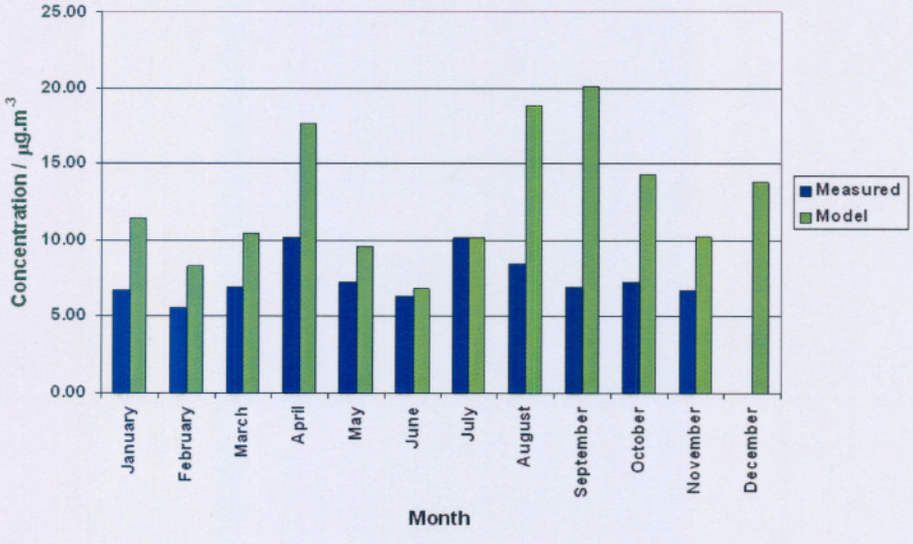

Figure 5.12: A comparison of monthly modelled NO_2 results versus measured NO_2 results for the Elandsfontein station during 2000

Table 5.5: Seasonally averaged concentrations for SO_2, SO_4^{2-} (shown in brackets) and NO_2 in $\mu g.m^{-3}$ for 1996 to 1998 (Mphepya, 2002) , compared to modelled results for 2000

		SO_2 and (SO_4^{2-})				NO_2			
Site	**Year**	**Autumn**	**Winter**	**Summer**	**Autumn**	**Winter**	**Spring**	**Summer**	
Cape Point	1996	n/a	n/a	n/a	n/a	n/a	n/a	n/a	n/a
	1997	n/a	n/a	n/a	n/a	n/a	n/a	n/a	n/a
	1998	n/a	n/a	n/a	n/a	n/a	n/a	n/a	n/a
	2000	**1.70 (0.19)**	**1.24 (0.10)**	**1.30 (0.12)**	**1.57 (0.14)**	**4.35**	**3.05**	**3.21**	**3.92**
Amersfoort	1996	-	-	-	-	-	-	-	-
	1997	-	10.9	8.0	10.9	-	5.0	4.3	4.0
	1998	5.9	8.2	7.4	10.1	2.6	3.1	4.3	3.3
	2000	**4.41 (1.52)**	**4.96 (0.94)**	**7.30 (1.57)**	**3.69 (1.29)**	**3.65**	**4.33**	**5.90**	**3.16**
Louis Trichardt	1996	1.3	3.7	2.1	1.3	2.1	0.9	1.4	1.5
	1997	2.4	2.4	1.9	1.3	0.7	1.0	1.2	1.0
	1998	5.1	6.1	5.1	3.7	0.9	1.2	1.2	1.2
	2000	**0.54 (0.44)**	**0.46 (0.29)**	**0.77 (0.40)**	**0.46 (0.40)**	**0.80**	**0.76**	**1.05**	**0.77**
Elandsfontein	1996	15.5 (7.1)	33.1 (7.3)	24.9 (6.9)	26.3 (3.6)	10.3	15.9	10.7	10.9
	1997	23.8 (4.9)	37.5 (6.8)	17.3 (5.7)	15.9 (13.3)	10.3	12.9	8.4	7.9
	1998	20.6 (21.6)	29.8 (18.6)	17.9 (19.3)	16.3 (18.5)	14.1	13.9	14.9	-
	2000	**16.60 (3.51)**	**15.27 (2.01)**	**19.47 (2.75)**	**14.73 (2.98)**	**12.51**	**11.90**	**14.87**	**11.16**
Palmer	1996	13.6 (6.8)	13.1 (5.7)	6.6 (3.6)	3.1 (4.4)	7.0	7.6	4.8	3.2
	1997	7.5 (4.5)	14.8 (9.1)	4.7 (9.9)	3.3 (11.8)	4.4	5.3	3.9	2.5
	1998	9.9 (16.5)	16.7 (18.0)	4.8 (11.0)	3.3 (9.3)	4.9	9.9	4.4	4.3
	2000	**7.79 (2.31)**	**6.13 (1.18)**	**7.75 (1.72)**	**7.16 (2.07)**	**6.58**	**5.41**	**6.61**	**6.06**

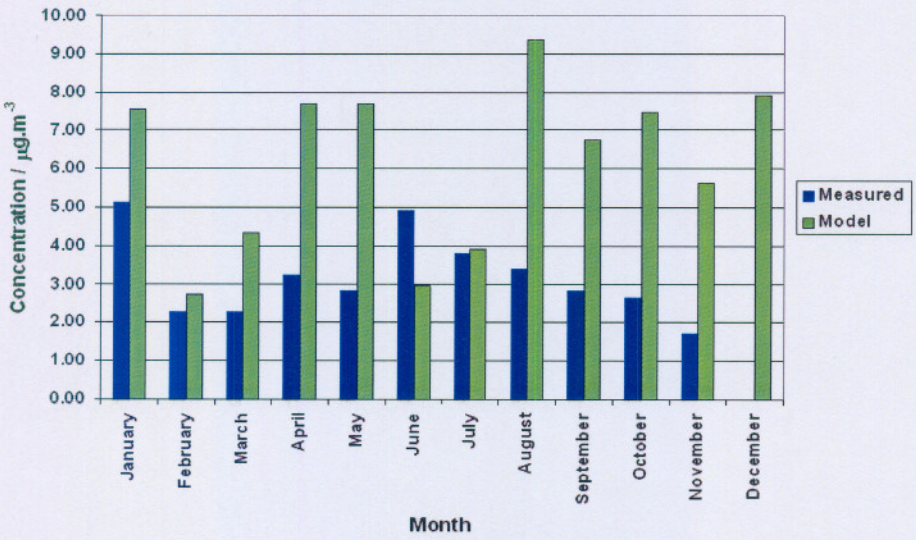

Figure 5.13: A comparison of monthly modelled NO_2 results versus measured NO_2 results for the Palmer station during 2000

An important atmospheric pathway for the removal of pollutant species from the atmosphere is through the process of dry and wet deposition. However, these processes lead to degradation of fragile environments typical for the region, or in some cases a supply of nutrients to the ecosystems.

Table 5.6 recapitulates the monthly dry deposition totals as calcualted by LED for the year 2000 for the selected DEBITS sites. Unfortunately, no data sets are available for the region to compare with the calculated results. In the study by Mphepya (2002) seasonal dry deposition totals for the DEBITS sites for the years 1996 to 1998 are presented. These results for sulphur and nitrogen species, as well as calculated LED dry deposition results for 2000, are presented in Tables 5.7 and 5.8. The general conclusion which can be made on the basis of these data sets is that LED generates dry deposition values that do not deviate from the observed quantities.

Similarly the LED results for the monthly wet deposition totals for sulphur and nitrogen species at the DEBITS sites are presented in Table 5.9. Once again no wet deposition results are available to evaluate the modelled performance.

Tables 5.10 and 5.11 taken from Mphepya (2002) as well calculated LED results for the year 2000, exhibit the annual mean wet deposition totals for the years 1996 to 1998 at the selected DEBITS sites. Calculated results confirm the ability of LED to calculate wet deposition values which is in the range of the observed quantities.

Table 5.6: Monthly dry deposition totals (kg.ha^{-1}), of S from SO_2 and SO_4^{2-}, as well as N from NO and NO_2 as modelled by LED for 2000

Site	Specie	Jan	Feb	Mar	Apr	May	Jun	Jul	Aug	Sep	Oct	Nov	Dec
Cape Point	SO_2 as S	0.08	0.07	0.08	0.07	0.09	0.06	0.05	0.06	0.05	0.06	0.07	0.06
	SO_4^{2-} as S	0.01	0.01	0.01	0.01	0.01	0.01	0.01	0.01	0.00	0.01	0.01	0.01
	NO as N	0.01	0.01	0.01	0.01	0.01	0.01	0.01	0.01	0.01	0.01	0.01	0.01
	NO_2 as N	0.05	0.04	0.05	0.04	0.05	0.04	0.03	0.03	0.03	0.04	0.04	0.04
Amersfoort	SO_2 as S	0.16	0.10	0.13	0.25	0.14	0.17	0.19	0.20	0.26	0.33	0.20	0.25
	SO_4^{2-} as S	0.07	0.05	0.07	0.14	0.05	0.04	0.07	0.06	0.08	0.11	0.08	0.10
	NO as N	0.01	0.01	0.01	0.02	0.01	0.01	0.01	0.02	0.03	0.01	0.01	0.01
	NO_2 as N	0.03	0.02	0.03	0.05	0.03	0.03	0.04	0.05	0.07	0.06	0.04	0.05
Louis Trichardt	SO_2 as S	0.03	0.01	0.02	0.02	0.04	0.02	0.01	0.03	0.02	0.03	0.04	0.02
	SO_4^{2-} as S	0.04	0.00	0.02	0.02	0.04	0.02	0.00	0.03	0.01	0.02	0.04	0.03
	NO as N	0.00	0.00	0.00	0.00	0.00	0.00	0.00	0.00	0.00	0.00	0.00	0.00
	NO_2 as N	0.01	0.00	0.01	0.01	0.01	0.01	0.00	0.01	0.01	0.01	0.01	0.01
Elandsfontein	SO_2 as S	0.72	0.44	0.60	0.95	0.62	0.38	0.56	0.74	0.57	0.83	0.57	0.85
	SO_4^{2-} as S	0.20	0.12	0.17	0.28	0.16	0.06	0.14	0.15	0.14	0.19	0.14	0.20
	NO as N	0.03	0.02	0.02	0.04	0.02	0.02	0.02	0.06	0.07	0.03	0.02	0.03
	NO_2 as N	0.13	0.08	0.11	0.18	0.11	0.07	0.11	0.17	0.15	0.16	0.11	0.15
Palmer	SO_2 as S	0.40	0.12	0.22	0.40	0.42	0.15	0.20	0.34	0.23	0.37	0.28	0.39
	SO_4^{2-} as S	0.16	0.04	0.08	0.15	0.18	0.04	0.07	0.10	0.07	0.14	0.09	0.16
	NO as N	0.02	0.01	0.01	0.02	0.02	0.01	0.01	0.03	0.02	0.02	0.01	0.02
	NO_2 as N	0.08	0.03	0.04	0.08	0.08	0.03	0.04	0.09	0.06	0.08	0.06	0.08

Table 5.7: Seasonal dry deposition totals for each year ($kg.ha^{-1}$) of S from SO_2 and SO_4^{2-} respectively, as well as annual totals of S deposition for 1996 to 1998 (Mphepya, 2002), compared against modelled results for 2000

		SO_2 as S				SO_4^{2-} as S				Annual
Site	**Year**	**Autumn**	**Winter**	**Spring**	**Summer**	**Autumn**	**Winter**	**Spring**	**Summer**	**Total S**
Cape Point	1996	n/a	n/a	n/a	n/a	n/a	n/a	n/a	n/a	n/a
	1997	n/a	n/a	n/a	n/a	n/a	n/a	n/a	n/a	n/a
	1998	n/a	n/a	n/a	n/a	n/a	n/a	n/a	n/a	n/a
	2000	**0.24**	**0.16**	**0.18**	**0.21**	**0.03**	**0.02**	**0.02**	**0.02**	**0.89**
Amersfoort	1996	-	-	-	-	n/a	n/a	n/a	n/a	-
	1997	0.40	0.52	0.57	1.14	n/a	n/a	n/a	n/a	2.63
	1998	0.45	0.42	0.52	1.02	n/a	n/a	n/a	n/a	2.41
	2000	**0.52**	**0.56**	**0.79**	**0.51**	**0.26**	**0.16**	**0.27**	**0.23**	**3.31**
Louis Trichardt	1996	0.10	0.18	0.15	0.13	n/a	n/a	n/a	n/a	0.56
	1997	0.18	0.11	0.13	0.13	n/a	n/a	n/a	n/a	0.55
	1998	0.39	0.29	0.36	0.36	n/a	n/a	n/a	n/a	0.44
	2000	**0.08**	**0.06**	**0.09**	**0.06**	**0.08**	**0.05**	**0.07**	**0.07**	**0.56**
Elandsfontein	1996	1.55	1.71	1.87	3.34	0.16	0.17	0.35	0.09	9.24
	1997	1.87	2.05	1.49	2.38	0.14	0.22	0.23	0.48	8.86
	1998	1.96	1.62	1.49	2.06	0.68	0.48	0.84	0.84	9.97
	2000	**2.16**	**1.67**	**1.96**	**2.00**	**0.61**	**0.35**	**0.47**	**0.52**	**9.74**
Palmer	1996	1.48	0.10	0.06	0.32	0.19	0.20	0.41	0.19	2.95
	1997	0.10	0.13	0.06	0.05	0.14	0.31	0.44	0.36	1.59
	1998	0.09	0.84	0.07	0.08	0.48	0.58	0.46	0.28	2.88
	2000	**1.04**	**0.69**	**0.88**	**0.91**	**0.41**	**0.20**	**0.30**	**0.36**	**4.79**

Table 5.8: Seasonal dry deposition totals for each year (kg.ha^{-1}) of N from NO and NO_2, respectively, as well as annual totals of N deposition for 1996 to 1998 (Mphepya, 2002), compared against modelled results for 2000

		NO as N				NO_2^- as N				Annual
Site	Year	Autumn	Winter	Spring	Summer	Autumn	Winter	Spring	Summer	Total N
Cape Point	1996	n/a	n/a	n/a	n/a	n/a	n/a	n/a	n/a	n/a
	1997	n/a	n/a	n/a	n/a	n/a	n/a	n/a	n/a	n/a
	1998	n/a	n/a	n/a	n/a	n/a	n/a	n/a	n/a	n/a
	2000	**0.03**	**0.02**	**0.02**	**0.03**	**0.15**	**0.10**	**0.10**	**0.13**	**0.57**
Amersfoort	1996	n/a	n/a	n/a	n/a	-	-	-	-	-
	1997	n/a	n/a	n/a	n/a	0.062	0.060	0.082	0.160	0.392
	1998	n/a	n/a	n/a	n/a	0.056	0.037	0.082	0.132	0.307
	2000	**0.03**	**0.03**	**0.05**	**0.02**	**0.11**	**0.13**	**0.17**	**0.10**	**0.64**
Louis Trichardt	1996	n/a	n/a	n/a	n/a	0.045	0.011	0.027	0.060	0.143
	1997	n/a	n/a	n/a	n/a	0.015	0.012	0.023	0.040	0.090
	1998	n/a	n/a	n/a	n/a	0.019	0.014	0.023	0.048	0.104
	2000	**0.01**	**0.01**	**0.01**	**0.01**	**0.03**	**0.02**	**0.03**	**0.02**	**0.13**
Elandsfontein	1996	n/a	n/a	n/a	n/a	0.150	0.190	0.200	0.410	0.950
	1997	n/a	n/a	n/a	n/a	0.320	0.160	0.180	0.350	1.010
	1998	n/a	n/a	n/a	n/a	0.410	0.170	0.320	-	> 0.900
	2000	**0.09**	**0.09**	**0.12**	**0.07**	**0.40**	**0.35**	**0.41**	**0.36**	**1.90**
Palmer	1996	n/a	n/a	n/a	n/a	0.150	0.090	0.080	0.110	0.430
	1997	n/a	n/a	n/a	n/a	0.110	0.060	0.060	0.080	0.310
	1998	n/a	n/a	n/a	n/a	0.090	0.120	0.090	0.160	0.460
	2000	**0.04**	**0.04**	**0.05**	**0.04**	**0.21**	**0.16**	**0.19**	**0.19**	**0.94**

Table 5.9: Monthly wet deposition totals (kg.ha^{-1}), of S from SO_4^{2-} , and N from NO_3^- respectively, modelled for 2000

Site	Specie	Jan	Feb	Mar	Apr	May	Jun	Jul	Aug	Sep	Oct	Nov	Dec
Cape Point[1]	SO_4^{2-} as S	0.08	0.07	0.08	0.05	0.06	0.05	0.04	0.05	0.02	0.04	0.07	0.05
	NO_3^{1-} as N	0.07	0.06	0.07	0.04	0.05	0.05	0.04	0.04	0.02	0.03	0.05	0.04
Amersfoort[1]	SO_4^{2-} as S	0.59	0.45	0.56	0.70	0.27	0.33	0.55	0.48	0.42	0.54	0.63	0.79
	NO_3^{1-} as N	0.29	0.20	0.26	0.31	0.13	0.12	0.24	0.23	0.17	0.20	0.26	0.33
Louis	SO_4^{2-} as S	0.34	0.04	0.12	0.10	0.21	0.14	0.04	0.23	0.07	0.09	0.29	0.20
Trichardt[1]	NO_3^{1-} as N	0.19	0.03	0.08	0.06	0.10	0.07	0.02	0.15	0.03	0.05	0.16	0.13
Elandsfontein	SO_4^{2-} as S	1.63	1.02	1.42	1.41	0.76	0.50	1.13	1.30	0.72	0.95	1.13	1.59
	NO_3^{1-} as N	0.62	0.37	0.54	0.52	0.27	0.16	0.45	0.53	0.29	0.34	0.44	0.59
Palmer	SO_4^{2-} as S	1.33	0.33	0.67	0.73	0.87	0.32	0.54	0.85	0.33	0.67	0.78	1.32
	NO_3^{1-} as N	0.56	0.14	0.29	0.29	0.33	0.12	0.24	0.39	0.13	0.28	0.34	0.58

Table 5.10: Annual three-year mean wet deposition ($kg.ha^{-1}.yr^{-1}$) for 1996 to 1998 (Mphepya, 2002), compared against modelled results for 2000

	SO_4^{2-} as S					NO_3^- as N				
Site	**1996**	**1997**	**1998**	**Mean**	**2000**	**1996**	**1997**	**1998**	**Mean**	**2000**
Cape Point	n/a	n/a	n/a	n/a	**0.67**	n/a	n/a	n/a	n/a	**0.55**
Amersfoort	3.10	5.90	4.60	4.50	**6.32**	1.11	2.10	2.30	1.84	**2.73**
Louis Trichardt	1.40	1.70	1.60	1.50	**1.89**	0.49	0.49	1.14	0.71	**1.07**
Elandsfontein	n/a	n/a	n/a	n/a	**13.57**	n/a	n/a	n/a	n/a	**5.12**
Palmer	n/a	n/a	n/a	n/a	**8.75**	n/a	n/a	n/a	n/a	**3.70**

Table 5.11: Mean seasonal and annual wet deposition (kg.ha^{-}1) of S from SO_4^{2-}, and N from NO_3^- respectively, during the period March 1996 to December 1999 (Mphepya, 2002), compared against modelled results for 2000

		SO_4^{2-} as S					NO_3^- as N				
Site	**Year**	**Autumn**	**Winter**	**Spring**	**Summer**	**Annual**	**Autumn**	**Winter**	**Spring**	**Summer**	**Annual**
Cape Point	1996 – 1999	n/a	n/a	n/a	n/a	n/a	n/a	n/a	n/a	n/a	n/a
	2000	**0.20**	**0.15**	**0.13**	**0.20**	**0.67**	**0.16**	**0.12**	**0.10**	**0.17**	**0.55**
Amersfoort	1996 – 1999	2.66	0.48	5.34	5.12	13.60	0.89	0.22	2.61	1.77	5.49
	2000	**1.53**	**1.36**	**1.59**	**1.84**	**6.32**	**0.69**	**0.59**	**0.64**	**0.81**	**2.73**
Louis Trichardt	1996 – 1999	1.99	0.06	0.97	1.51	4.53	0.44	0.01	0.99	0.64	2.08
	2000	**0.43**	**0.42**	**0.46**	**0.58**	**1.89**	**0.24**	**0.24**	**0.24**	**0.36**	**1.07**
Elandsfontein	1996 - 1999	n/a	n/a	n/a	n/a	n/a	n/a	n/a	n/a	n/a	n/a
	2000	**3.59**	**2.93**	**2.81**	**4.25**	**13.57**	**1.34**	**1.14**	**1.07**	**1.58**	**5.12**
Palmer	1996 – 1999	n/a	n/a	n/a	n/a	n/a	n/a	n/a	n/a	n/a	n/a
	2000	**2.27**	**1.71**	**1.78**	**2.99**	**8.75**	**0.91**	**0.75**	**0.75**	**1.29**	**3.70**

5.4 EVALUATION OF EMISSION DATA

The importance of the quality of emission data can not be underestimated in any air quality model, and it is generally acknowledged in the modelling community as a major source of uncertainty.

The emission data utilized by LED was the one accepted by the SAFARI 2000 research plan (Flemming and Van der Merwe, 2000), see Figure 4.12. In Figures 5.15 and 5.17 the ambient concentration and dry deposition fields for SO_2 are illustrated, which were produced utilizing the SAFARI 2000 emission database. A disturbing fact in these figures is the absence of any output fields around the well known Zambian Copperbelt, whose SO_2 emission rates are comparable to those of the highly industrialized Mpumalanga Highveld region in South Africa (See EDGAR 2000 Emission database: Figure 5.12). There is also no significant output over Zimbabwe for the ambient concentrations.

The obvious advantage of the international EDGAR emission database, which properly depicts the Zambian Copperbelt led, to the repetition of the calculation of ambient concentration as well as dry deposition for the winter season during 2000. The aim was to evaluate the importance of the quality of emission rates for producing reliable air pollution outputs. In Figures 5.16 and 5.18 the same fields as in Figures 5.15 and 5.17 are shown. Comparisons of the fields between these two sets of figures clearly demonstrate the deficiency of the SAFARI 2000 emission dataset. As a result of the use of the international data set the anticipated ouput fields around the Zambian Copperbelt are visible. Even without quantitative analysis, output fields in these figures demonstrate that the environmental impact of the Zambian Copperbelt is comparable to the industrialized Mpumalanga Highveld region.

Further one can anticipate that the use of more reliable emission data may improve the already discussed discrepancy of the modelled against measured results at the Louis Trichardt station. Clearly this station, which is closely located near Zimbabwe and Zambia, can not get any input from these countries if the model is used based on the Flemming and Van der Merwe database (Figure 5.15). The opposite is true for the results in Figure 5.16 where the industrial activities in the Zambian Copperbelt and Zimbabwe may increase the pollution levels at the station.

This discussion leads to the recommendation of revisiting the local SAFARI 2000 emission dataset.

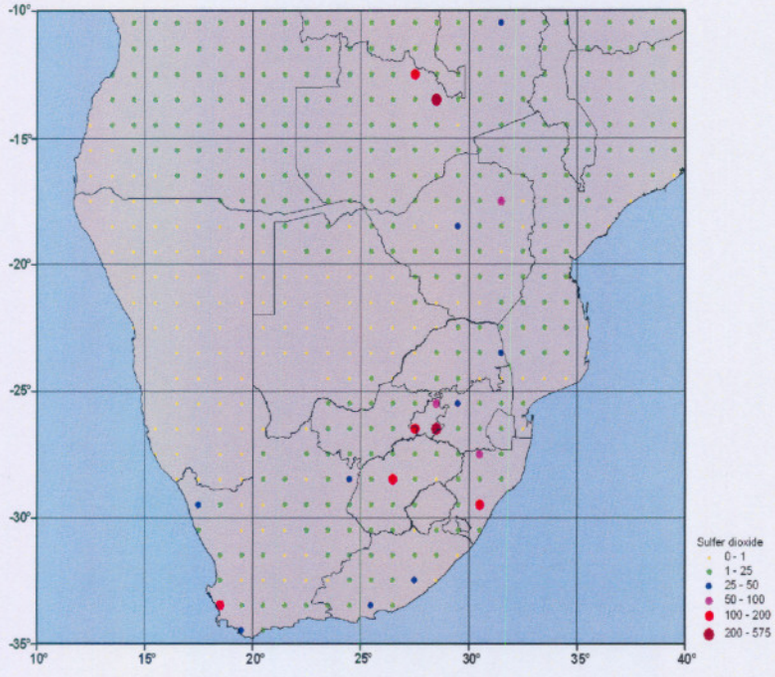

Figure 5.14: Sulphur dioxide (SO_2) emissions in Gg/annum for the modelling region based on the EDGAR 2000 emission database (EDGAR 2000, 2005)

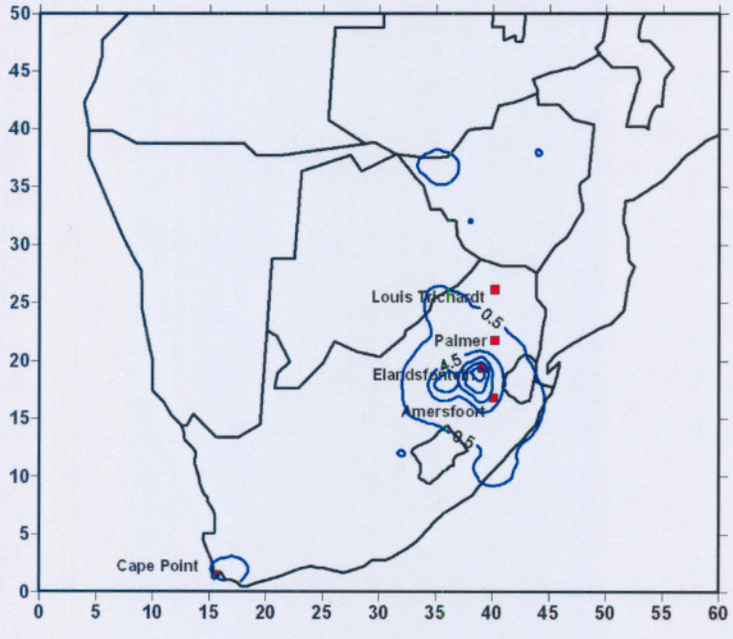

Figure 5.15: Mean ambient SO_2 concentrations ($\mu g.m^{-3}$) for the winter season during 2000 based on the emission database from Flemming and Van der Merwe (2000)

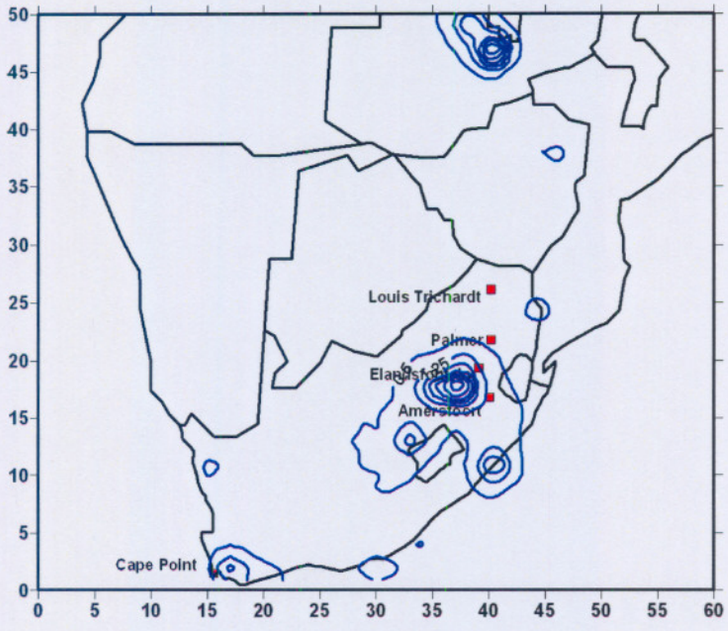

Figure 5.16: Mean ambient SO_2 concentrations ($\mu g.m^{-3}$) for the winter season during 2000 based on the EDGAR 2000 emission database

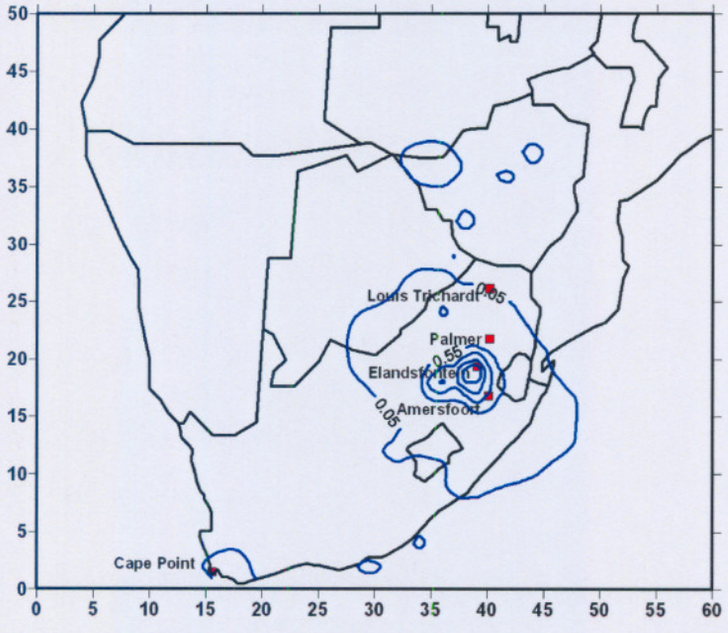

Figure 5.17: Accumulated dry deposition, SO_x as S ($kg.ha^{-1}.3\ months^{-1}$) for the winter season during 2000 based on the emission database from Flemming and Van der Merwe (2000)

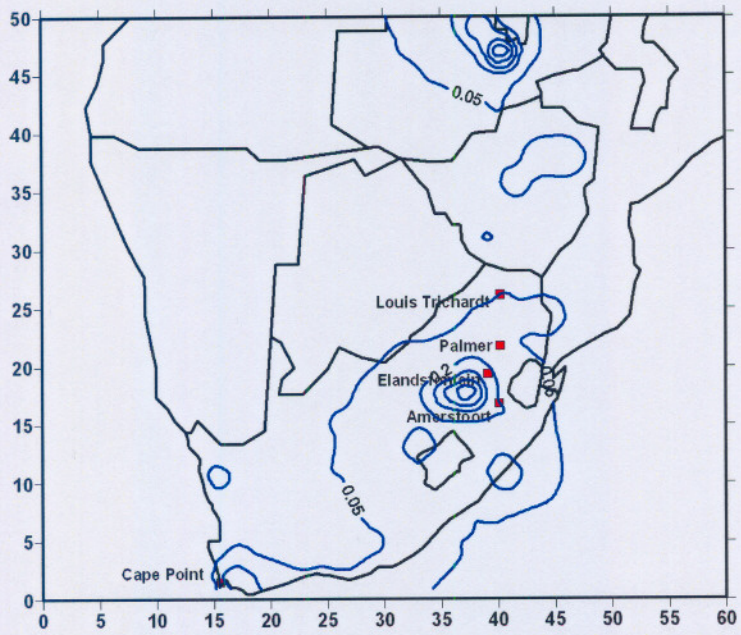

Figure 5.18: Accumulated dry deposition, SO_x as S ($kg.ha^{-1}.3\ months^{-1}$) for the winter season during 2000 based on the EDGAR 2000 emission database

5.5 SUMMARY

LED model results for ambient concentrations, as well as deposition fields were produced for all months during the year 2000, and compared with the available experimental data at the DEBITS sites. Data obtained for the evaluation were in the framework of SAFARI 2000 research campaign. However, the ground measurements needed for the evaluation of LED were not sufficient due to the small number of observation pionts (5), and geographical location which does not comply with the WMO criteria for baseline regional air quality stations.

Another shortcoming stems from the fact that some of the DEBITS stations were not fully operational during the year 2000. The predetermined SAFARI 2000 research plan for the period of integration (2000), did not allow the use of previous years measured data (where the availability of experimental data is somewhat more complete) for the evaluation exercise. Therefore data from before the year 2000, has been used to only evaluate LED capability of producing results which are in the range of the inter-annual observations.

Despite these inherent difficulties of not having a complete set of experimental data for the evaluation process, this chapter presents enough evidence of LED to produce reliable results. The annual quantities compare quite accurately. The bigger variation in differences of the monthly quantities is also within the acceptable range. The numerical experiment carried out with the alternative emission data set (EDGAR), clearly shows the importance of revisiting the existing emission data set accepted by the SAFARI 2000 research group, and gives a reasonable explanation for some of the monthy deviations observed at the most northen DEBITS station.

Chapter 6

LONG-RANGE TRANSPORT OF SO_x AND NO_x FROM SOUTH AFRICA

In this Chapter...

The objective of this chapter is briefly stated (Section 6.1). Section 6.2 gives a detailed description of the input parameters for the LED model that were used in this study, while Section 6.3 focuses on the discussions of the results obtained from the LED model. Section 6.4 summarizes areas of application of the LED model.

6.1 OBJECTIVES

The Mpumalanga Highveld region in South Africa is the industrial hub of South African industries, with an enormous environmental footprint.

Major sources of SO_2 in this region includes power stations, petrochemical plants, various other industries (e.g., brick works, ferro-alloy smelters, steel works, fertilizer plants, pulp and paper mills), colliery discard dumps, as well as biomass burning. Particulate sulphate is also emitted by some of these sources. According to Siversten *et. al.* (1995), 66 % of the annual total of 1.1 Mt of sulphur emitted into the southern African atmosphere originates in South Africa and of this 90 % is from the Mpumalanga Highveld (Wells *et. al.*, 1996).

In this section, the LED model was be utilized to establish and assess the impacts of emissions emanating from this industrialized highveld region of Mpumalanga, South Africa, on the southern African region. Special emphasis is on the airborne SO_x and NO_x species emanating from this region.

6.2 MODELLING PARAMETERS AND MODELLING SCENARIO

The converted emission database by Fleming and Van der Merwe (2000) as described in Chapter 4 was utilized as the baseline emission database for this study (as illustrated in Figure 4.12). Emissions for SO_2 and NO_x species were extracted for the specific highveld

region, and these emissions were converted into a region-specific emission database for input into LED. A graphical illustration of the highveld specific emission database that was utilized in LED is illustrated in Figure 6.1.

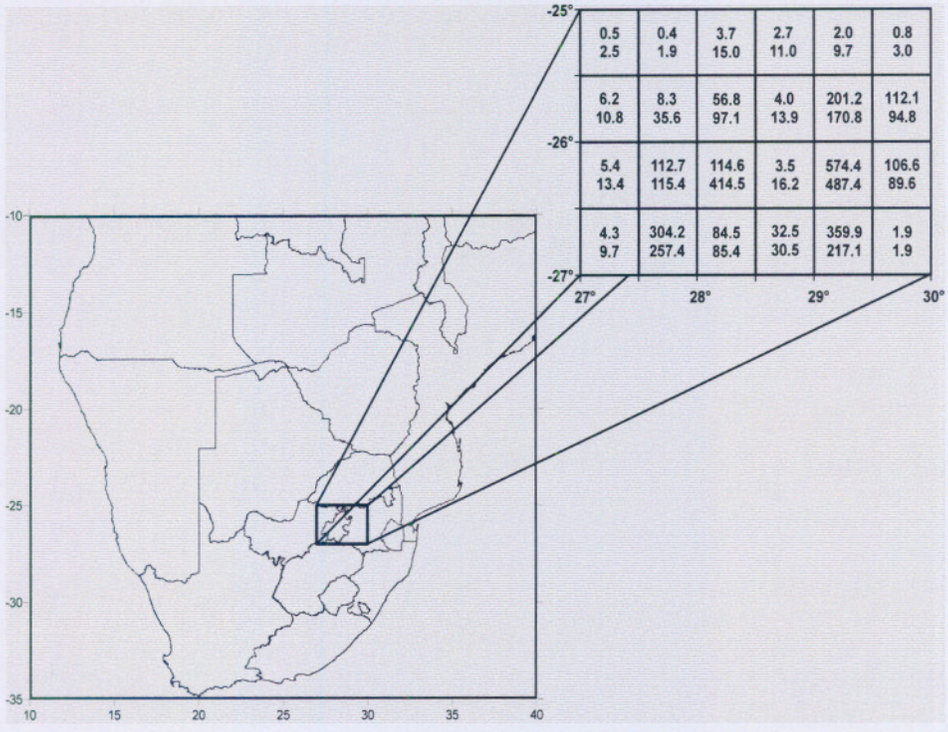

Figure 6.1: Gridded SO_2 (top) and NO_X (bottom) emissions (Gg per annum) for the greater Highveld region during 2000 (from Fleming and Van der Merwe, 2000)

Monthly meteorological data files for 2000 were utilized in this modelling scenario. A detailed description of the meteorological data was given in Chapter 4.

Results from the LED model include seasonal (summer and winter), as well as annual ambient concentrations, dry deposition and wet deposition profiles for SO_x and NO_x species over the southern African region, which illustrate the environmental footprint of this highly industrialized region.

6.3 RESULTS AND DISCUSSIONS

Monthly runs for 2000 were executed by the LED model for emissions emanating from the highveld region. The monthly results obtained from the LED model were averaged for ambient concentration results, and summed up for deposition results, to obtain seasonal ambient and deposition results for 2000. As previously mentioned, assumptions were made that the summer season consists of January, February and December; autumn consists of March, April and May; winter consists of June, July and August; and spring consists of September, October and November. Results from the LED model were superimposed on the Cartesian grid utilized in the LED model for graphical illustrations of these results.

Figures 6.2 and 6.3 illustrate the mean ambient SO_2 concentrations ($\mu g.m^{-3}$) for the summer and winter seasons during 2000, while Figures 6.4 and 6.5 illustrate the mean ambient SO_4 concentrations ($\mu g.m^{-3}$) for the summer and winter seasons during 2000.

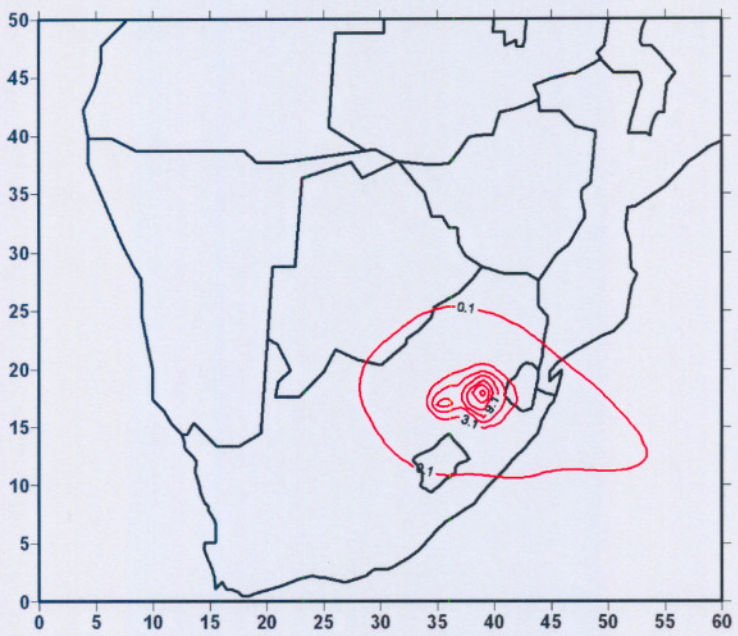

Figure 6.2: Mean ambient SO_2 concentrations ($\mu g.m^{-3}$) for the summer season during 2000

The comparison of Figures 6.2 and 6.3 reveals a resemblance of the extent of the environmental footprint, which is due to the similarity of the predominant wind direction for the two seasons during 2000. The main difference in the meteorological data is in the more frequent inversion layers, and stable planetary boundary layer during the winter season. This is reflected in the increase by 35% on average of the maximium ambient concentration experienced during the winter season of 2000. It should also be noted that the maximum values calculated by LED are located over, or in close proximity of the emission region.

Figures 6.4 and 6.5 illustrate the mean ambient NO_2 concentrations ($\mu g.m^{-3}$) for the summer and winter seasons during 2000. Analysis of the ambient NO_2 concentration fields in these two figures confirms the findings for the SO_2 concentration fields as discussed in the previous paragraph.

Figures 6.6 and 6.7 illustrate the accumulated dry deposition of SO_x as S ($\mu g.m^{-3}$) for the summer and winter seasons during 2000, while Figures 6.8 and 6.9 illustrates the accumulated dry deposition of NO_x as N ($\mu g.m^{-3}$) for the summer and winter seasons during 2000.

Figures 6.6 to 6.9 show the accumulated SO_x and NO_x during 2000. Once again the appearance of the dry deposition output fields reflects the approximate similarity of the predominant wind direction for the summer and winter season during 2000.

The deposition total for the winter season for these quantities are lower due to the suppresed turbulence during this season. A comparison of the range of calculated accumulated dry deposition values from LED, with experimental data from Mhpepya (2002) (summary of this data is presented in Table 5.7, Chapter 5), shows that LED produces reliable estimates.

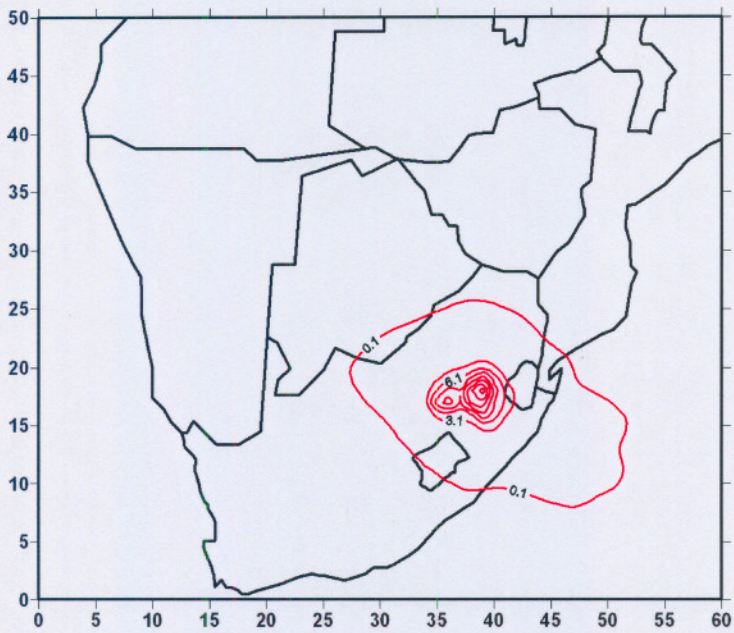

Figure 6.3: Mean ambient SO_2 concentrations ($\mu g.m^{-3}$) for the winter season during 2000

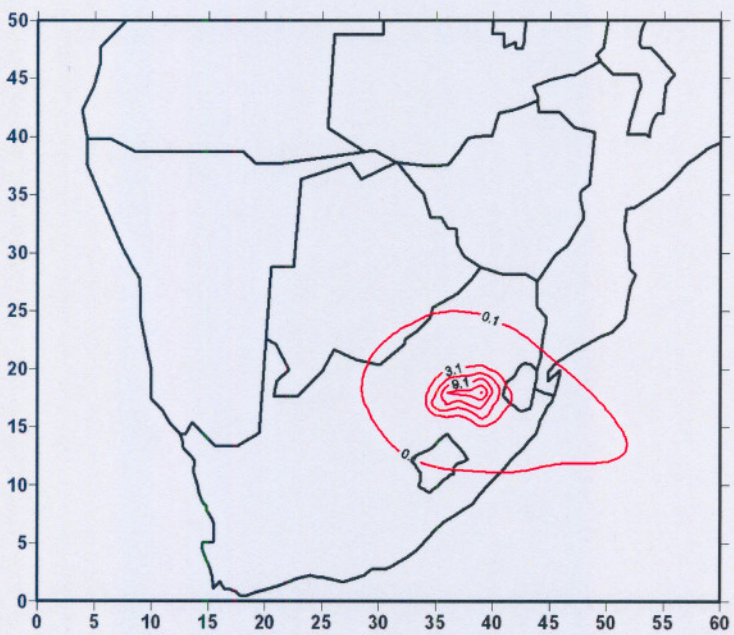

Figure 6.4: Mean ambient NO_2 concentrations ($\mu g.m^{-3}$) for the summer season during 2000

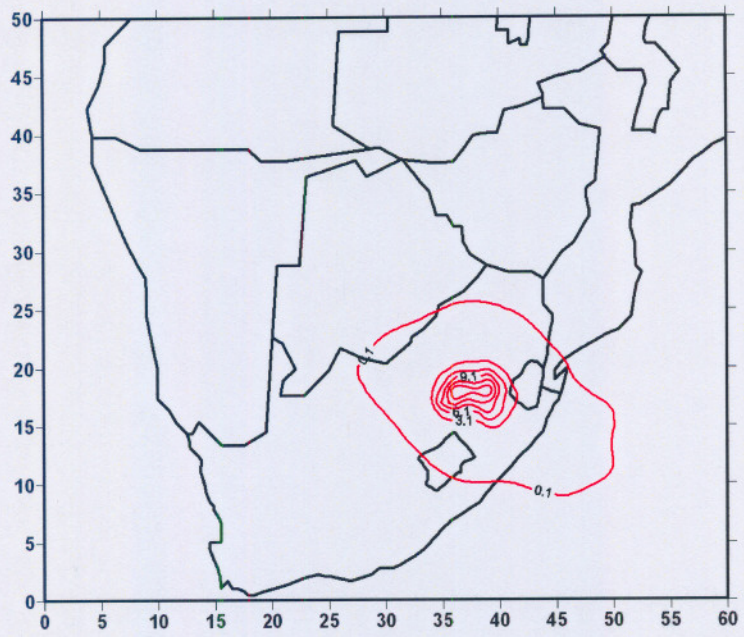

Figure 6.5: Mean ambient NO_2 concentrations ($\mu g.m^{-3}$) for the winter season during 2000

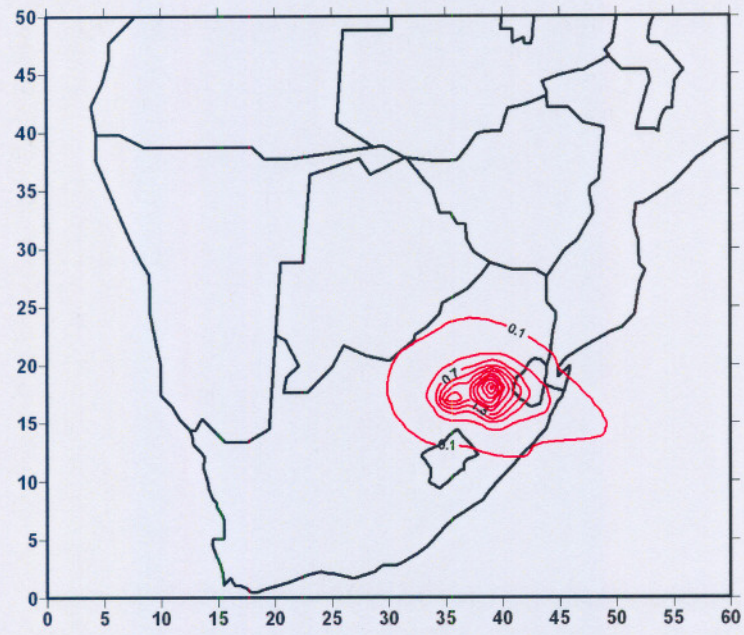

Figure 6.6: Accumulated dry deposition, SO_x as S ($kg.ha^{-1}.3\ months^{-1}$) for the summer season during 2000

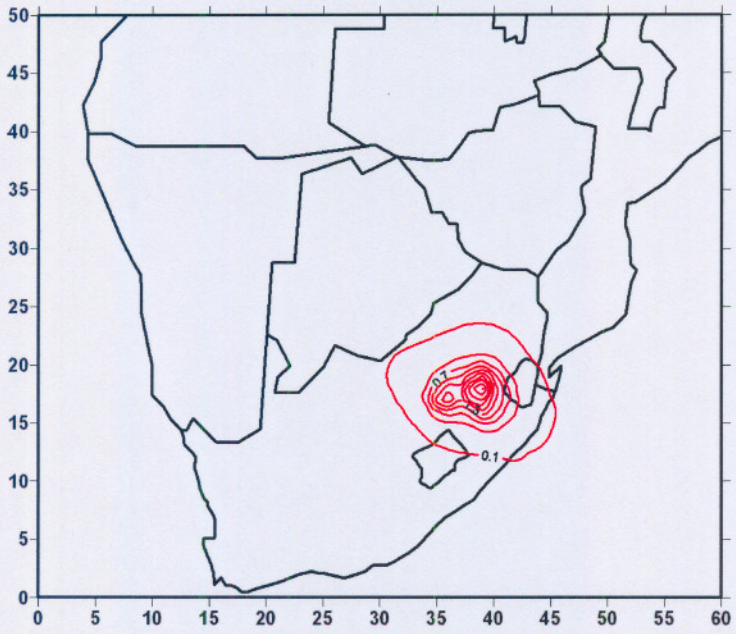

Figure 6.7: Accumulated dry deposition, SO_x as S ($kg.ha^{-1}.3\ months^{-1}$) for the winter season during 2000

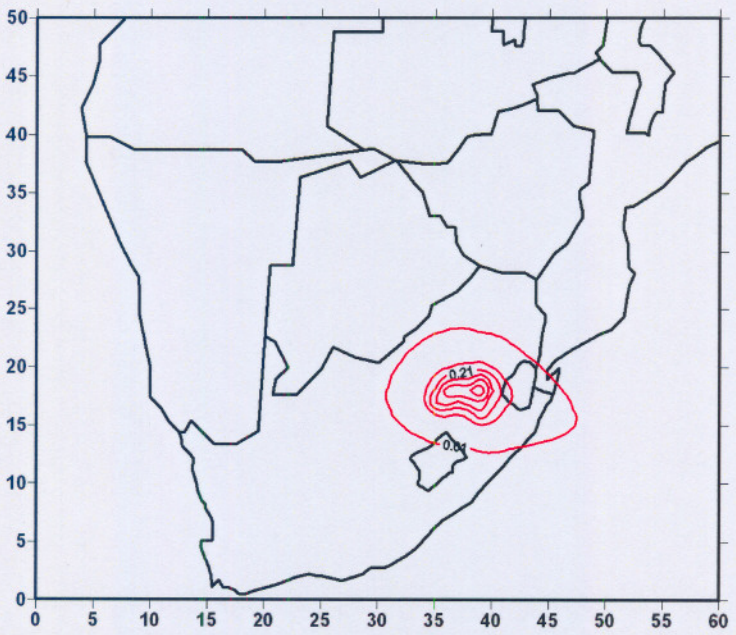

Figure 6.8: Accumulated dry deposition, NO_x as N ($kg.ha^{-1}.3\ months^{-1}$) for the summer season during 2000

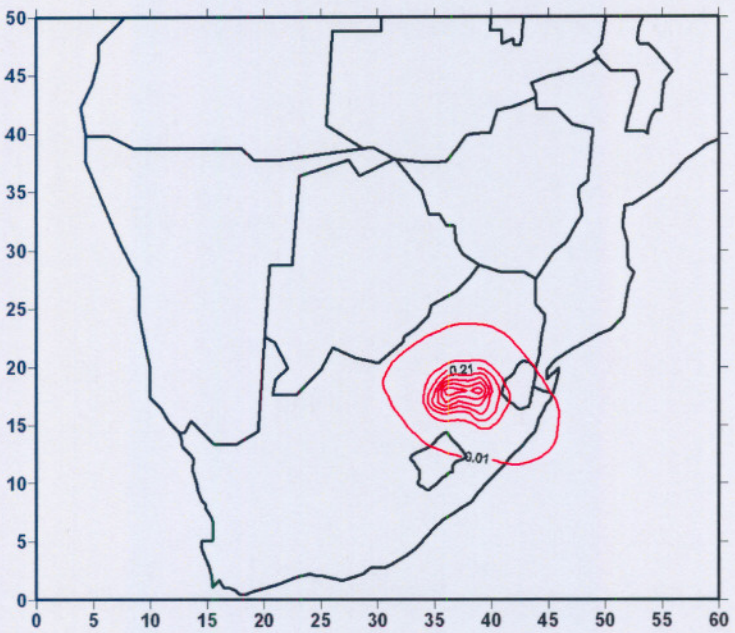

Figure 6.9: Accumulated dry deposition, NO_x as N (kg.ha^{-1}.3 months^{-1}) for the winter season during 2000

Figures 6.10 and 6.11 illustrates the accumulated wet deposition of SO_x as S (μg.m^{-3}) for the summer and winter seasons during 2000, while Figures 6.12 and 6.13 present the accumulated wet deposition of NO_x as N (μg.m^{-3}) for the summer and winter seasons during 2000.

Similarily to the accumulated dry deposition, Figures 6.10 to 6.13 illustrates the accumulated wet deposition of SO_x as S (μg.m^{-3}) for the summer and winter seasons during 2000. LED produced lower maximum wet deposition values during the winter season, which is attributed to the meteorological phenomina of minimal rain events during the winter season in the southern African region. It should be pointed out that the range of values for the wet deposition produced by LED during 2000, compares favourably with the experimental data set of Mhpepya (2002) for the DEBITS sites.

Figures 6.13 and 6.14 illustrate the pH values of precipitation for the summer and winter seasons during 2000 as calculated by LED.

The complicated distribution of pH values in the region reflects the inherent patchiness of the rain events, which are mainly connected with strong convective type of cloud activities. The range of calculated pH values falls well within the results produced by other models and observational data (Mphepya *et. al.*, 2004). It can be noted that the lowest pH values (higher acidity) occurs over the industrialized part of southern Africa, from where the emissions emanate. This must be anticipated by revisiting the calculated ambient SO_2 and NO_2 concentration fields as presented in Figures 6.2 to 6.5. The need for southern African data sets, especially for pH values, to fully validate or correlate modelled results can be emphasized again.

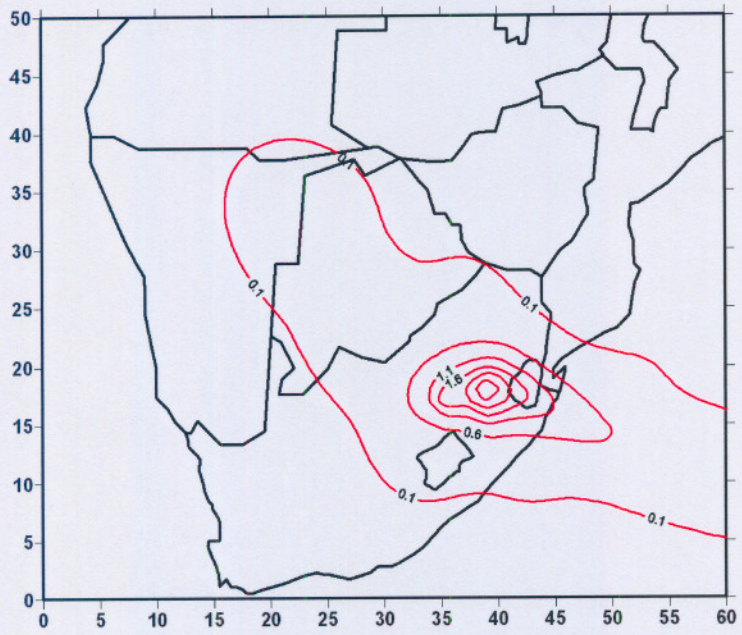

Figure 6.10: Accumulated wet deposition, SO_x as S ($kg.ha^{-1}.3\ months^{-1}$) for the summer season during 2000

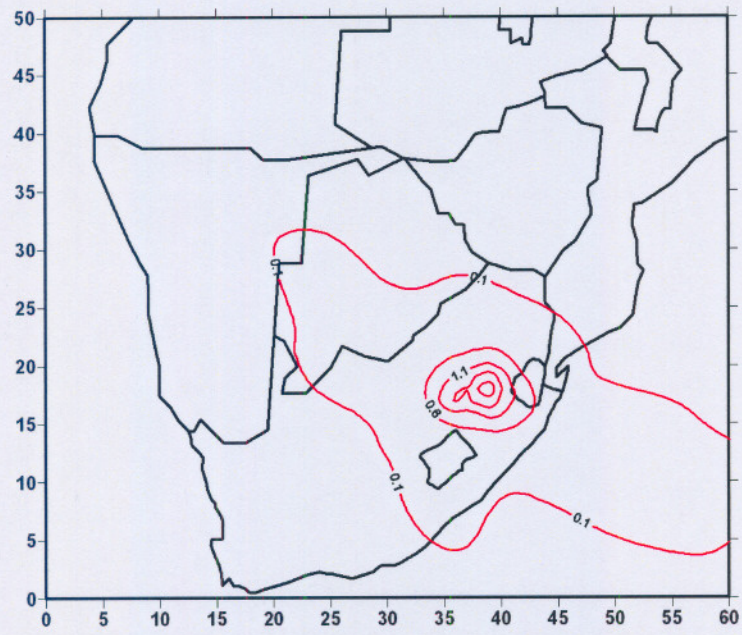

Figure 6.11: Accumulated wet deposition, SO_x as S ($kg.ha^{-1}.3\ months^{-1}$) for the winter season during 2000

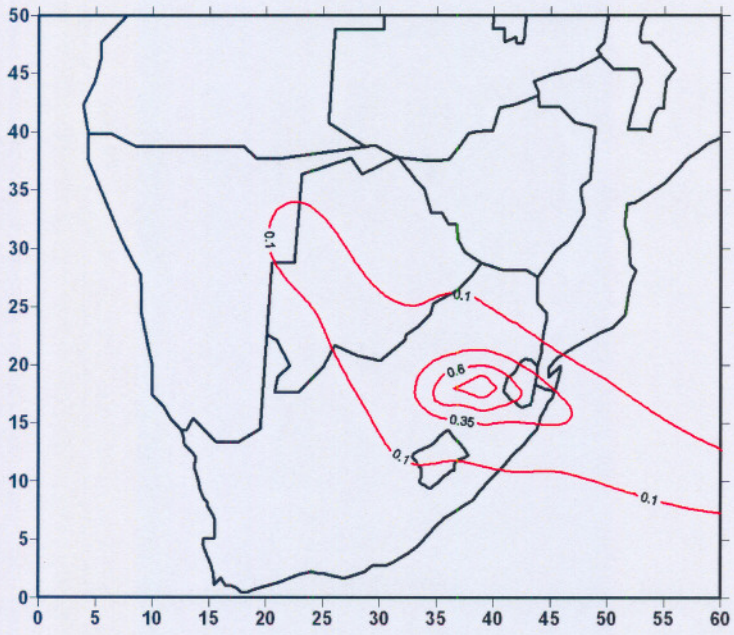

Figure 6.12: Accumulated wet deposition, NO_x as N (kg.ha^{-1}.3 months^{-1}) for the summer season during 2000

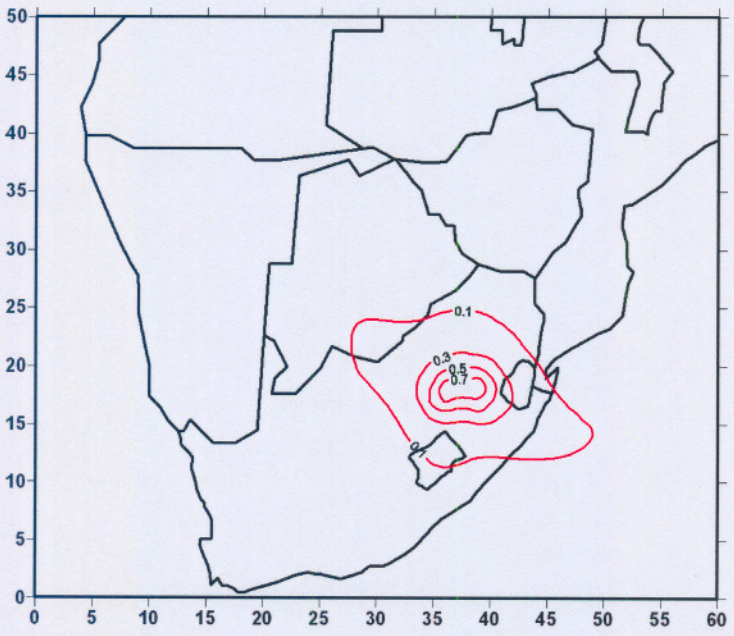

Figure 6.13: Accumulated wet deposition, NO_x as N (kg.ha^{-1}.3 months^{-1}) for the winter season during 2000

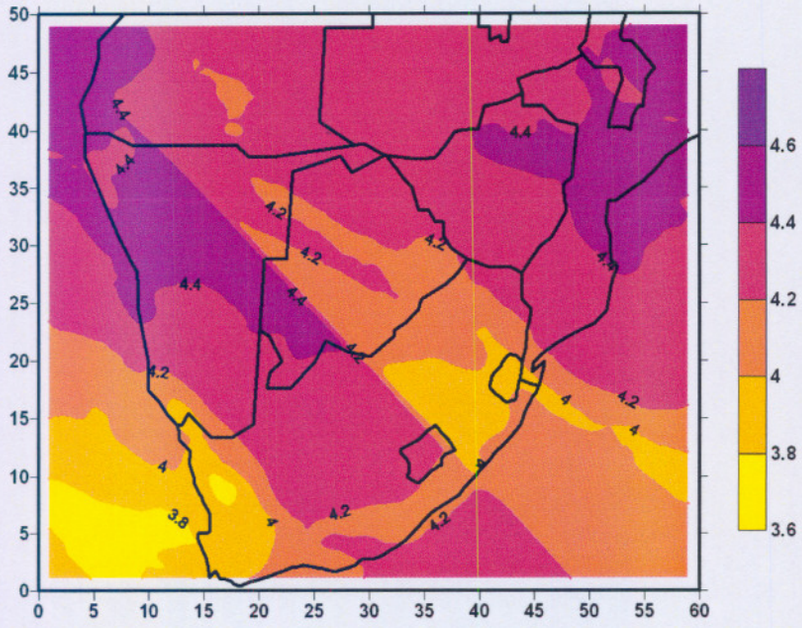

Figure 6.14: Calculated pH values for the summer season during 2000

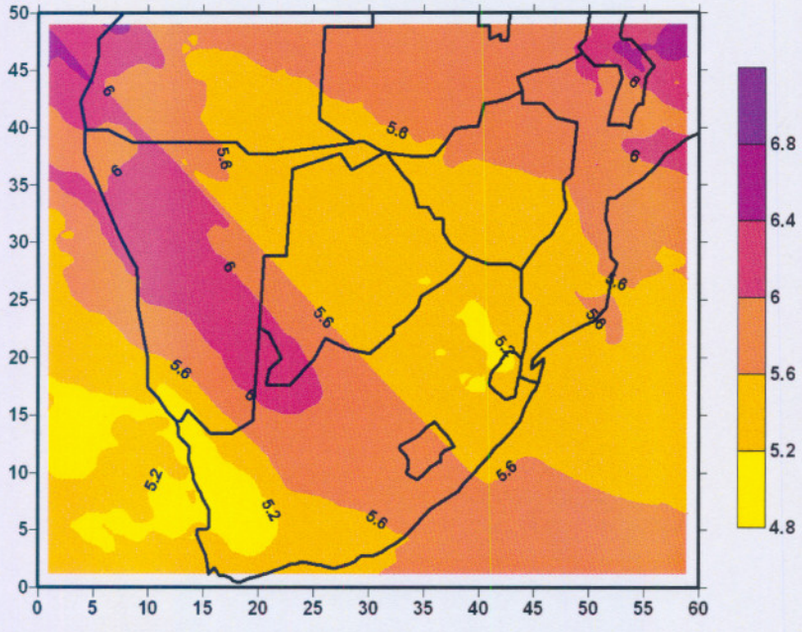

Figure 6.15: Calculated pH values for the winter season during 2000

6.4 SUMMARY

This case study implementation of LED to study the long-range transport from the highly industrialized Highveld region of South Africa, demonstrates the versitality of the LED model. This include the calculation of ambient concentration fields, accumulated dry- and wet deposition fields, as well as pH values of precipitation over the modelling region.

As demonstrated, the output allows the environmental footprint characteristics to be determined. In the case under consideration, the environmental impact region is located approximately 500 to 600 kilometers around the industrial region.

The comparison of the calcualted model results with limited experimental data for the region, and lack of outputs from other models and observations, substantiate the use of LED for environmental impact studies, regulatory purposes and decision making.

Chapter 7

A DEPOSITION MATRIX FOR SOUTHERN AFRICA

In this Chapter...

The objective of this chapter is briefly stated (Section 7.1). Section 7.2 gives a detailed description of the parameters utilized for this specific modelling scenario, while Section 7.3 discusses the results obtained from the LED model. Section 7.4 concludes the chapter.

7.1 OBJECTIVES

The transboundary transport of air pollutants in the southern African region is of great concern due to the quantity of fossil fuels being utilized, as well as the unique synoptic circulation patterns which prevails over this subcontinent.

Moreover, agricultural activities are imperative for the existance of many of the inhabitants of this region. Deposition of specific species may pose a significant environmental risk, more specifically, crop production throughout the modelling region.

As previously highlighted in Chapter 2, new air quality legislation was promulgated during September 2005 in South Africa. The National Environmental Management: Air Quality Act, 2004 (Act No. 39 of 2004) demands a total paradigm shift from permitting scheduled processes, to ambient air quality standards. Ambient concentration standards for specific pollutant species are set down by the Department of Environmental Affairs and Tourism (DEAT) for specific pollutants, and the latter should not be exceeded. Chapter 6 of the National Environmental Management: Air Quality Act, 2004 in South Africa deals specifically with the issue of International Air Quality Management and transboundary air pollution.

In this section, the LED model will be utilised to establish and assess the impacts of emissions emanating from individual countries in the southern African region. Country-to-country dry- and wet deposition matrices will be developed to illustated the contribution of individual countries on the other countries in the region. These matrices will give guidance in establishing a regional air quality management plan for the modelling domain.

7.2 MODELLING PARAMETERS AND SCENARIO

Monthly meteorological data files for 2000 were utilized in this modelling scenario. A detailed description of the meteorological data is given in Chapter 4.

The converted emission database by Fleming and Van der Merwe (2000) as discussed in Chapter 4, was utilized as the baseline emission database. The geographical distribution of the emission sources and their associated strenghts are illustrated in Figure 4.12, Chapter 4. This emission database was converted into a country-specific emission database for input into LED.

Modelling runs were conducted with LED for the year 2000, utilizing these country specific emission files. Country-to-country deposition quantities are obtained as a final result from the LED model. Figures 7.1 and 7.2 present graphical illustrations of the country specific emission database (files) obtained for South Africa and Zambia respectively from the original SAFARI 2000 database from Fleming and Van der Merwe (2000).

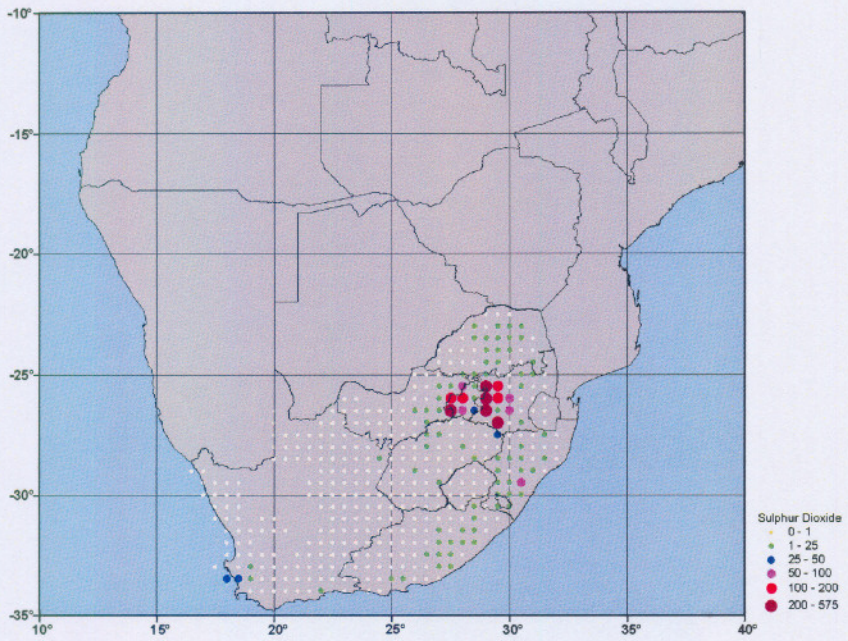

Figure 7.1: Sulphur dioxide (SO_2) emissions in Gg/annum for South Africa

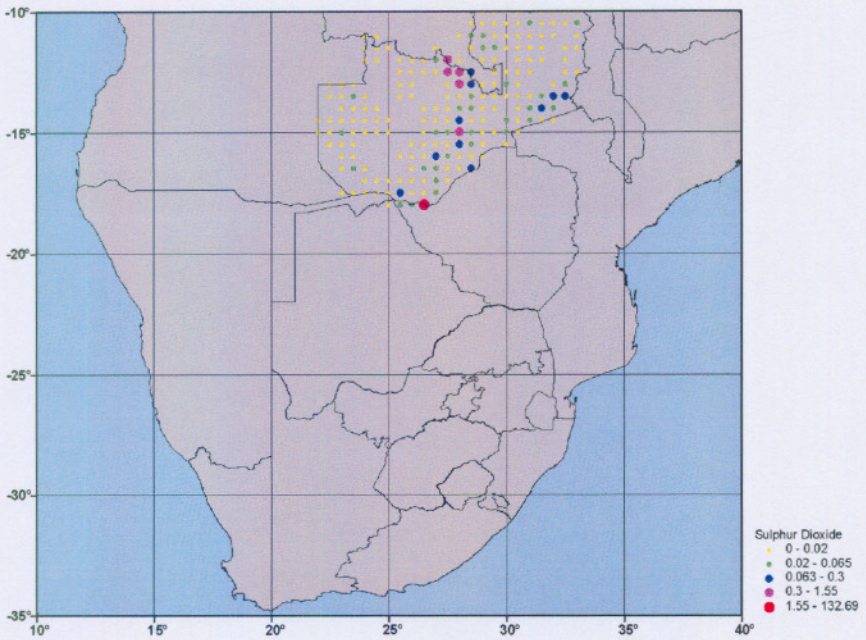

Figure 7.2: Sulphur dioxide (SO_2) emissions in Gg/annum for Zambia

7.3 RESULTS AND DISCUSSIONS

Monthly runs for 2000 for all individual countries in the modelling region, were executed with the LED model. The monthly deposition results can be used to obtain seasonal and annual deposition quantities on a country-to-country basis.

For illustrative purposes only, Figure 7.3 presents the SO_x as S, annual dry deposition pattern for 2000 over the southern African region for SO_2 emissions emanating from South Africa.

Tables 7.1 and 7.2 summarize LED results for the country-to-country dry deposition matrices for 2000, based on the country-specific emissions.

The top values in both Tables 7.1 and 7.2 indicate the persentage deposition recieved from the specified emitter indicated on the left hand side in the matrix. Therefore every top horisontal line represents the partition of the deposition to its own and the other countries. It is obvious that the sum of the partition percentage quantities should add up to 100%. The bottom values in the horizontal lines are the deposition quantities (percentages) expressed in tonnes per annum.

The vertical coulumn drawn on the right hand side for each specific reciever country in Table 7.2, contains the percentage contribution to the deposition from the reciever countries. Again the sum of these percentages adds up to 100%.

These tables can be used to perform the following analysis. To illustrate the analysis Botswana will be used as an example using Tables 7.1 and 7.2.

During 2000, and treating the SO_2 emissions exclusively from Botswana, only 32.58% of these emissions were deposited over Botswana. While 3.5% of these emissions were deposited

Table 7.1: Annual country-to-country dry deposition matrix of SO_x as S for 2000 (Top value: Percentage of total deposition received; Bottom value: tons.annum^{-1} received). Ang: Angola, Bot: Botswana, Mal: Malawi, Moz: Mozambique, Nam: Namibia, Ocn: Oceans, RSA: South Africa, Zam: Zambia, Zim: Zimbabwe

	RECEIVER									
EMITTER	**Ang**	**Bot**	**Mal**	**Moz**	**Nam**	**Ocn**	**RSA**	**Zam**	**Zim**	**Total**
Ang	96.61 4.55×10^{2}	0.01 4.85×10^{-2}	0.00 0.00	0.00 0.00	2.85 1.34×10^{1}	0.35 1.66	0.00 0.00	0.18 8.48×10^{-1}	0.00 0.00	100 -
Bot	3.50 2.56×10^{3}	32.58 2.38×10^{4}	0.15 1.13×10^{2}	4.77 3.49×10^{3}	2.76 2.02×10^{3}	4.91 3.59×10^{3}	38.08 2.78×10^{4}	3.47 2.53×10^{3}	9.77 7.15×10^{3}	100 -
Mal	0.53 8.05×10^{-1}	0.17 2.61×10^{-1}	10.67 1.63×10^{1}	78.72 1.20×10^{2}	0.13 1.93×10^{-1}	0.30 4.63×10^{-1}	0.14 2.11×10^{-1}	8.56 1.30×10^{1}	0.78 1.19	100 -
Moz	0.07 2.68	1.20 4.49×10^{1}	1.94 7.27×10^{1}	50.81 1.90×10^{3}	8.04 3.01×10^{2}	27.95 1.05×10^{3}	7.81 2.92×10^{2}	0.35 1.32×10^{1}	1.83 6.86×10^{1}	100 -
Nam	16.68 2.90×10^{2}	3.51 6.11×10^{1}	0.00 1.12×10^{-3}	0.70 1.22×10^{1}	75.88 1.32×10^{3}	2.13 3.70×10^{1}	1.05 1.82×10^{1}	0.02 2.70×10^{-1}	0.04 6.64×10^{-1}	100 -
Ocn	0.00 0.00	0.00 0.00	0.00 0.00	0.00 0.00	0.00 0.00	0.00 0.00	0.00 0.00	0.00 0.00	0.00 0.00	0.00 -
RSA	1.68 1.47×10^{4}	6.88 6.00×10^{4}	0.10 8.92×10^{2}	5.23 4.56×10^{4}	2.00 1.74×10^{4}	12.41 1.08×10^{5}	68.82 6.00×10^{5}	1.15 1.00×10^{4}	1.72 1.50×10^{4}	100 -
Zam	9.37 3.90×10^{3}	4.51 1.87×10^{3}	0.83 3.47×10^{2}	4.08 1.69×10^{3}	2.56 1.07×10^{3}	0.83 3.46×10^{2}	1.37 5.72×10^{2}	57.47 2.39×10^{4}	18.97 7.89×10^{3}	100 -
Zim	4.52 1.22×10^{3}	4.49 1.21×10^{3}	1.53 4.13×10^{2}	22.53 6.09×10^{3}	1.71 4.62×10^{2}	1.20 3.23×10^{2}	1.74 4.69×10^{2}	17.88 4.83×10^{3}	44.40 1.20×10^{4}	100 -

Table 7.2: Annual country-to-country dry deposition matrix of SO_x as S for 2000 (Top value: Percentage of total deposition received; Bottom value: Origin of deposition load in persentage). Ang: Angola, Bot: Botswana, Mal: Malawi, Moz: Mozambique, Nam: Namibia, Ocn: Oceans, RSA: South Africa, Zam: Zambia, Zim: Zimbabwe

	RECEIVER																					
EMITTER	Ang		Bot		Mal		Moz		Nam		Ocn		RSA		Zam		Zim		Total
Ang	96.61	-	0.01	-	0.00	-	0.00	-	2.85	-	0.35	-	0.00	-	0.18	-	0.00	-	100
	-	1.97	-	0.00	-	0.00	-	0.00	-	0.06	-	0.00	-	0.00	-	0.00	-	0.00	-
Bot	3.50	-	32.58	-	0.15	-	4.77	-	2.76	-	4.91	-	38.08	-	3.47	-	9.77	-	100
	-	11.09	-	27.39	-	6.11	-	5.93	-	8.93	-	3.16	-	4.43	-	6.14	-	16.98	-
Mal	0.53	-	0.17	-	10.67	-	78.72	-	0.13	-	0.30	-	0.14	-	8.56	-	0.78	-	100
	-	0.00	-	0.00	-	0.88	-	0.20	-	0.00	-	0.00	-	0.00	-	0.03	-	0.00	-
Moz	0.07	-	1.20	-	1.94	-	50.81	-	8.04	-	27.95	-	7.81	-	0.35	-	1.83	-	100
	-	0.01	-	0.05	-	3.92	-	3.23	-	1.33	-	0.92	-	0.05	-	0.03	-	0.16	-
Nam	16.68	-	3.51	-	0.00	-	0.70	-	75.88	-	2.13	-	1.05	-	0.02	-	0.04	-	100
	-	1.26	-	0.07	-	0.00	-	0.02	-	5.85	-	0.03	-	0.00	-	0.00	-	0.00	-
Ocn	0.00	-	0.00	-	0.00	-	0.00	-	0.00	-	0.00	-	0.00	-	0.00	-	0.00	-	0.00
	-	0.00	-	0.00	-	0.00	-	0.00	-	0.00	-	0.00	-	0.00	-	0.00	-	0.00	-
RSA	1.68	-	6.88	-	0.10	-	5.23	-	2.00	-	12.41	-	68.82	-	1.15	-	1.72	-	100
	-	63.49	-	68.94	-	48.13	-	77.40	-	77.06	-	95.29	-	95.36	-	24.21	-	35.59	-
Zam	9.37	-	4.51	-	0.83	-	4.08	-	2.56	-	0.83	-	1.37	-	57.47	-	18.97	-	100
	-	16.88	-	2.16	-	18.71	-	2.88	-	4.72	-	0.30	-	0.09	-	57.88	-	18.74	-
Zim	4.52	-	4.49	-	1.53	-	22.53	-	1.71	-	1.20	-	1.74	-	17.88	-	44.40	-	100
	-	5.29	-	1.40	-	22.26	-	10.34	-	2.05	-	0.28	-	0.07	-	11.70	-	28.51	-
Total	-	100	-	100	-	100	-	100	-	100	-	100	-	100	-	100	-	100	-

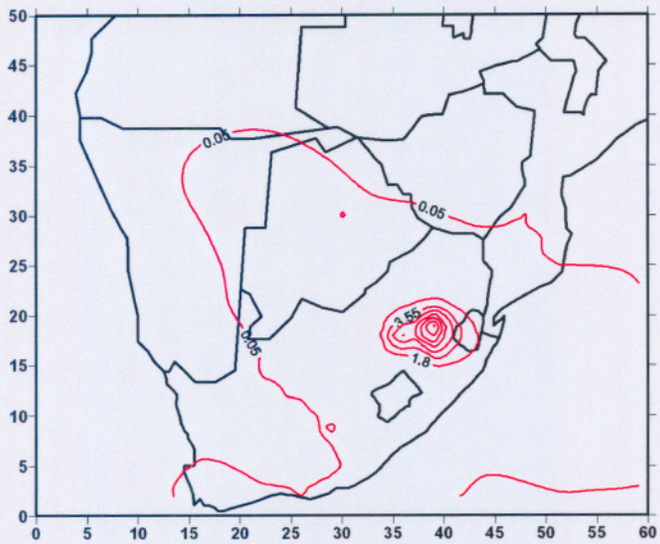

Figure 7.3: Accumulated dry deposition, SO_x as S (kg.ha^{-1}.annum^{-1}) for 2000, emanating from South Africa

over Angola (Ang) and 0.15%, 4.77%, 2.76%, 4.91%, 38.08%, 3.47% and 9.77% were deposited over Malawi (Mal), Mozambique (Moz), Namibia (Nam), the oceans (OCN), South Africa (RSA), Zambia (Zam) and Zimbabwe (Zim) respectively.

Therefore the analysis of the horizontal rows for each country allows the quantification in percentage (top value in Table 7.1), and absolute values (bottom values in Table 7.1) of the distribution of the emitter country to the deposition pattern in all receiving countries.

The analysis of the vertical column drawn on the right hand side for each specific receiver country in Table 7.2, allows one to identify where each country's deposition load originates from. For example Botswana as a receiver obtains 0.0% from Angola, 27.4% from itself, 0.0% from Malawi, 0.1% from Mozambique, 0.1% from Namibia, 69.0% from South Africa, 2.2% from Zambia and 1.4% from Zimbabwe. Again the sum of these percentages should add up to 100%. The percentage deposition received from the specified emitter indicated on the left hand side in the matrix is indicated by the left column in Table 7.2, and is similar to Table 7.1.

Tables 7.3 and 7.4 summarize LED results for the country-to-country wet deposition matrices for 2000, based on the country-specific emissions. The analysis for the wet deposition matrices (Tables 7.3 and 7.4), can be executed in the same manner as for the dry deposition matrices (Tables 7.1 and 7.2).

It is clear from the examples considered above, that if the Botswana goverment decides to prepare an air quality management plan, the country-to-country matrices indicates that emissions emanating from South Africa is responsible for 69% of all dry deposition in Botswana.

This illustration, based on one country, shows the importance of the country-to-country deposition matrices in a holistic air-quality management plan for the region as a whole. Analysis of these matrices clearly indicate the seriousness and complexity of transboundary transport of air pollutants in this specific region. However, these matrices are only representative for the year 2000, and are based on the emission database of Flemming and Van der Merwe (2000), which clearly needs upgrading (See Chapter 6).

Table 7.3: Annual country-to-country wet deposition matrix of SO_x as S for 2000 (Top value: Percentage of total deposition received; Bottom value: tons.annum^{-}1 received). Ang: Angola, Bot: Botswana, Mal: Malawi, Moz: Mozambique, Nam: Namibia, Ocn: Oceans, RSA: South Africa, Zam: Zambia, Zim: Zimbabwe

	RECEIVER									
EMITTER	**Ang**	**Bot**	**Mal**	**Moz**	**Nam**	**Ocn**	**RSA**	**Zam**	**Zim**	**Total**
Ang	92.68 $5.46\text{x}10^{2}$	0.01 $6.46\text{x}10^{-2}$	0.00 0.00	0.00 0.00	6.58 $3.88\text{x}10^{1}$	0.67 3.97	0.00 0.00	0.06 $3.46\text{x}10^{-1}$	0.00 0.00	100 -
Bot	6.13 $1.04\text{x}10^{4}$	26.72 $4.55\text{x}10^{4}$	0.26 $4.39\text{x}10^{2}$	6.26 $1.07\text{x}10^{4}$	5.05 $8.59\text{x}10^{3}$	12.92 $2.20\text{x}10^{4}$	27.80 $4.73\text{x}10^{4}$	5.78 $9.84\text{x}10^{3}$	9.08 $1.55\text{x}10^{4}$	100 -
Mal	1.82 3.25	0.67 1.20	12.76 $2.28\text{x}10^{1}$	56.49 $1.01\text{x}10^{2}$	0.53 $9.39\text{x}10^{-1}$	2.32 4.13	0.55 $9.82\text{x}10^{-1}$	21.93 $3.91\text{x}10^{1}$	2.93 5.22	100 -
Moz	0.19 $1.08\text{x}10^{1}$	2.72 $1.51\text{x}10^{2}$	1.08 $6.02\text{x}10^{1}$	30.17 $1.68\text{x}10^{3}$	5.59 $3.11\text{x}10^{2}$	43.08 $2.40\text{x}10^{3}$	12.50 $6.96\text{x}10^{2}$	0.86 $4.77\text{x}10^{1}$	3.82 $2.13\text{x}10^{2}$	100 -
Nam	14.37 $3.23\text{x}10^{2}$	6.12 $1.38\text{x}10^{2}$	0.00 $1.98\text{x}10^{-3}$	0.39 8.85	72.09 $1.62\text{x}10^{3}$	5.36 $1.21\text{x}10^{2}$	1.56 $3.51\text{x}10^{1}$	0.03 $7.40\text{x}10^{-1}$	0.07 1.54	100 -
Ocn	0.00 0.00	0.00 0.00	0.00 0.00	0.00 0.00	0.00 0.00	0.00 0.00	0.00 0.00	0.00 0.00	0.00 0.00	0.00 -
RSA	3.09 $6.38\text{x}10^{4}$	10.27 $2.12\text{x}10^{5}$	0.18 $3.67\text{x}10^{3}$	6.77 $1.40\text{x}10^{5}$	3.73 $7.72\text{x}10^{4}$	25.50 $5.27\text{x}10^{5}$	45.89 $9.49\text{x}10^{5}$	2.09 $4.31\text{x}10^{4}$	2.48 $5.12\text{x}10^{4}$	100 -
Zam	13.65 $1.36\text{x}10^{4}$	6.56 $6.55\text{x}10^{3}$	1.38 $1.38\text{x}10^{3}$	6.52 $6.51\text{x}10^{3}$	4.23 $4.23\text{x}10^{3}$	2.72 $2.72\text{x}10^{3}$	2.29 $2.29\text{x}10^{3}$	48.38 $4.84\text{x}10^{4}$	14.27 $1.43\text{x}10^{4}$	100 -
Zim	7.55 $4.44\text{x}10^{3}$	6.59 $3.87\text{x}10^{3}$	2.17 $1.28\text{x}10^{3}$	17.55 $1.03\text{x}10^{4}$	3.05 $1.79\text{x}10^{3}$	3.50 $2.06\text{x}10^{3}$	2.89 $1.70\text{x}10^{3}$	25.25 $1.48\text{x}10^{4}$	31.45 $1.85\text{x}10^{4}$	100 -

Table 7.4: Annual country-to-country wet deposition matrix of SO_x as S for 2000 (Top value: Percentage of total deposition received; Bottom value: Origin of deposition load in persentage). Ang: Angola, Bot: Botswana, Mal: Malawi, Moz: Mozambique, Nam: Namibia, Ocn: Oceans, RSA: South Africa, Zam: Zambia, Zim: Zimbabwe

	RECEIVER																					
EMITTER	**Ang**		**Bot**		**Mal**		**Moz**		**Nam**		**Ocn**		**RSA**		**Zam**		**Zim**		**Total**
Ang	92.68	-	0.01	-	0.00	-	0.00	-	6.58	-	0.67	-	0.00	-	0.06	-	0.00	-	100
	-	0.59	-	0.00	-	0.00	0.00	0.00	-	0.04	-	0.00	-	0.00	-	0.00	-	0.00	-
Bot	6.13	-	26.72	-	0.26	-	6.26	-	5.05	-	12.92	-	27.80	-	5.78	-	9.08	-	100
	-	11.20	-	16.93	-	6.41	-	6.30	-	9.16	-	3.95	-	4.73	-	8.47	-	15.51	-
Mal	1.82	-	0.67	-	12.76	-	56.49	-	0.53	-	2.32	-	0.55	-	21.93	-	2.93	-	100
	-	0.00	-	0.00	-	0.33	-	0.06	-	0.00	-	0.00	-	0.00	-	0.03	-	0.01	-
Moz	0.19	-	2.72	-	1.08	-	30.17	-	5.59	-	43.08	-	12.50	-	0.86	-	3.82	-	100
	-	0.01	-	0.06	-	0.88	-	0.99	-	0.33	-	0.43	-	0.07	-	0.04	-	0.21	-
Nam	14.37	-	6.12	-	0.00	-	0.39	-	72.09	-	5.36	-	1.56	-	0.03	-	0.07	-	100
	-	0.35	-	0.05	-	0.00	-	0.01	-	1.73	-	0.02	-	0.00	-	0.00	-	0.00	-
Ocn	0.00	-	0.00	-	0.00	-	0.00	-	0.00	-	0.00	-	0.00	-	0.00	-	0.00	-	0.00
	-	0.00	-	0.00	-	0.00	-	0.00	-	0.00	-	0.00	-	0.00	-	0.00	-	0.00	-
RSA	3.09	-	10.27	-	0.18	-	6.77	-	3.73	-	25.50	-	45.89	-	2.09	-	2.48	-	100
	-	68.47	-	79.08	-	53.65	-	82.70	-	82.32	-	94.73	-	94.80	-	37.09	-	51.41	-
Zam	13.65	-	6.56	-	1.38	-	6.52	-	4.23	-	2.72	-	2.29	-	48.38	-	14.27	-	100
	-	14.63	-	2.44	-	20.09	-	3.85	-	4.51	-	0.49	-	0.23	-	41.60	-	14.31	-
Zim	7.55	-	6.59	-	2.17	-	17.55	-	3.05	-	3.50	-	2.89	-	25.25	-	31.45	-	100
	-	4.76	-	1.44	-	18.64	-	6.09	-	1.91	-	0.37	-	0.17	-	12.76	-	18.54	-
Total	-	100	-	100	-	100	-	100	-	100	-	100	-	100	-	100	-	100	-

A matrix representative for longer than a one year period (e.g. a decade) can easily be calculated using LED. This particular matrix, together with an appropriate optimization algorithm (maximises the benefit for all countries in the region), can be used as a tool for the development of a regional, mutually agreed upon environmental protection plan.

7.4 SUMMARY

The results in this chapter clearly demonstrate that the phenomena of long-range transport of air pollutants is a serious, complex and significant problem for the countries in the southern African region. The results also indicate that impacts from highly industrial countries in the region may pose significant risks to developing countries, who relies for example on agriculture as a major contributor to the specific country's gross domestic product (GDP).

The LED model supplies objective data, which lays the foundation for the development of holistic regional air quality management plans. The implementation of such a management plan will be obviously beneficial to all countries in the region. The results obtained from this modelling scenario highlights the complexity of transboundary air pollutant transport, and serious developmental consequences, as well as the availability of reliable data for modelling as well as validation purposes.

Chapter 8

CRITICAL EVALUATION

In this Chapter...

In this chapter the thesis as a whole is critically evaluated in terms of the goals stated and the results obtained. Section 8.1 summarizes the main results, whilst Section 8.2 deals with challenges and opportunities for future research.

8.1 RESEARCH PROJECT EVALUATION

The research project forming the basis of this thesis was initiated in the framework of the LEAD/SAFARI 2000 research initiative. The LEAD/SAFARI 2000 research plan considered the development of a long-range air pollutant transport and transformation air quality model, as a main tool for understanding linkages among physical, chemical, biological and anthropogenic processes in southern African systems.

In achieving the main goal set by the LEAD/SAFARI 2000 science initiative the thesis succeeded in the following aspects:

- To develop a comprehensive air quality long-range transport and transformation model. The model includes the appropriate description of the large scale and atmospheric planetary boundary layer dynamics, linear inorganic chemical transformation mechanisms for the oxidation of primary atmospheric pollutants, mechanisms responsible for the wet and dry deposition of pollutants and calculation of the pH value of rain. In the design and development of the LED model, the most recent theoretical understanding and experimental data was utilized. The adopted modular architecure of the LED model allows for easy incorporation of knowledge and inputs from various branches of scientific fields of meteorology, chemistry, physics and biological sciences. It can be noted due to the contribution of the SAFARI 2000 scientific team and international scholars, that LED is the first model designed and proven to be applicable to southern African conditions;

- In addition to the development of LED, software tools usefull and essential for running of this type of model have been developed for meteorological and emission data preprocessing;

- The model evaluation has shown LED's capability in reasonably accurate calculating of averaged atmospheric concentration, deposition fields and pH values;

- The model methodology for calculating country-to-country (emitter-receiver) matrices provides a valuable tool for development of regional air quality improvement plans, legislative initiatives and decision making information, applicable to abatement policies within the Southern African Development Community (SADC) region.

The model performance evaluation during 2000 provides assurance that LED can be used for operational purposes. In the absence of a sufficient number of properly located observation sites, LED is the only tool available for the generation of historical environmental data.

8.2 FUTURE CHALLENGES AND RESEARCH OPPORTUNITIES

The development of a comprehensive long-range air-pollutant transport and transformation air-quality model like LED, requires input from various science disciplines, as well as knowledge and organization of goal specific databases.

The experience gained during the realization of LED, as well as input and discussions with the SAFARI 2000 project team, allowed the following challenges and research opportunities, that will lead to the improvement and optimization of the LED model, to be identified.

- An appropriate research topic relevant to the region, is the quantification of pollution caused by domestic and natural biomass burning. LED can be implemented for this task, keeping in mind that the preliminary estimates show that the total emissions from domestic sources is almost equal to the emissions from industial sources.

- The updated SAFARI 2000 emission database should be compared with available global emission databanks, in order to improve its quality and reliability, especially for the countries outside the borders of South Africa.

- The ground observation network over the region is not sufficient, and does not function on a continuous basis. There is a need for its extention, for which LED can supply information for optimal development. However, the ground measurements needed for the evalaution of LED were also not sufficient due to the small number of observation pionts (5), and geographical location which does not comply with the WMO criteria for baseline regional air quality stations.

- The chemical transformation module implemented in LED can be essentially improved by incorporating new chemical species relevant to the region, as well as a non-linear chemistry mechanism. An additional improvement in the chemistry model of LED, would be the inclusion of an ozone chemistry mechanism. Improvent of the oxidation mechanism is also a consideration.

- The planetary boundary layer (PBL) science has achieved a major theoretical improvement of the understanding of its dynamics during unstable and stable conditions. This necessitates the upgrade of the PBL model to incorporate the new emerging knowledge in the non-local turbulent transport phenomenon which is very relevant to the atmospheric conditions of tropical regions.

- Further research on the rain formation peculiarities (especially duration and spatial distribution) in-cloud and below-cloud intake of pollutant mechanisms is needed to improve the pH calculation scheme.
- An area of future development in LED is the calculation of vertical concentration profiles. This will allow for its verification using remote sensing data (e.g. satellites).

In conclusion, it can be noted that the present thesis has filled a definite gap in the scientific tools available for the southern African region. Many scientific and practical problems associated with the long-range transport and transformation of pollutants can be assessed utilizing the unique features of the LED model. The develpoment of the LED model has also identified new horizons for multi diciplinary scientific research in environmental science.

Chapter 9

REFERENCES

1. Alloway, B.J. and Ayres, D.C., 1993. *Chemical principles of environmental pollution*, Springer, 2^{nd} ed., Great Britain, 291 pp.

2. Al-Ourabi, H. and Lacaux, J.P., 1999. Measurement of the Atmospheric Concentrations of NH_3, NO_2, HNO_3 in Tropical Africa by Use of Diffusive Samplers. *International Global Atmospheric Chemistry (IGAC) Symposium*, September 13-19 1999, Bologna, Italia.

3. Andreae, M.O., Atlas, E., Cachier, H., Cofer, W.R., Harris, G.W., Helas, G., Koppman, R., Lacaux, J. and Ward, D.E., 1996. Trace gas and aerosol emissions from savanna fires. Levine, J.S. (ed.), *Biomass Burning and Global Change*, MIT Press, Cambridge, 278-294.

4. Annegarn, H.J., Kneen, M.A., Piketh, S.J., Horne, A.R., Hlapolosa, H.P.S. and Kirkman, G.A., 1993. Evidence of large-scale circulation of anthropogenic sulphur over southern Africa. Paper No. 57, *Proceedings of the 24^{th} National Association for Clean Air Conference, Clean Air Challenges in a changing South Africa*, Dikololo Game Lodge, Brits, 7 pp.

5. Annegarn, H.J., Turner, C.R., Helas, G., Tosen, G.R. and Rorich, R.P., 1996. Gaseous Pollutants, Chapter 6 in *Air Pollution and its Impacts on the South African Highveld*, eds. G. Held, B.J. Gore, A.D. Surridge, G.R. Tosen, C.R. Turner and R.D. Walmsley, Environmental Scientific Association, Cleveland, 144 pp.

6. Arya, S.P.S. and Sundarajan, A., 1976. An Assessment of Proposed Similarity Theories for the Atmospheric Boundary Layer. *Bound. Layer Met.*, 10, 149-166.

7. Arya, S.P.S., 1974. Geostrophic Drag and Heat Transfer Relation for the Atmospheric Boundary Layer. *Quart. J. Roy. Meteorol. Soc.*, 101, 147-161.

8. Bachmann, J., 2003. *Intercontinental Air Pollution: Introduction to the Topic.* Air & Waste Management Association's Magazine for Environmental Managers: 11, December 2003.

9. Barrie, L.A., 1988. Scavenging ratios, wet deposition and in-cloud oxidation: An application to the oxides of sulphur and nitrogen. *J. Geophys. Res.*, 90, 5789-5799.

10. Batterman, S., 1997. Air Quality Modeling, Monitoring and Control, A Short Course, University of Michigan, Environmental and Industrial Health, 109 Observatory, Ann Arbor, MI 48109-2029.

11. Beloussov, S. and Miatch, L., 1978. On the data gathering in the First Global Experiment GARP. *Meteorology and Hydrology*, 1, 94-103.

12. Black, T. 1994. The new NMC mesoscale ETA model: description and forecast examples. *Wea. Forecasting*, 9, 265-278.

13. Brodzinsky, R., Cantrell, B.K., Endlich, R.M. and Bhumralkar, C.M. (1984) A long range air pollution transport model for Eastern North America-II. Nitrogen oxides, *Atmos. Environ.*, 18, 2361-2366.

14. Burger, J.W., 1993. *Die rol van atmosferiese ysterverbindings in die oksidasie-prosesse van swawel(IV)oksied met suurstof.* MSc Thesis, Potchefstroomse Universiteit vir CHO, Potchefstroom, 80 pp.

15. Calvert, J.G., Bottenheim, J.W. and Strausz, O., 1978. Mechanism of the homogeneous oxidation of sulphur dioxide in the troposphere. *Atmos. Environ.*, 12, 197-226.

16. Calvert, J.G., Lazrus, A., Kok, G.L., Heikes, B.G., Walega, J.G., Lind, J. and Cantrell, C.A., 1985. Chemical mechanisms of acid generation in the troposphere. *Nature*, 317, 27-35.

17. Campbell, G.W., 1997. *Acid Deposition in the United Kingdom 1992-1994.* AEA Technology, London, 176 pp.

18. Cohen, S., Chang, S.G., Markkowitz, S. and Novakov, T., 1981. Role of fly ash in catalytic oxidation of S(IV) slurries. *American Chemical Society*, 15, 1498-1502.

19. Conrad, R., 1997. Production and consumption of methane in the terrestrial biosphere. In: Biogenic Volatile Organic Compounds in the Atmosphere, eds G. Helas, J. Slanina and R. Steinbrecher, SPB Academic Publishing, Amsterdam, 27-44.

20. Cox, W.M. and Tikvart, J.A., 1991. A statistical procedure for determining the best performing air quality simulation model. *Atmos. Environ.*, 21a, 2387-2395.

21. Data Catalog GARP, 1979-1980, Ed. 1-5-M, World Data Centre B.

22. Davidson, E.A., 1991. Fluxes of nitrous oxide and nitric oxide from terrestrial ecosystems. In: Rogers, J.E. and Whitman, W. (Editors), Microbial Production and Consumption of Greenhouse Gases: Methane, Nitrogen Oxides, and Halo methanes. American Society for Microbiology, Washington, 219-235 pp.

23. Deardorff, J. W., 1974. Three-Dimensional Numerical Study of the Height and Mean Structure of the Heated Planetary Boundary Layer. *Bound. Layer Met.*, 7, 81-106.

24. DEBITS, 2005. [Online]. [Accessed 13 May 2005]. Available from the World Wide Web: <http://medias.obs-mip.fr/idaf/measurements/gas/index>.

25. Djolov, G.D., 1991. *Modelling of dynamic and diffusion processes in the planetary boundary layer.* PhD Thesis, Bulgarian Academy of Science, Sofia, Bulgaria, (In Bulgarian).

26. Djolov, G.D. and Syrakov, D.E., 1971. Non-isotropic turbulent diffusion from ellipsoidal source with Gaussian distribution of the concentration in the initial moment. *Meteorology and Hydrology*, 1, 3-8.

27. Djolov, G.D., Syrakov, D.E. and Yordanov, D.L., 1983. Investigation of long-range transport in the region of South-East Europe. *Bulgarian Geophysical Journal*, IX, No. 3, 36-45.

28. Djolov, G.D., Yordanov, D.L. and Syrakov, D.E., 1987. Modelling the Long Range Transport of Air Pollutants with Atmospheric Boundary Layer Chemistry. *Bound. Layer Met.*, 41, 407-416.

29. Dovland, H. and Saltbones, J., Emissions of sulphur dioxides in Europe in 1978, Rep. EMEP/CCC, 2/79, 31 pp.

30. du Vachat, R. and Musson-Genon, L, 1982. Rossby Similarity and Turbulent Formulations. *Bound. Layer Met.*, 23, 47-49.

31. eia.dov.gov, 2004. [Online]. [Accessed 19 August 2005]. Available from the World Wide Web: <http://www.eia.doe.gov/emeu/cabs/safrenv.html>.

32. Eliassen, A., Hov, O., Isaksen, I., Saltbones, J. and Stordal, F., 1982. A lagrangian transport model with atmospheric boundary layer chemistry. *J. of Appl. Met.*, Vol. 21, No. 11, 1645-1661.

33. Endlich, R., Nitz, K., Brodzinsky, R. and Bhumralkar, C.M., 1984. A long-range air pollution transport model for Eastern North America-I. Sulphur Oxides. *Atmos. Environ.*, Vol. 18, No. 11, 2345-2360.

34. Erisman, J.W. and Draaijers, G.P.J., 1995. *Atmospheric deposition in relation to acidification and eutrophication*, Elsevier, Netherlands, 405 pp.

35. Eskom, 2001. Eskom Annual Report 2000, Eskom, Johannesburg (most parts are also available on: http://www.eskom.co.za/annreport01/).

36. Ferm, M. and Rodhe, H., 1997. Measurements of air concentrations of SO_2, NO_2 and NH_3 at rural and remote sites in Asia. *J. Atmos. Chem.*, 27, 17-29.

37. Finlayson-Pitts, B.J. and Pitts, J.N., 1986. *Atmospheric Chemistry: Fundamentals and Experimental Techniques.* John Wiley and Sons, New York, 1098 pp.

38. Fleming, G. and van der Merwe, M., 2000. Spatial Disaggregation of Greenhouse Gas Emission Inventory Data for Africa South of the Equator. ESRI. [Online]. [Accessed 25 March 2004]. 9pp. Available from the World Wide Web: <http://gis.esri.com/library/userconf/proc00/profesional/papers/PAP896/p896.htm>

39. Fourie, G.D., 2000. *Modelling Atmospheric Chemical Transformations under South African Conditions.* MSc Thesis, Potchefstroomse Universiteit vir CHO, Potchefstroom, 155 pp.

40. Fourie, G.D., 2002. *Air Pollution Modelling Needs in the Sasol Environment.* Sastech R&D - Research Report, Sasol Technology Research & Development, Sasolburg, South Africa, 24 pp.

41. Galy-Lacaux, C. and Modi, A.I., 1998. Precipitation chemistry in the Sahelian Savanna. *J. Atmos. Chem.*, 30, 319-343.

42. Ganzeveld, L. and Lelieveld, J., 1995. Dry deposition parameterization in a chemistry general circulation model and its influence on the distribution of reactive trace gases. *J. Geophys. Res.*, 100, 20999-21012.

43. Ganzeveld, L., Lelieveld, J. and Roelofs, G-J., 1998. A dry deposition parameterization for sulfur oxides in a chemistry and general circulation model. *J. Geophys. Res.*, 103, 5679-5694.

44. Ganzeveld, L.N., Lelieveld, J., Dentener, F.J., Krol, M.C., Bouwman, A.J. and Roelofs, G-J., 2002a. Global soil-biogenic NO_x emissions and the role of canopy processes. *J. Geophys. Res.*, 107, No. D16, 10.1029/2001JD000684.

45. Ganzeveld, L.N., Lelieveld, J., Dentener, F.J., Krol, M.C. and Roelofs, G-J., 2002b. Atmosphere-biosphere trace gas exchanges simulated with a single-column model. *J. Geophys. Res.*, 107, No. D16, 10.1029/2001JD0001289.

46. Garrat, J., 1992. *Atmospheric Boundary Layer.* Cambridge University Press, 316 pp.

47. Garstang, M., Tyson, P.D., Swap, R.J., Edwards, M., Kallberg, P. and Lindsay, J.A., 1996. Horizontal and vertical transport of air over southern Africa. *J. Geophys. Res.*, 101, 23721-23736.

48. Gifford, F.A., 1975. *Atmospheric Dispersion Models for Environmental Pollution Applications*, Lectures on Air Pollution and Environmental Impact Analyses, American Meteorological Society, Boston, MA.

49. Graedel, T.E. and Crutzen, P.J., 1997. *Atmosphere, Climate, and Change*, Scientific American Library, United States of America, 113-141.

50. Guenther, A., Hewitt, C., Erickson, D., Fall, R., Geron, C., Graedel, T., Harley, P., Klinger, L., Lerdau, M, McKay, W., Pierce, T., Scholes, R., Steinbrecher, R., Tallamraju, R., Taylor, J. and Zimmerman, P., 1995. A global model of natural volatile organic compound emissions. *J. Geophys. Res.*, 100, 8873-8892.

51. Helas, G. and Pienaar, J.J., 1996. Biomass Burning Emissions. Chapter 3 in: G Held, BJ Gore, AD Surridge, GR Tosen, CR Turner and RD Walmsley (Editors), *Air pollution and its impacts on the South African Highveld*, Environmental Scientific Association, Cleveland, 12-15.

52. Held, G., Scheifinger, H., Snyman, G.M., Tosen, G.R. and Zunckel, M., 1996. The climatology and meteorology of the highveld. Chapter 9 in: G Held, BJ Gore, AD Surridge, GR Tosen, CR Turner and RD Walmsley (Editors), *Air pollution and its impacts on the South African Highveld*, Environmental Scientific Association, Cleveland, 60-71.

53. Held, G., Scheifinger, H., Snyman, G.M., 1994. Recirculation of pollutants in the Atmosphere. *SA J. Sci.*, 90, 91-97.

54. Hicks, B.B., Baldocchi, D.D., Meyers, T.P., Hosker Jr, R.P. and Matt, D.R., 1987. A preliminary multiple resistance routine for deriving dry deposition velocity from measured quantities. *Water, Air and Soil Pollution*, 36, 311-330.

55. Hough, A. and Johnson, C., 1991. Modelling the role of nitrogen oxides, hydrocarbons and carbon monoxide in the global formation of tropospheric oxidants. *Atmos. Environ.*, 25A, 1819-1835.

56. Intergovernmental Panel on Climate Change (IPCC). 1996. *Revised guidelines for national greenhouse gas inventories.* http://www.ipcc.ch.

57. Isaksen, I.S.A. and Hov, O., 1987. Calculations of trends in tropospheric concentrations of O_3, OH, CO, CH_4 and NO_x. *Tellus*, 39, 271-285.

58. Jacobson, M.Z., 1999. *Fundamentals of Atmospheric Modelling*, Cambridge University Press, USA, 656 pp.

59. Kostadinov, L. and Djolov, G., 1977, The Universal Functions in the Resistance Laws for Ekman Boundary Layer. *Izv. Atm. Ocean Phys.*, 13, 984-988.

60. Lacaux, J.P. and Cachier, H., 1993. Biomass burning in Africa: An overview of its impacts on atmospheric chemistry. In: Crutzen, P.J. and Goldammer, J., (eds.) *Fire in the Environment: The ecological, atmospheric and climatic importance of vegetation fires.* John Wiley, New York, 159-191.

61. Lacaux, J.P., Delmas, R., Kouadio, G., Cros, B. and Andreae, M.O., 1992. Precipitation chemistry in the Moyombe forest of equatorial Africa. *J. Geophys. Res.*, 97, 6195-6206.

62. Lacaux, J.P., 1998. An overview of the IGAC's DEBITS activity. *Proceedings of the Fourth CAAP Workshop*, Chulalongkorn University, Bangkok, 9-12 November 1998, 125 pp.

63. Lacaux, J.P., 1999. DEBITS's Activity in Africa: Atmospheric Deposition in Northern Hemisphere of Tropical Africa. International Global Atmospheric Chemistry (IGAC) Symposium, September 13-19, 1999, Bologna, Italia.

64. Langner, J., Rodhe, P., Crutzen, P. and Zimmerman, P., 1992. Anthropogenic influence on the distribution of tropospheric sulphate aerosol. *Nature*, 359, 712-715.

65. Levine, J.S., Winstead, L.E., Parsons, D.A.B., Scholes, M.C., Scholes, R.J., Cofer, W.R., Cahoon, D.R. and Sebacher, D.I., 1996. Biogenic soil emissions of nitric oxide (NO) and nitrous oxide (N_2O) from savannas in South Africa. *J. Geophys. Res.*, 101, 23089-23697.

66. Levine, J.S., Parsons, D.A.B., Zepp, R.G., Burke, R.A., Cahoon, D.R., Cofer, W.R., Miller, W.L., Scholes, M.C., Scholes, R.J., Sebacher, D.I., Sebacher, S. and Winstead, E.L., 1997. Southern African savannas as a source of atmospheric gases. *In: Fire in Southern African Savannas: Ecological and Atmospheric Perspectives*, eds. B.W. van

Wilgen, M.O. Andreae, J.G. Goldhammer and J.A. Lindesay, Witwatersrand University Press, Johannesburg, 135-160.

67. Logan, J.A., 1983. Nitrogen oxides in the troposphere: global and regional budgets. *J. Geophys. Res.*, 88, 10785-10807.

68. Ludwig, J., Marufu, L.T., Huber, B., Andreae, M.O. and Helas, G., 2003. Domestic combustion of biomass fuels in developing countries - A major source of atmospheric pollutants. *J. Atmos. Chem.*, 44, 23-37.

69. Moller, D., 1980. Kinetic model of atmospheric SO_2 oxidation based on published data. *Atmos. Environ.*, 14, 1067-1079.

70. Marufu, L., Dentener F.J., Lelieveld J., Andreae M.O., Helas G., 2000. Photochemistry of the African troposphere: Influence of biomass burning emissions. *J. Geophys. Res.*, 105, 14513-14530.

71. Marufu, L., Ludwig, J., Andreae, M.O., Meixner, F.X., and Helas, G., 1997. Domestic biomass burning in rural and urban Zimbabwe - Part A. *Biomass and Bioenergy*, 12, 53-68.

72. McDowell, W.H., 1988. Potential effects of acid deposition on tropical terrestrial ecosystems, In: *Acidification in Tropical Countries*, H. Rodhe and R. Herrera (eds), Scope 36, John Wiley & Sons, New York, 117-140.

73. McNaughton, D.J., 1981. Relationships between sulfate and nitrate ion concentrations and rainfall pH for use in modeling applications. *Atmos. Environ.*, 15, 1075-1079.

74. Meetham, A.R., 1981. *Atmospheric Pollution: It's History, Origin and Preventions.* Pergamon Press, Oxford, 219 pp.

75. Mesinger, F., Z. I. Janjic, S. Nickovic, D. Gavrilov, and D. G. Deaven. 1988. The stepmountain coordinate: model description and performance for cases of alpine lee cyclogenesis and for a case of an Appalachian redevelopment. *Mon. Wea. Rev.*, 116, 1493-1518.

76. Mesinger, F. 1984. A blocking technique for representation of mountains in atmospheric models. *Riv. Meteor. Aeronaut.*, 44, 195-202.

77. Moussiopoulos, N., Berge, E., Bohler, T., De Leeuw, F., Gronskei, K-E., Mylona, S. and Tombrou, M., 1996, Ambient Air Quality, Pollutant Dispersion and Transport Models, EEA Report, Copenhagen.

78. Mphepya, J.N., 2002. *Atmospheric Deposition Characteristics of Sulphur and Nitrogen Compounds in South Africa.* PhD Thesis, Potchefstroomse Universiteit vir CHO, Potchefstroom, 122 pp.

79. Mphepya, J.N., Pienaar, J.J., Galy-Lacaux, C., Held, G., 2004. An estimate of wet an dry deposition of sulphur and nitrogen in semi-arid areas of southern Africa. *J. Atmos. Chem.*, 47, 1-24.

80. Muller, J-F., 1992. Geographical distribution and seasonal variation of surface emissions and deposition velocities of atmospheric trace gases. *J. Geophys. Res.*, 97, 3787-3804.

81. Munn, R.E. and Bolin, B., 1971. Global air pollution-meteorological aspects: A survey. *Atmos. Environ.* 5, 363-402.

82. Musson-Genon, L. and du Vachat, R., 1992. Rossby Similarity and Turbulent Formulations. *Bound. Layer Met.*, 23, 47-49.

83. Olson, J., 1992. World ecosystems (WE1.4): Digital raster data on a 10 min geographic 1080x2160 grid square, in *Global Ecosystems Database, Version 1.0: DISC A*, edited by NOAA Natl. Geophys. Data Cent., Boulder, Colorado.

84. Orlanski, J., 1975. A rational subdivision of scales for atmospheric processes. *Bull. Amer. Meteorol. Soc.*, 56, 527-530.

85. Otter, L.B., Marufu, L. and Scholes, M.C., 2001. Biogenic, biomass and biofuel sources of trace gases in southern Africa. *SA J. Sci.*, 97, 131-138.

86. Piketh, S.J. and Prangley, A.R., 1998. *Trajectory climatology of transboundary transport for the Highveld.* TRR/T98/038, Eskom, Johannesburg, 24 pp.

87. Piketh, S.J. and Walton, N.M., 2004. Characteristics of Atmospheric Transport of Air Pollution for Africa. The Handbook of Environmental Chemistry, Vol. 4, Part G: 173-195.

88. Piketh, S.J., Annegarn, H.J. and Kneen, M.A., 1996. Regional scale impacts of biomass burning emissions over southern Africa, In: Biomass Burning and Global Change, J.S. Levine (ed), MIT Press, Cambridge, Massachusetts, 320-326.

89. Piketh, S.J., Formenti, P., Freiman, T., Maenhaut, W., Annegarn, H.J. and Tyson, P.D., 1998. Industrial pollutants at a remote site in South Africa, In: 11^{th} *World Clean Air & Congress, IUAPPA, Durban, 14-18 September, Conference Proceedings, Volume 6*, p. 17E-5, Natl. Assoc. for Clean Air, Parklands, South Africa.

90. Potter, C.S., Matson, P.A., Vitousek, P.M. and Davidson, E.A., 1996. Process modeling of controls on nitrogen trace gas emissions from soils worldwide. *J. Geophys. Res.*, 101, 1361-1377.

91. Preston-Whyte, R.A. and Tyson, P.D., 1977. *The atmosphere and weather of southern Africa.* Oxford University Press, Cape Town, 374 pp.

92. Rani, A., Prasad, D.S.N., Madnawat, P.V.S. and Gupta, K.S., 1992. The role of free fall atmospheric dust in catalysing autoxidation of aqueous sulphur dioxide. *Atmos. Environ.*, 16, 1647-1656.

93. Raupach, M.R., 1992. Drag and Drag Partition on Rough Surfaces. *Bound. Layer Met.*, 60, 375-395.

94. Raupach, M.R., 1994. Simplified expressions for vegetation roughness length and zero-plane displacement as functions of canopy height and area index. *Bound. Layer Met.*, 71, 211-216.

95. SAWB, 1986. *Climate of South Africa. Climate statistics up to 1984.* WB 40, South African Weather Bureau, Department of Environment Affairs, Pretoria, 474 pp.

96. South African Weather Service (SAWS). 2004. SAFARI 2000 ETA Atmospheric Model Data, Wet and Dry Seasons 2000. Data set. Available on-line [http://daac.ornl.gov/] from Oak Ridge National Laboratory Distributed Active Archive Center, Oak Ridge, Tennessee, U.S.A.

97. Scholes, M.C. and Andreae, M.O., 2000. Biogenic and pyrogenic emissions from Africa and their impact on the global atmosphere. *Ambio.*, 29, 23-29.

98. Scholes, R.J., Kendall, J. and Justice, C.O., 1996. The quantity of biomass burned in southern Africa. *J. Geophys. Res.*, 101 (D19), 23667-23676.

99. /item Scholes, R.J., Ward, D.E. and Justice, C.O., 1996. Emissions of trace gases and aerosol particles due to vegetation burning in southern hemisphere Africa. *J. Geophys. Res.*, 101 (D19), 23677-23682.

100. Schulze, B.R., 1965. *Climate of South Africa, Part 8, General Survey.* WB 28, South African Weather Bureau, Department of Environment Affairs, Pretoria, 330 pp.

101. Scott B.C., 1978. Parameterization of Sulfate Removal by Precipitation. *J. of Appl. Met.*, 17, 1375-1389.

102. Seigneur, C., 1987. Computer simulation of air pollution chemistry. *Environ. Software*, 2, 116.

103. Seinfeld, J.H. and Pandis, S.N., 1998. *Atmospheric Chemistry and Physics: From Air Pollution to Climate Change.* John Wiley & Sons, New York, 1326 pp.

104. Serca, D., Delmas, R., Le Roux, X., Parsons, D.A.B., Scholes, M.C., Abbadie, L., Lensi, R., Ronce, O. and Labroue, L., 1998. Comparison of nitrogen monoxide emissions from several African tropical ecosystems and influence of season and fire. *Global Biogeochem. Cycles*, 12, 637-651.

105. Serca, D., Delmas, R., Jambert, C. and Labroue, L., 1994. Emissions of nitrogen oxides from equatorial rainforests in central Africa: origin and regulation of NO emissions from soils. *Tellus*, 46B, 143-254.

106. Sheih, C-M., Wesely, M.L. and Hicks, B.B., 1979. Estimated dry deposition velocities of sulfur over the eastern United States and surrounding regions. *Atmos. Environ.*, 13, 1361-1368.

107. Shir, C.C. and Bornstein, R.D., 1977. Eddy Exchange Coefficients in Numerical Models of the Planetary Boundary Layer. *Bound. Layer Met.*, 11, 171-186.

108. Siversten, B., Matal, C. and Rereira, L.M.R., 1995. *Sulphur emissions and transfronteir air pollution in southern Africa.* Report 35, SADC ELMS, Lesotho, 117 pp.

109. Smeda, M.S., 1979. Bulk Model for the Atmospheric Planetary Boundary Layer. *Bound. Layer Met.*, 7, 411-467.

110. Summers, P.W., 1992. Role of clouds in the chemistry, transport, transformation and deposition of air pollutants: general concepts, current understanding and future research needs, in WMO WMP Rep. No. 17, World Meteorological Organization, Geneva, 27-45.

111. Syrakov, D., Djolov, G. and Yordanov, D., 1983. Incorporation of planetary boundary layer dynamics in a numerical model of long-range air pollutant transport. *Bound. Layer Met.*, 26, 1-13.

112. Tosen, G.R. and Jury, M., 1986. *The winter nocturnal wind jet over the Eastern Transvaal - a case study sequence.* TRR/N86/006, Eskom, Johannesburg, 20 pp.

113. Tosen, G.R. and Jury, M., 1988. Climatology of the winter boundary layer over the Eastern Transvaal. *SA J. Sci.*, 84, 247-253.

114. Tyson, P.D., Garstang, M., Swap, R., Edwards, M. and Kallberg, P., 1988. *Atmospheric Pollution and its Implications in the Eastern Transvaal Highveld.* S. Afr. National Scientific Programmes Report 150, Foundation for Research and Development, Pretoria, 114 pp.

115. Tyson, P.D. and D'Abreton, P., 1998. Transport and recirculation of aerosols off southern Africa – Macroscale plume structure. *Atmos. Environ.*, 32, 1511-1524.

116. Tyson, P.D., 1998. Regional Transport of Aerosols and Trace Gases over southern Africa and Adjacent Oceans: Implications for the Future, 11^{th} World Clean Air & Environment Congress, 2G-2, 3 pp.

117. Tyson, P.D., Garstang, M., Swap, R.J., Edwards, M. and Kallberg, P., 1996. An air transport climatology for subtropical southern Africa. *International Journal of Climatology*, 16, 151-163.

118. Tyson, P.D., Garstang, M., Swap, R.J., Edwards, M. and Kallberg, P., 1996. An air transport climatology for subtropical southern Africa. *International Journal of Climatology*, 16, 265-91.

119. Wesely M.L. and Hicks, B.B., 1977. Some factors that affect the deposition rates of sulfur dioxide and similar gases on vegetation. *Journal of Air Pollution Control Association*, 27, 1110-1116.

120. Wesely, M.L. and Hicks, B.B., 2000. A review of the current status of knowledge on dry deposition. *Atmos. Environ.*, 34, 2261-2282.

121. Whelpdale, D.M. and Kaiser, M.S., 1996. *Global Acid Deposition Assessment.* WMO No. 106, Global Atmosphere Watch, World Meteorological Organization, Geneve.

122. Williamson, S.J., 1973. *Fundamentals of Air Pollution*, Addison-Wesley, Reading, Massachusetts.

123. Wills, G.E. and Deardorff, J.W., 1976. A laboratory model of diffusion into a convective planetary boundary layer. *Quart. J. Roy. Meteor. Soc.*, 102, 427-445.

124. Wippermann, F., 1972. Universal Profiles in the Barotropic Planetary Boundary Layer. *Beitr. Phys. Atm.*, 45, 148-163.

125. Wippermann, F., 1973. Numerical Study of the Effects Controlling the Low-Level Jet. *Beitr. Phys. Atm.*, 46, 137-154.

126. WMO, 1997a (1998, 1999). Nineteenth (Twentieth and Twentyfirst) acid rain performance survey. World Precipitation Chemistry Center of the WMO QA/SAC, State University of New York, Albany.

127. WMO, 1997b. Global acid deposition assessment. In: D.M. Whelpdale and M.S. Kaiser (eds), *A global overview of acid deposition.* WMO Report TD No. 777, Global Atmosphere Watch, World Meteorological Organization, Geneva, Switzerland.

128. WMO, 1996. Global Acid Deposition Assessemnt, Report No. 106, World Meteorological Organization, Geneva, Switzerland.

129. Yordanov, D.L., Penenko, V.V., and Aloyan, A.E., 1978. Parametrization of Stratified Baroclinic Planetary Boundary Layer for the Numerical Modeling of Atmospheric Processes. *Izv. Atm. Ocean Phys.*, 14,815-823.

130. Yordanov, D., Syrakov, D. and Djolov, G., 1983. A barotropic planetary boundary layer. *Bound. Layer Met.*, 25, 363-373.

131. Yordanov, D., 1975. A Simple Baroclinic Model for the Planetary Boundary Layer. *Izv. Atm. Ocean Phys.*, 11,630-634.

132. Yordanov, D., 1976. On the Universal Function in the Resistance Law for the Baroclinic Planetary Boundary Layer. *Izv. Atm. Ocean Phys.*, 12, 769-772.

133. Yordanov, D., 1977. On the Height of Surface Air Layer. *Izv. Atm. Ocean Phys.*, 13,781-783.

134. Zannetti, P., 1990. *Air Pollution Modelling: Theories, Computational Methods and Available Software*, Computational Mechanics Publication, Southampton.

135. Zannetti, P., 1993. *Numerical simulation modelling of air pollution: an overview, in Air Pollution* (P. Zannetti et al., eds.), Computational Mechanics Publication, Southampton, Chp. 3-14.

136. Zilitinkevich, S.S., 1970. *Dynamics of Atmospheric Boundary Layer*, Leningrad, *Gidrometeorological Press* (in Russian).

137. Zilitinkevich, S.S., 1975. Resistance Laws and Prediction Equations for the Depth of the Planetary Boundary Layer. *J. Atm. Sc.*, 32, 741-752.